


For Reference

NOT TO BE TAKEN FROM THIS ROOM



Ex LIBRIS
UNIVERSITATIS
ALBERTAENSIS





Digitized by the Internet Archive
in 2018 with funding from
University of Alberta Libraries

<https://archive.org/details/Masuda1955>

thesis
1955
#20

THE UNIVERSITY OF ALBERTA

APPARENT VISCOSITIES OF SELECTED ALBERTA CRUDE OILS

BY PILOT PIPELINE

A DISSERTATION

SUBMITTED TO THE SCHOOL OF GRADUATE STUDIES IN
PARTIAL FULFILLMENT OF THE REQUIREMENTS FOR THE DEGREE
OF MASTER OF SCIENCE

FACULTY OF ENGINEERING

DEPARTMENT OF CHEMICAL AND PETROLEUM ENGINEERING

by

A. MASUDA

EDMONTON, ALBERTA

APRIL, 1955.

ABSTRACT

From experimental pressure drop and flow rate data of the pilot pipeline tests, the apparent viscosities of various crude oils, for the temperature range of 20 to 80°F., were calculated. Possible viscosity dependency on shear rate, as for a non-Newtonian fluid, was investigated by variation in flow rates.

The relationship between the calculated apparent viscosity and temperature was defined by a single curve for a specific crude for both laminar and turbulent flow patterns regardless of the apparent shear rate at the wall, the diameter of the test line or the storage tank temperature of the crude oil. Apparent viscosity data for both turbulent and laminar flow conditions were found to be identical in the relatively wax-free range of 40 to 80°F. The crude oils showed linear apparent viscosity-temperature relationship for oil temperatures in the range 80 to 65°F. Below 55°F the apparent viscosity of all crudes increased rapidly with decrease in temperature. The transition occurred in the range 65 to 55°F.

Even under laminar conditions of flow, the pilot pipeline investigations showed the flow of crude oil through the test lines to be characterized by high apparent shear rates at the wall. The shear rates observed may have been large enough to give the limiting viscosity characteristic of a pseudoplastic

fluid at infinite shear. The pseudoplastic nature of similar crudes at temperatures below their "wax points" where precipitated wax is held in suspension within the fluid, has been reported by previous investigators. The maximum shear rates used by these investigators were approximately 40 reciprocal seconds while minimum shear rates at the wall, obtained in the pilot pipeline tests, were rarely below 1000 reciprocal seconds and exceeded 100,000 reciprocal seconds at the higher rates of flow. The results indicate that, within the operating range of the pilot pipeline, the crudes tested behave as Newtonian liquids. However, pseudoplasticity cannot entirely be disregarded in view of the high shear rates encountered in the pipeline tests.

ACKNOWLEDGEMENT

Acknowledgement by the writer for assistance
in the completion of this phase of the project is extended to:

Dr. G. W. Govier, for his supervision and
criticism;

Interprovincial Pipe Line Company Limited
for their Fellowship;

P. Buckland and other members of the staff
of Interprovincial Pipe Line Company Limited
who have aided in the collection of crude
oil samples and pipeline data;

and to all those not mentioned here whose
advice, criticism and assistance helped to
make this dissertation possible.

TABLE OF CONTENTS

	<u>Page</u>
INTRODUCTION.....	3
THEORY AND LITERATURE REVIEW	
Classification of Fluids.....	5
Pipeline Flow Equations for Newtonian Fluids.....	12
A. Reynolds Criterion of Flow.....	12
B. The Flow Equation.....	13
C. Friction Factor Equations.....	14
D. Shear Stress and Shear Rate.....	17
Pipeline Flow Equations for Non-Newtonian Fluids....	19
Nomenclature: Definition of Symbols in Theory and Literature Review.....	24
DESCRIPTION OF EXPERIMENTAL EQUIPMENT.....	27
OPERATION OF THE PILOT PIPELINE.....	37
RESULTS.....	39
DISCUSSION OF RESULTS	
A. Thermal Behaviour of Crude Oil in Test.....	46
B. Apparent Viscosity Characteristics of Crude Oils Tested.....	48
(1) Redwater Sample No. 1.....	49
(2) Redwater Sample No. 2.....	52
(3) Stettler D2-D3 Blend.....	53
(4) Duhamel-Malmo-New Norway Blend.....	53
(5) Leduc-Woodbend Blend.....	54
(6) Nisku Blend.....	54
C. Generalized Effect of Crude Oil Gravity on Apparent Viscosity.....	55
CONCLUSION.....	67
BIBLIOGRAPHY.....	69
APPENDIX A	
(1) Sample Computations of Experimental Data	
(2) Sample Computations of Formulae Used in Computation of Results	
(3) Sample Computations of Detailed Results	
(4) Sample Computations of Viscosity Conversions	

APPENDIX B: Experimental Data of Pilot Pipeline

APPENDIX C: Detailed Results of Computation of Pilot Pipeline Tests

APPENDIX D: Refrigeration Studies

LIST OF TABLES

TABLE	I-B	Test Line Dimensions of the Pilot Pipeline.....	1B
TABLE	II-B	Record of Crudes Tested.....	1B
TABLE	III-B	Density Determinations by Gravitometer.....	2B
TABLE	IV-B	Experimental Data of Pilot Pipeline Tests for Redwater Sample No. 1 in 0.249 and 0.386 Inch Line.....	4B
TABLE	V-B	Experimental Data of Pilot Pipeline Tests for Redwater Sample No. 2 in 0.249 Inch Line.....	7B
TABLE	VI-B	Experimental Data of Pilot Pipeline Tests for Stettler D2-D3 Blend in 0.249 Inch Line.....	9B
TABLE	VII-B	Experimental Data of Pilot Pipeline Tests for Duhamel-Malmo-New Norway Blend in 0.249 Inch Line	9B
TABLE	VIII-B	Experimental Data of Pilot Pipeline Tests for Leduc-Woodbend Blend in 0.249 Inch Line.....	11B
TABLE	IX-B	Experimental Data of Pilot Pipeline Tests for Nisku Blend in 0.249 Inch Line.....	11B
TABLE	I-C	Summary of Formulae Used in Computations Reported in Appendix A, Section 2.....	1C
TABLE	II-C	Detailed Results of Computations for Pilot Pipeline Tests on Redwater Sample No. 1.....	2C
TABLE	III-C	Detailed Results of Computations for Pilot Pipeline Tests on Redwater Sample No. 2.....	13C
TABLE	IV-C	Detailed Results of Computations for Pilot Pipeline Tests on Stettler D2-D3 Blend.....	16C
TABLE	V-C	Detailed Results of Computations for Pilot Pipeline Tests on Duhamel-Malmo-New Norway Blend	17C
TABLE	VI-C	Detailed Results of Computations for Pilot Pipeline Tests on Leduc Woodbend Blend.....	21C
TABLE	VII-C	Detailed Results of Computations for Pilot Pipeline Tests on Nisku Blend.....	22C

TABLE VIII-C	Apparent Viscosity Comparisons for Redwater Crudes.....	23C
TABLE IX-C	Summary of Apparent Viscosity Correlations.....	24C
TABLE X-C	Apparent Viscosity Conversion to Kinematic and Saybolt Universal Viscosities.....	25C
TABLE I-D	Experimental Data for Refrigeration Studies on Pilot Pipeline.....	2D
TABLE II-D	Tabulation of Results of Heat Transfer Computations.....	19D

LIST OF ILLUSTRATIONS

Fig. 1	The Pilot Pipeline.....	1
Fig. 2	Schematic Diagram of Pilot Pipeline.....	2
Fig. 3	Simplified Shear Diagrams for Newtonian, Bingham Plastic, Pseudoplastic and Dilatant Materials..	6
Fig. 4	General Shear Diagram for Bingham Plastic.....	6
Fig. 5	Shear Diagram for a Thixotropic Material.....	6
Fig. 6	Shear Stress Distribution in Circular Conduit.....	17
Fig. 7	Typical End Assembly of Pilot Pipeline.....	30
Fig. 8	Equilibrium Line and Upstream Pressure Tap Section..	31
Fig. 9	View of Upstream Portion of Pilot Pipeline Showing Refrigeration and Cooling Section.....	32
Fig. 10	End View of Upstream Manifold.....	33
Fig. 11	End View of Downstream Manifold and Pressure Taps..	34
Fig. 12	View of Crude Oil Measuring Tanks, Freon-12 Storage Tanks and Instrument Panel.....	34
Fig. 13	Typical Pressure Tap Assembly.....	35
Fig. 14	Instrument Panel for Pilot Pipeline.....	36
Fig. 15	Density Variation with Temperature.....	40
Fig. 16	Thermal Behaviour of Duhamel-Malmo-New Norway Blend	47
Fig. 17	Apparent Viscosity of 34.5 A.P.I. Redwater Crude by Pilot Pipeline (0.249" line).....	56
Fig. 18	Apparent Viscosity of 34.5 A.P.I. Redwater Crude by Pilot Pipeline (0.386" line).....	57
Fig. 19	Apparent Viscosity of 34.2 A.P.I. Redwater Crude by Pilot Pipeline.....	58
Fig. 20	Apparent Viscosity of 29.1 A.P.I. Stettler D2-D3 Blend by Pilot Pipeline.....	59

Fig. 21	Apparent Viscosity of 37.1 A.P.I. Duhamel-Malmö-New Norway Blend by Pilot Pipeline.....	60
Fig. 22	Apparent Viscosity of 38.5 A.P.I. Leduc-Woodbend Blend by Pilot Pipeline.....	61
Fig. 23	Apparent Viscosity of 32.6 A.P.I. Nisku Blend by Pilot Pipeline.....	62
Fig. 24	Apparent Viscosities of Crude Oils Tested by Pilot Pipeline (Arithmetic Plot).....	63
Fig. 25	Apparent Viscosities of Some Alberta Crude Oils by Pilot Pipeline (Semi-Logarithmic Plot).....	64
Fig. 26	Saybolt Universal Viscosities Computed from Apparent Viscosities of Pilot Pipeline Results.....	65
Fig. 27	Generalized Effect of Crude Oil Gravity on Apparent Viscosity.....	66

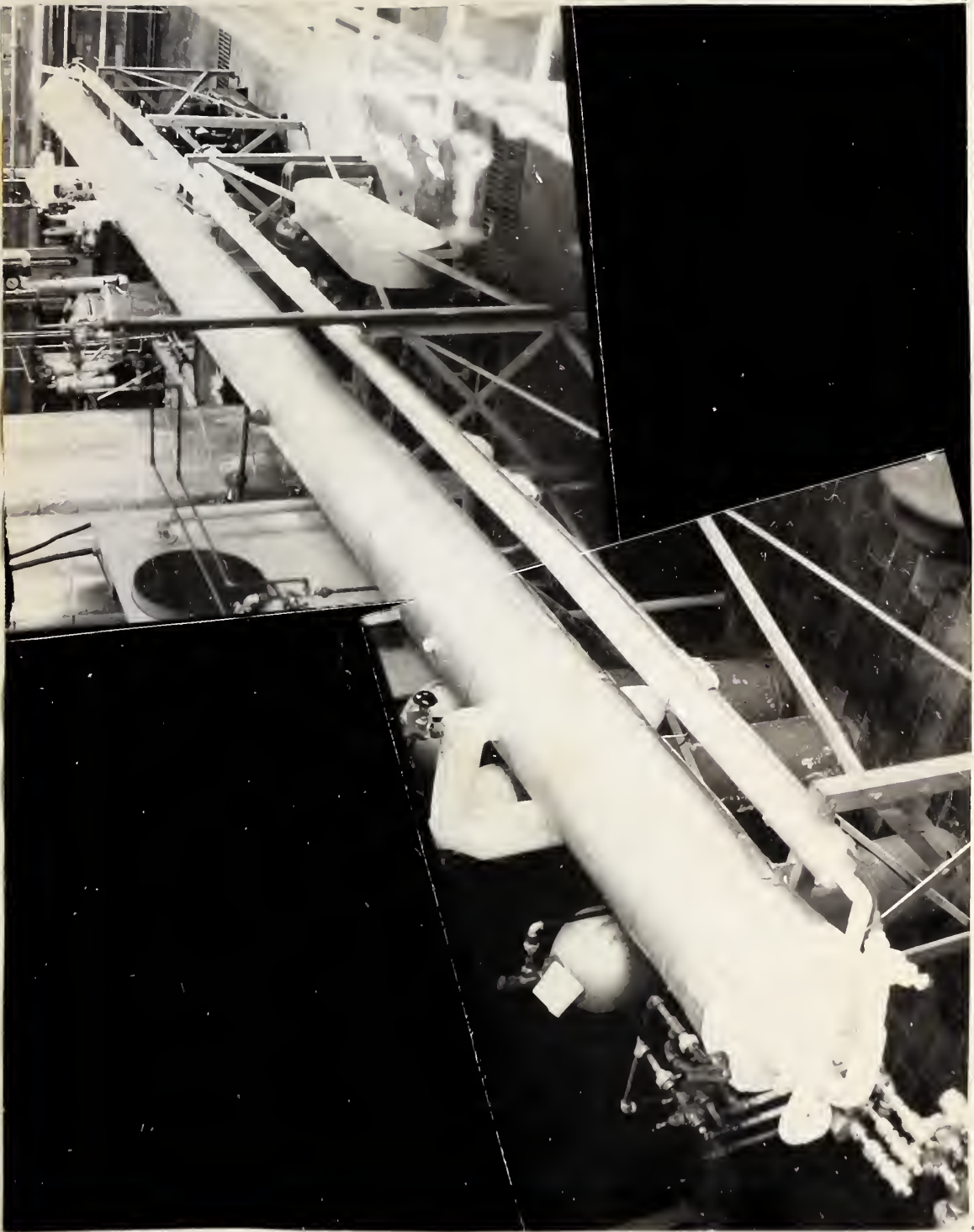


Figure 1. The Pilot Pipeline

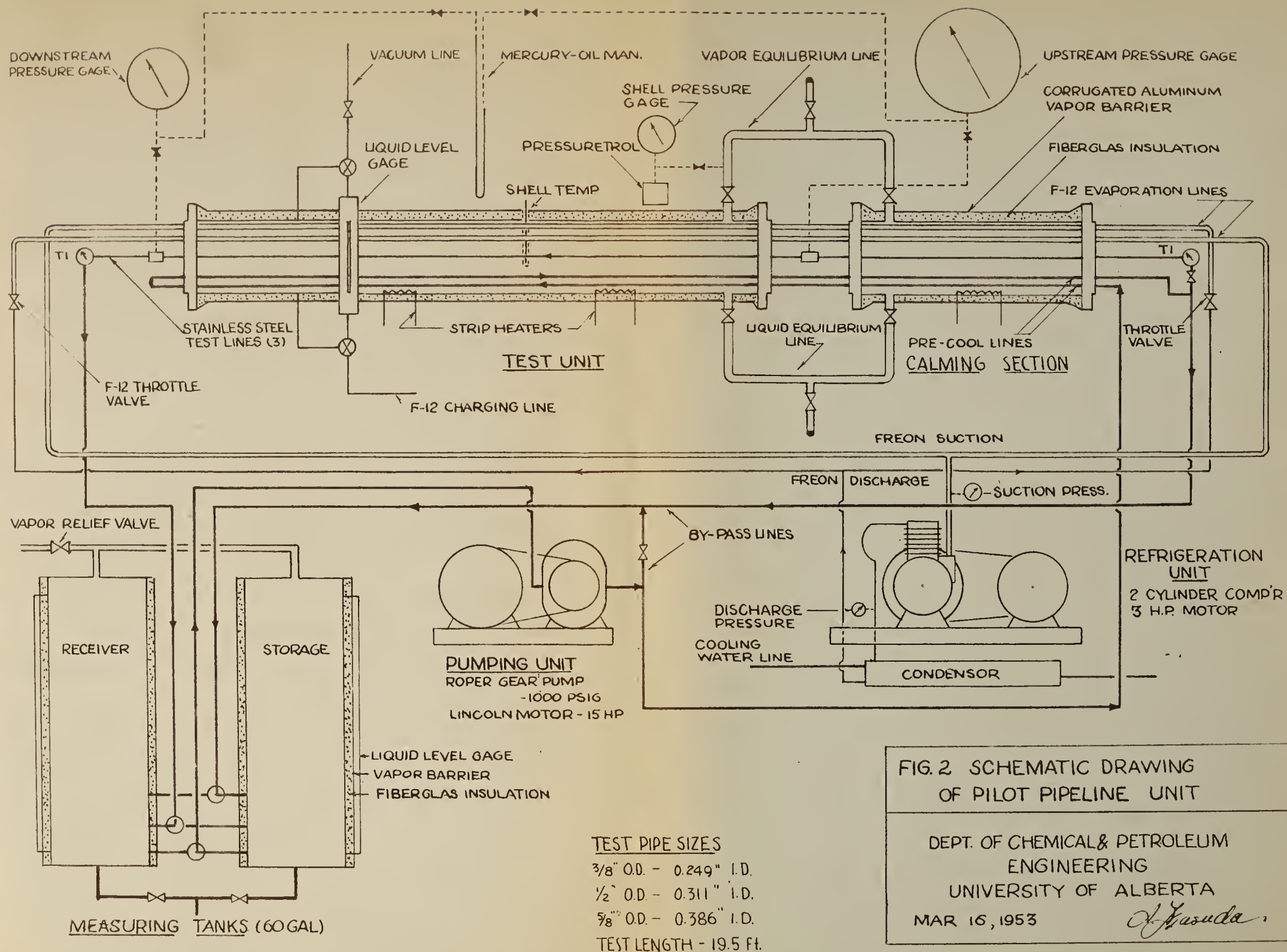


FIG. 2 SCHEMATIC DRAWING
OF PILOT PIPELINE UNIT

DEPT. OF CHEMICAL & PETROLEUM
ENGINEERING
UNIVERSITY OF ALBERTA

MAR 16, 1953

A. Yasuda

INTRODUCTION

The investigation into the viscosity characteristics of Alberta crude oils was initiated at the University of Alberta in 1950. The purpose of this research program was to obtain rheological data on various Alberta crude oils which could be used to predict the power requirements of existing pipelines or used in the design of pipelines handling Alberta crude stocks.

The research program in chronological order has been:

- (1) The laboratory investigations by W. Sidjak (17) on the rheological properties of some Alberta crudes using the MacMichael viscometer.
- (2) The design, assembly, and preliminary testing of pilot pipeline using stove oil and Redwater crude oil by M. M. Chmilar (9).
- (3) An investigation of the viscosity characteristics of Alberta crudes using the pilot pipeline. The result of this investigation is presented in this dissertation.

An evaluation of the consistency of the liquid is necessary to determine the pressure drops encountered in the pipeline flow of liquids. The consistency of a Newtonian liquid is independent of the rate of shear and is commonly known as the viscosity of the liquid. For such liquids, pressure drops may be calculated by standard formulae from a single evaluation of viscosity at the flow temperature.

The consistency of a non-Newtonian liquid is dependent on the rate of shear, flow temperature, and for certain liquids, upon previous thermal treatment. For these fluids, data relating "viscosity" to shear rate and temperature is needed for the computation of pressure drops. Without such data, the calculation of pressure drops becomes little better than guesswork.

Most Alberta crudes behave as Newtonian fluids at temperatures above the "wax point". Previous investigations by Sidjak (17) and Bauer and Ruston (5) on some Alberta crude oils indicate wax points in the region 50 to 60 degrees F. "Viscosity" - temperature relationships have been found to be near linear above these critical points. Below "wax point" temperatures, however, some crude oils tested have shown non-Newtonian characteristics. Sidjak (17) has shown that these crudes at temperatures below the "wax point" will behave as pseudoplastic materials.

THEORY AND LITERATURE REVIEW

Classification of Fluids

Fluids are classified according to the relationship of shear stress to the rate of shear, i.e., the shape of shear stress - rate of shear curves as shown in Figure 3, (Alves, Boucher and Pigford 2). A fluid subjected to a shear stress undergoes continuous deformation and the resistance by the fluid to the applied stress is called its consistency. Numerically the measure of consistency is the ratio:

$$\frac{\hat{\tau} \xi_c}{-(dv/dr)} \quad (1)$$

where $\hat{\tau}$ = unit shear stress,

$-(dv/dr)$ = rate of shear at the point of stress.

ξ_c = conversion constant

At any given temperature, Newtonian fluids are characterized by a constant ratio between the rate of shear and the applied shearing stress (Figure 3, curve A). For such substances, the consistency is called viscosity and defined by the equation:

$$\hat{\tau} = - \frac{\mu}{\xi_c} \left(\frac{dv}{dr} \right) \quad (2)$$

where μ is the coefficient of viscosity or simply, viscosity and is indicated by the slope of curve A.

If the consistency is dependent on the rate of shear at constant temperature, the fluid is said to be non-Newtonian.

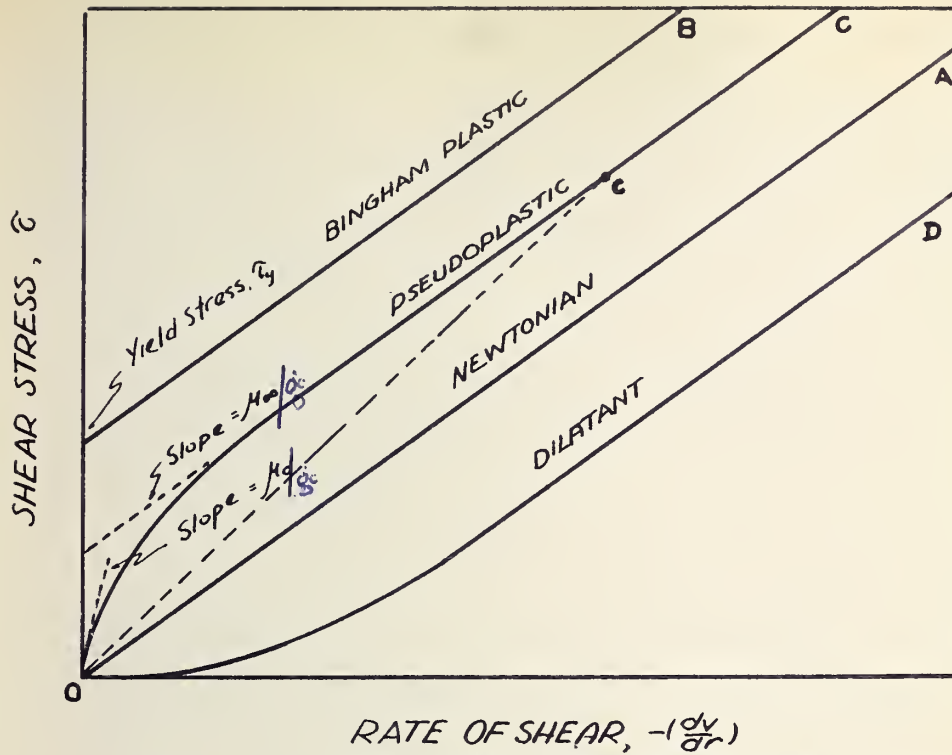


FIG. 3 Simplified Shear Diagrams for Newtonian, Bingham Plastic, Pseudoplastic and Dilatant Materials

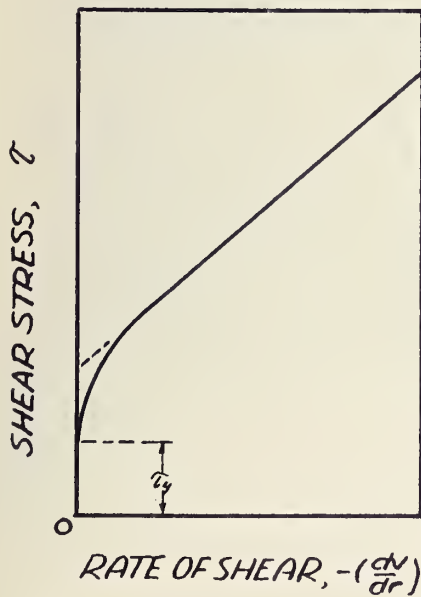


FIG. 4 General Form of Shear Diagram for Bingham Plastic

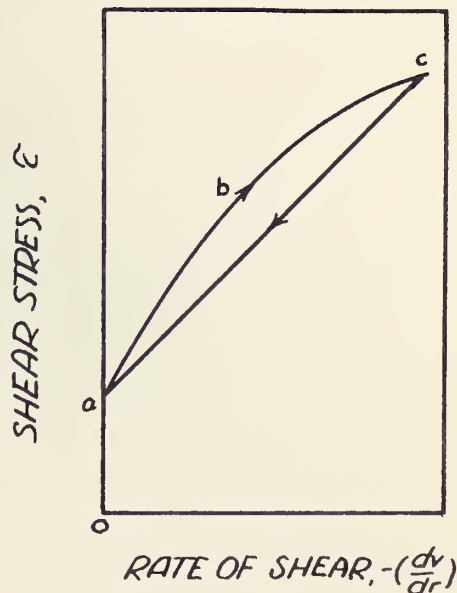


FIG. 5 Shear Diagram for a Thixotropic Material

For these fluids, the property corresponding to the viscosity of a Newtonian has been described in a multiplicity of terms, e.g. plasticity, rigidity, apparent viscosity and plastic viscosity. Non-Newtonian fluids have been further classified into distinct types such as Bingham plastics, pseudoplastics, thixotropes, dilatants, etc., and present shear rate - shear stress relationships which differ from each other and from a Newtonian as illustrated in Figures 3, 4 and 5 (Alves 1).

1. Bingham Plastic (Curve B, Figure 3)

The Bingham plastic exhibits a yield stress τ_y , which must be exceeded before motion is imparted to the fluid. At values greater than the yield stress, the ratio of shear stress to shear rate is constant and is called the coefficient of rigidity or plastic viscosity (Green, 11). The coefficient of rigidity, η , is defined by the equation:

$$\eta = \frac{(\tau - \tau_y) \, g_c}{-(\frac{dv}{dr})} \quad (3)$$

where τ_y = yield stress

Experimental data on Bingham plastics give shear stress - shear rate relationships similar to Figure 4, and at very low shear rates, the straight line relationship between shear stress and shear rate degenerates as shown.

Sewage sludge and grain suspensions in water are materials which exhibit Bingham plastic behaviour.

2. Pseudoplastic (Curve C, Figure 3)

Pseudoplastic fluids flow under any deforming force, but the consistency of these materials decreases at increasing rates of shear as shown by the decreasing slope of curve C. The limiting viscosity at infinite rate of shear (μ_∞) is indicated by the slope of the straight line, and the slope of the tangent at zero rate of shear indicates the viscosity at zero rate of shear, μ_0 . These two limits are dependent on the system and temperature, but are independent of rate of shear and the dimensions of the confining tube (Winding, Baumann and Kranich, 21).

The consistency curve of a pseudoplastic fluid is best represented by a complex function:

$$\tau = \tau_y \left(- \frac{dv}{dr} \right)^{1/n} / g_c \quad (4)$$

An approximation of the curve in the region where linearity exists between shear stress and rate of shear is given by the equation:

$$(\tau - \tau_y) = \frac{\eta'}{g_c} \left(- \frac{dv}{dr} \right) \quad (5)$$

where τ_y represents effective yield value and η' , the effective coefficient of rigidity.

In the evaluation of the consistency of pseudoplastic fluids, the term "apparent viscosity" has been used, and has been

defined as "the viscosity of a pseudoplastic if it were a Newtonian material with a consistency curve passing through the point of measurement" (Green, 11). Referring to curve C of Figure 3, the apparent viscosity of a pseudoplastic is indicated by the slope of line O-c if c represents the point of measurement.

Winding, et al (21) in discussing the pseudoplastic behaviour of GRS latices, suggest that the suspension of finite particles in a liquid may result in decrease of apparent viscosity at high rates of shear. The decrease may be attributed to any one or a combination of elongation of spherical particles by disintegration of aggregates, alignment of particles possessing rod-like structures, or through the breakdown of solvation layers of fluid about the particle.

When temperature conditions are favorable, precipitation of wax takes place in many crude oils. These particles could influence the rheological behavior of crude oils through one or more of the mechanisms previously suggested. Sidjak (17) found that when temperature conditions resulted in wax precipitation the crude oil behaved in a pseudoplastic manner. Padgett (14) found that petroleum wax could crystallize out in several different forms, e.g. as plate crystals, needle crystals, or in a mal-crystalline form, and that the type of crystal formed was dependent on the characteristics of the wax present in the

oil, the concentration of wax, the rate of cooling and on the influence of crystal forms upon one another. Investigations by Sidjak (17) and Bauer and Ruston (5) showed that apparent viscosities of certain Alberta crudes were also influenced by the thermal treatment, to which the oil has been subjected prior to viscosity measurement. The thermal treatment of the crude may have caused formation of different crystal forms.

3. Dilatant Materials (Curve D, Figure 3)

Dilatant materials are defined by the general relationship between shear stress and rate of shear as shown by curve D. The consistency of these fluids increases with increasing shear stress. A characteristic feature of the dilatant material is that a stiffening of the material takes place when it is subjected to a shearing stress.

Dilatancy is typical of heavy suspensions in which particles have settled into a position of "minimum voids." The disturbance of particles under shear will expand or "dilate" the volume of voids resulting in an insufficiency of fluid vehicle, consequently, a dry appearance and stiffening of the suspension takes place (Green, 11). A common material which exhibits dilatancy is wet sand whose water-to-sand ratio is just sufficient to fill the voids when the voids are at their minimum volume.

Dilatant behaviour has not been observed in crude oils.

4. Thixotropic Materials (Figure 5)

Thixotropic materials possess a structure, the breakdown of which is a function of time as well as of the rate of shear. These structures can rebuild themselves, if not prevented from doing so by externally applied forces. As a simple illustration of thixotropy, the addition of a suitable amount of electrolyte to a strong sol of ferric oxide or alumina results in a jelly if allowed to stand. Shaking the jelly will reform the sol which will set again on standing.

Data from rotational viscometers for thixotropic materials give shear stress-rate of shear diagram similar to Figure 5 with the characteristic hysteresis loop which is an indication of the degree of thixotropy of the material. Referring to Figure 5, curve abc is obtained while the material is being continually broken down, increased shear rate resulting in decreased consistency. If the downcurve ca is run immediately after the completion of upcurve abc, no further breakdown occurs, hence higher rates of shear are obtained for the corresponding shear stresses. A repetition of loop abca is obtained if the thixotropic material is retested after being allowed to stand (Alves, et al, 2).

An application of thixotropic behaviour is found in drilling muds. Water alone is not adequate as a drilling fluid since it is not heavy enough and cuttings may easily settle out and freeze the drill. Thixotropic suspensions of bentonite are used as boring fluids to maintain the required hydrostatic head and to bring up the cuttings. These muds set to soft jels which are easily liquidied (Weiser,19).

Other materials exhibiting thixotropic behaviour are paints and printing inks. The thixotropic behaviour of some crude oils has been reported. This is not surprising since some crude oils will gel if allowed to stand at low temperatures.

Pipeline Flow Equations for Newtonian Fluids

A. Reynolds Criterion of Flow.

The flow of Newtonian fluids may take place in a viscous, transitional, or turbulent manner. Viscous flow is characterized by the movement of the fluid in layers or laminae, and turbulent flow by the presence of eddying and turbulence in the flowing stream. Laminar, transitional or turbulent flow is dependent on the numerical value of the dimensionless ratio $\frac{DV\rho}{\mu}$, which is called the Reynolds number N_R . Experimental results indicate that laminar flow exists when values of Reynolds number are less than 2100 (Walker, Lewis, McAdams and Gilliland, 18). The value of 2100 is called the lower critical value of Reynolds number. The upper critical value, which indicates the lowest value of Reynolds number for which complete turbulence is present, is reported by Brown (7) as 3000 while Binder (6) reports an upper critical value of 4000. Values lying between these two critical Reynolds numbers indicate a state of transition where flow is neither laminar or turbulent but a mixture of these two states.

B. The Flow Equation

For the solution of problems involving steady state flow of essentially noncompressible fluids, Walker et al (18) present the mechanical energy equation in the form:

$$\omega' - \int_1^2 dP = (x_2 - x_1) \frac{g}{g_c} + \frac{v_2^2 - v_1^2}{2g_c} + F \quad (6)$$

where ω' = external work done on the flowing fluid

v = specific volume of flowing fluid

x = height above datum.

P = pressure

V = velocity

g = acceleration due to gravity

g_c = conversion constant

F = total friction due to flow.

In the case of fluid flow in a horizontal pipe of constant cross-section where change in specific volume of the fluid is very small, and in the absence of external work, equation (6) reduces to:

$$\frac{\Delta P}{\rho_{av}} = F \quad (7)$$

where ρ_{av} = average density of fluid.

The friction term in equation (7) may be evaluated by the Fanning equation which expresses pressure drop in terms of fluid density, flow rate, pipeline geometry and a friction factor:

$$\frac{\Delta P}{\rho} = \frac{fV^2L}{2g_cD} \quad (8)$$

where D = internal diameter of pipe

L = length of pipe section

f = friction factor

In some engineering texts equation (8) is presented as

$$\frac{\Delta P}{\rho} = \frac{2f'V^2L}{g_cD}$$

$$\text{where } f' = \frac{f}{4}$$

In this dissertation the values of friction factor will be defined by equation (8).

C. Friction Factor Equations

Experimental data have shown that the friction factor is dependent on two dimensionless ratios, the Reynolds number, $\left(\frac{DVP}{\mu}\right)$, and the relative roughness, $\left(\frac{e}{D}\right)$, i.e., the ratio of the absolute roughness, (e), to the diameter of the pipe, (D).

In laminar flow, relative roughness of the pipe wall has no effect upon the friction factor and the experimentally determined relationship between Reynolds number and friction factor is:

$$f = \frac{64}{N_R} \quad (9)$$

$$\text{where } N_R = \frac{DVP}{\mu}, \text{ Reynolds number}$$

Poiseuille's equation states that the pressure drop, encountered in the laminar flow of a fluid through a tube, is directly proportional to the product of viscosity, average velocity and length and inversely proportional to the square of the diameter,

that is:

$$\Delta P = \frac{32 \mu V L}{\epsilon_c D^2}$$

This equation, while derived theoretically, is equivalent to the combination of equations (8) and (9).

Empirical formulae have been developed to show the relationship between friction factor, Reynolds number and relative roughness in turbulent flow. For smooth tubes the equations are given in terms of Reynolds number and friction factor. Equations commonly used for smooth tubes are:

Blasius equation (4)

$$f = 0.316 \left(\frac{1}{N_R} \right)^{0.25} \quad (10)$$

Koo equation (15, 18)

$$f = .0056 + \frac{0.50}{N_R^{0.32}} \quad (11)$$

Karman, Nikuradse and Prandtl equation (6,16)

$$\frac{1}{\sqrt{f}} = 2 \log_{10} N_R \sqrt{f} - 0.8 \quad (12)$$

Stanton and Pannell equation (3)

$$f = \frac{0.3205}{(N_R)^{0.252}} \quad (13)$$

Heltzel's equations (3,12)

$$f = \frac{0.364}{(N_R)^{0.265}} \quad (14)$$

$$f = \frac{0.157}{N_R^{0.188}} \quad (15)$$

The Blasius equation is especially suited for Reynolds numbers ranging from 10,000 to 100,000. The Koo equation is based on a Reynolds number range from 3000 to 3,000,000. Anderson (3) showed that the Stanton and Pannell relationship could be used to compute friction factors in the Reynolds number range of 6000 to 130,000 for the transmission of some crude oils through large diameter lines (16, 20 and 30 inch). Equations (14) and (15) were the results of Heltzel's work on lines 6 to 12 inches in diameter. He found that friction factors, calculated in the flow of crude oil through these lines, could be closely represented by equation (14) for values of Reynolds numbers in the range 2,500 to 57,600 and by equation (15) for values of Reynolds numbers greater than 57,600.

In rough pipes, friction factors encountered in turbulent flow are influenced by the value of relative roughness as well as the Reynolds number. Furthermore, the friction factor approaches a limit dependent on the relative roughness. Karman's equation for the value of this limit in fully developed turbulent flow is given by Rouse (16) as:

$$\frac{1}{\sqrt{f}} = 2 \log_{10} \frac{e}{D} + 1.74 \quad (16)$$

In general, pressure drops in fluid flow are computed by using the Fanning friction factor equation and by evaluating friction

factors from the standard friction factor - Reynolds number plots given in fundamental engineering texts. Such plots present in graphical form, equation (9) for laminar flow and the equivalent of (12) for turbulent flow in smooth pipes. Parameters indicating lines of constant relative roughness show the effect of the wall roughness on the friction factor.

D. Shear Stress and Shear Rate

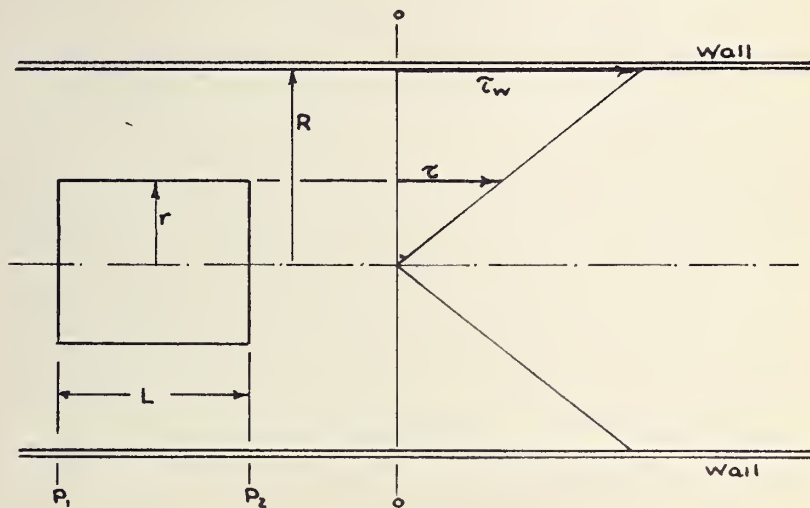


FIG. 6 Shear Stress Distribution in Circular Conduit

In the isothermal steady state flow of a cylindrical mass of fluid, consider the section of radius r and pressure drop,

$P_1 - P_2 = \Delta P$ (Figure 6). A force balance may be written:

$$\pi r^2 \Delta P = (2 \pi r L) \tau \quad (17)$$

$\eta r^2 (\Delta P)$ represents the difference in force between the two faces, and $2 \eta r L \tau$ represents the opposing force acting on the cylindrical surface of radius r . The shear stress is shown to be:

$$\tau = \frac{r \Delta P}{2L} \quad (18)$$

Similarly the shear stress at the wall may be shown to be:

$$\tau_w = \frac{D (\Delta P)}{4L} \quad (19)$$

Since no limitations were made as to the rheology of the fluid or the type of flow (laminar, transitional or turbulent), equation (18) shows that the steady state flow of all fluids will be in such a manner, that a linear shear stress distribution will be obtained (Figure 6).

For Newtonian fluids in laminar motion, the shearing force at the wall of the pipe is:

$$\tau_w = -\mu \left(\frac{dv}{dr} \right)_w \cdot \frac{1}{g_c}$$

Substituting this in equation (19), the rate of shear at the wall for a Newtonian fluid in laminar motion is:

$$-\left(\frac{dv}{dr} \right)_w = \frac{D g_c (\Delta P)}{4 \mu L} \quad (20)$$

Fluid flow through tubes and pipes is characterized by a velocity profile with maximum velocity at the axis and zero velocity at the wall. A boundary layer exists adjacent to the wall in which fluid is flowing in a laminar fashion while the main core of the stream may be turbulent, (Coulson, 10). The shear

rate at the wall is again given by equation (20) because of the laminar boundary layer.

Pipeline Flow Equations for Non-Newtonian Fluids

The mechanical energy equation (6) and the Fanning equation (8) may be used to estimate the pressure drops encountered in the pipeline flow of non-Newtonian fluids as well as Newtonian fluids. However, for non-Newtonians the equations relating the friction factor to the Reynolds number and the relative roughness for Newtonian fluids are no longer valid. If an apparent Reynolds number is defined for the flow of non-Newtonians, using some other consistency term for viscosity:

$$\text{apparent } N_R = \frac{DV\rho}{(\text{consistency of non-Newtonian})} \quad (21)$$

it is found that the apparent Reynolds number will vary throughout the cross section of the pipe since the consistency of non-Newtonians are dependent on the rate of shear which varies from maximum at the pipe wall to zero at the axis of the pipe. Establishment of the character of flow, i.e. laminar, transition or turbulent, has been done by most investigators by substituting coefficient of rigidity, limiting viscosity or apparent viscosity for the consistency term in the apparent Reynolds number.

Buckingham (11) in 1921 derived a theoretical expression for the capillary flow of a plastic based on the definition of a plastic,

equation (3). He pictured "plastic flow" to be made up of three parts:

- (1) the flow of a central plug in which no shear occurred.
- (2) a laminar layer enveloping the plug and
- (3) a lubricating layer adjacent to the wall with a finite slippage velocity v_R and thickness, ϵ .

Buckingham assumed that the thin lubricating layer exhibited a Newtonian viscosity. The final form of his equation is:

$$Q = \frac{\pi R^4 g_c}{8 \eta L} \left(\Delta P - \frac{4 \Delta p}{3} + \frac{\Delta p^4}{3 \Delta P^3} \right) + \frac{\pi R^3 \epsilon \Delta P}{2 \mu L} \quad (22)$$

where Q = volume rate of flow

R = radius of capillary

η = coefficient of rigidity

L = length of capillary

ΔP = total pressure drop

Δp = pressure required to initiate motion

μ = viscosity of a Newtonian fluid

ϵ = thickness of lubricating layer

Equation (22) shows that when $\Delta P = \Delta p$, the first term becomes zero, and the flow becomes entirely due to slippage. When ΔP is less than Δp , there is no flow since the total applied stress is less than the yield stress. When there is no slippage the last term vanishes and plug flow is not eliminated completely until the volume rate of flow becomes infinite. Although Buckingham's

theoretical equation is important in discussing the plug and laminar flow of plastics, the equation is not satisfactorily solved due to the numerous unknown quantities inherent in it. A simpler flow equation by Bingham, again based on the definition of a plastic and cited by Babbitt and Caldwell, (8) is:

$$Q = \frac{\pi R^4 g_c}{8 \eta L} \left(\Delta P - \frac{4 \Delta P}{3} + \frac{1}{3} \frac{\Delta P^4}{\Delta P^3} \right) \quad (23)$$

Bingham did not assume slippage at the wall but only assumed a central plug moving inside a laminar layer. In terms of velocity, the equation becomes:

$$V = \frac{D^2 g_c}{32 \eta L} \left(\Delta P - \frac{4 \Delta P}{3} + \frac{1}{3} \frac{\Delta P^4}{\Delta P^3} \right) \quad (24)$$

Substituting equation (24) in the Fanning equation results in the friction factor expression:

$$f = \frac{\Delta P}{\rho} \left(\frac{2 g_c D}{L} \left(\frac{32 \eta L}{D^2 g_c} \right)^2 \left(\Delta P - \frac{4 \Delta P}{3} + \frac{1}{3} \frac{\Delta P^4}{\Delta P^3} \right) \right)^{-2} \quad (25)$$

A dimensional analysis by Winning (22) on the properties assumed to influence the pipeline flow of plastics resulted in the expression:

$$f = 4 \left(\frac{DV \rho}{\eta} \right), \frac{e}{D}, \frac{D \bar{\epsilon}_y g_c}{V \eta} \quad (26)$$

From Winning's experimental data, a plot of $\frac{DV \rho}{\eta}$ vs. friction factor showed the effect of the "yield ratio", $\frac{D \bar{\epsilon}_y g_c}{V \eta}$, in the laminar flow region. For values of $\frac{DV \rho}{\eta}$ to 2000, lines of constant yield ratio were obtained parallel to the equation $f = 64 \left(\frac{2}{DV \rho} \right)$. In this

region, higher values of yield ratio corresponded to higher values of friction factor for any given value of $\frac{DV\rho}{\eta}$ and the line $f = 64 \left(\frac{1}{DV\rho} \right)$ represented a yield ratio value of zero.

Another method of evaluating friction factors in the laminar flow of non-Newtonian fluids has been through the use of "apparent viscosities". A modified Poiseuille equation in which apparent viscosity has been substituted for viscosity is:

$$\Delta P = \frac{32 \mu_a LV}{8_c D^2} \quad (27)$$

where μ_a is the apparent viscosity and depicts the net result of the consistency properties of the non-Newtonian in laminar flow through a tube. Substitution of equation (27) in the Fanning equation (8) gives:

$$f = 64 \left(\frac{\mu_a}{DV\rho} \right) \quad (28)$$

$$\text{or } f = \frac{64}{(N_R)_a}$$

where $(N_R)_a$ is apparent Reynolds number.

In fully developed turbulent flow, theoretical equations describing the flow of non-Newtonian fluids are not known. Experimental results of Winning, (22), Alves, Boucher and Pigford (2) Winding, Baumann and Kranich (21) show that non-Newtonians behave in a manner similar to Newtonians in the turbulent region, that is, the effective consistency is not influenced by the shear rates of the non-Newtonian fluids. The work of Alves et al (2) on the turbulent

flow of a plastic, an eighteen percent titanium dioxide slurry, over a range of apparent Reynolds numbers of 4,000 to 100,000 gave values of apparent viscosities of 1.5 to 1.6 centipoise. With these results they showed that the conventional friction factor - Reynolds number charts could be used to obtain values of friction factor using apparent Reynolds numbers. Winding, Baumann and Kranich (21) suggest that limiting viscosity at infinite shear, in the case of pseudoplastics or the coefficient of rigidity, in the case of plastics, can be used to compute apparent Reynolds numbers in turbulent flow and that these apparent Reynolds numbers can be used to determine friction factors from the standard friction factor - Reynolds number charts.

The literature review indicates that in fully developed turbulent flow of non-Newtonian fluids, friction factors may be evaluated by the method of using apparent Reynolds numbers. A suitable friction factor equation such as the Karman Prandtl equation (12) or the Heltzel equation (14) may be used in relating the apparent Reynolds number to the friction factor. For example, modification of the Heltzel equation becomes:

$$f = \frac{0.364}{(N_R)_a^{0.265}} = 0.364 \left(\frac{\mu_a}{DV\rho} \right)^{0.265} \quad (29)$$

As in the modified Poiseuille equation, the apparent viscosity term in equation (29) depicts the net effect of the consistency property of the non-Newtonian fluid in fully developed turbulent flow.

A few friction factor equations have been presented for non-Newtonian fluids. Since Alberta crude oils have been found to behave in a pseudoplastic manner at low temperatures (Sidjak, 17), the Buckingham, Bingham and Winning equations for plastic flow cannot be used. The method of apparent viscosities seems the effective method for evaluating friction factors, especially for the case of the pilot pipeline.

Nomenclature

Definition of Symbols Used in Theory and Literature Review.

$-\frac{dv}{dr}$ = velocity gradient or rate of shear, sec^{-1} .

$-\left(\frac{dv}{dr}\right)_w$ = rate of shear at the pipe wall, sec^{-1} .

D = internal diameter of pipe, ft.

e = absolute roughness of pipe wall, ft.

f = Fanning friction factor, dimensionless.

F = friction loss, $\frac{\text{lb}_f - \text{ft.}}{\text{lb}_m}$.

g = acceleration due to gravity, ft/sec^2

g_c = conversion constant = $32.2 \frac{\text{lb}_m - \text{ft.}}{\text{lb}_f - \text{sec}^2}$

L = length of pipe, ft.

$N_R = \frac{DV\rho}{\mu} = \text{Reynolds number, dimensionless}$

$(N_R)_a = \frac{DV\rho}{\mu_a} = \text{apparent Reynolds number, dimensionless}$

P = pressure, $\text{lb}/\text{ft.}^2$

Δp = pressure drop required to initiate flow for plastic, $\text{lb}/\text{ft.}^2$

ΔP = total pressure drop, $\text{lb}/\text{ft.}^2$

Q = volume rate of flow, $\text{ft}^3/\text{sec.}$

r = radial distance from pipe axis, ft.

R = internal radius of pipe, ft.

V = velocity of fluid $\text{ft}/\text{sec.}$

v = point velocity of fluid, $\text{ft}/\text{sec.}$

v_R = slippage velocity of plastic fluid, $\text{ft}/\text{sec.}$

w = external work done on flowing fluid, $\frac{\text{lb}_f - \text{ft.}}{\text{lb}_m}$

x = height above datum, ft.

ξ = thickness of lubricating layer in the Buckingham equation, ft.

ψ = function

μ = viscosity, $\text{lb}/\text{ft-sec.}$

μ_a = apparent viscosity, $\text{lb}/\text{ft-sec.}$

μ_0 = limiting viscosity of pseudoplastic at zero shear, lb/ft-sec.

μ_∞ = limiting viscosity of pseudoplastic at infinite shear, lb/ft-sec.

η = coefficient of rigidity, lb/ft-sec.

η' = effective coefficient of rigidity, lb/ft-sec.

ρ = fluid density, lb/ft.³

τ = shear stress, lb/ft.²

τ_w = shear stress at the wall, lb/ft.²

τ_y = yield stress for plastic, lb/ft.²

τ' = effective yield stress, lb/ft.²

v = specific volume of fluid, ft³/lb.

DESCRIPTION OF EXPERIMENTAL EQUIPMENT

The essential features of the pilot pipeline (Figures 1 and 2) are the refrigerated shell, refrigeration unit, test lines, precooling lines, crude oil storage and measurement tanks, Roper gear pump, and the control instruments.

Two lengths of eight inch pipe, fitted with dead end flanges (Figure 7), make up the outer casing of the refrigerated shell. An eight foot length encloses the calming section and an eighteen and a half foot length encloses the test section. The casings are connected by vapor and liquid equilibrium lines (Figure 8). The entire casing is insulated with glass wool and covered with a vapor barrier of corrugated aluminum sheet to prevent heat transfer from the surroundings into the shell. Arrangement of test, refrigeration and precooling lines within the shell is shown schematically in Figure 2. Test and precooling lines are immersed in a bath of liquid Freon-12. A pressuretrol, which is actuated by the vapor pressure of Freon-12 within the shell, controls the bath temperature. Settings on this controller turn on strip heaters if the pressure decreases and shut off the heaters if the pressure increases. By this means, a relatively constant pressure, and hence constant temperature may be maintained within the shell. Other accessories to the shell include the liquid level gauge, pressure gauge, thermometer and thermometer well.

Three stainless steel test lines are mounted on the unit as shown in Figure 7. The internal diameters of these lines are 0.249 inches, 0.311 inches and 0.386 inches. The manifold arrangement for selection of the test line is shown in Figures 10 and 11. The test section between pressure taps is 19.5 feet and is preceded by a calming section of 8.5 feet. Weston dial thermometers, of range -40 to 140°F., are inserted in each of the distributing manifolds to measure the flow temperature of the crude oil. Figure 13 shows a typical pressure tap assembly. Care was taken in fabrication to remove any burrs which could induce turbulence at the pressure taps.

Three pressure gauges are used to determine the pressure drop over the test section; an upstream Heise gauge of range 0 to 1000 psi. in 2 psi. intervals, a downstream Acragauge of range 0 to 100 psi. in one-half psi. intervals, and a mercury-under-oil differential manometer for low pressure drops (0 to 30 psi.).

Two 60 gal. capacity tanks (Figure 12), with sight glasses provide for the volumetric measurement of the fluid used in the tests. The valves and pipes are arranged so that either tank may be used as the reservoir or the measuring tank. Drainage pipes are installed for manual draining of tanks of fluid which cannot be pumped out. The tanks are completely enclosed to prevent weathering of the crude, however a safety relief valve is used

to prevent build-up of excessive tank pressures.

A Roper gear pump, capable of delivering pressures up to 1000 psi. is used to circulate the crude oil through the system. Piping and valves are arranged to permit part or all of the crude oil to be returned to the storage tank before or after precooling of the oil (Figure 2). When part of the oil stream is by-passed before cooling, the temperature of the storage tank oil remains essentially at the higher temperatures (50 to 70°F) since any cooling of the storage oil is due to the return of cold test oil to storage. When part of the oil stream is by-passed after precooling, greater cooling of the storage tank temperature is effected and tank temperatures may reach as low as 35°F.

A three horsepower Freon-12 vapor compression unit is used to refrigerate the shell (Figure 9). Freon-12 vapor taken on the suction side is compressed, cooled and liquified, and expanded from the half inch liquid line into a $1\frac{1}{8}$ inch copper refrigeration line which passes through the length of the shell. Cooling of the bath is accomplished by the vapors condensing on the refrigeration lines. This results in the lowering of vapor pressure and temperature of the liquid Freon in the bath. The crude oil is cooled by the transfer of heat through the walls of the precool and test lines into the liquid Freon bath.

Pressure gauges, magnetic controls and manual switches for the heaters, pump and refrigerating unit are mounted on an instrument panel board as shown in Figure 14.

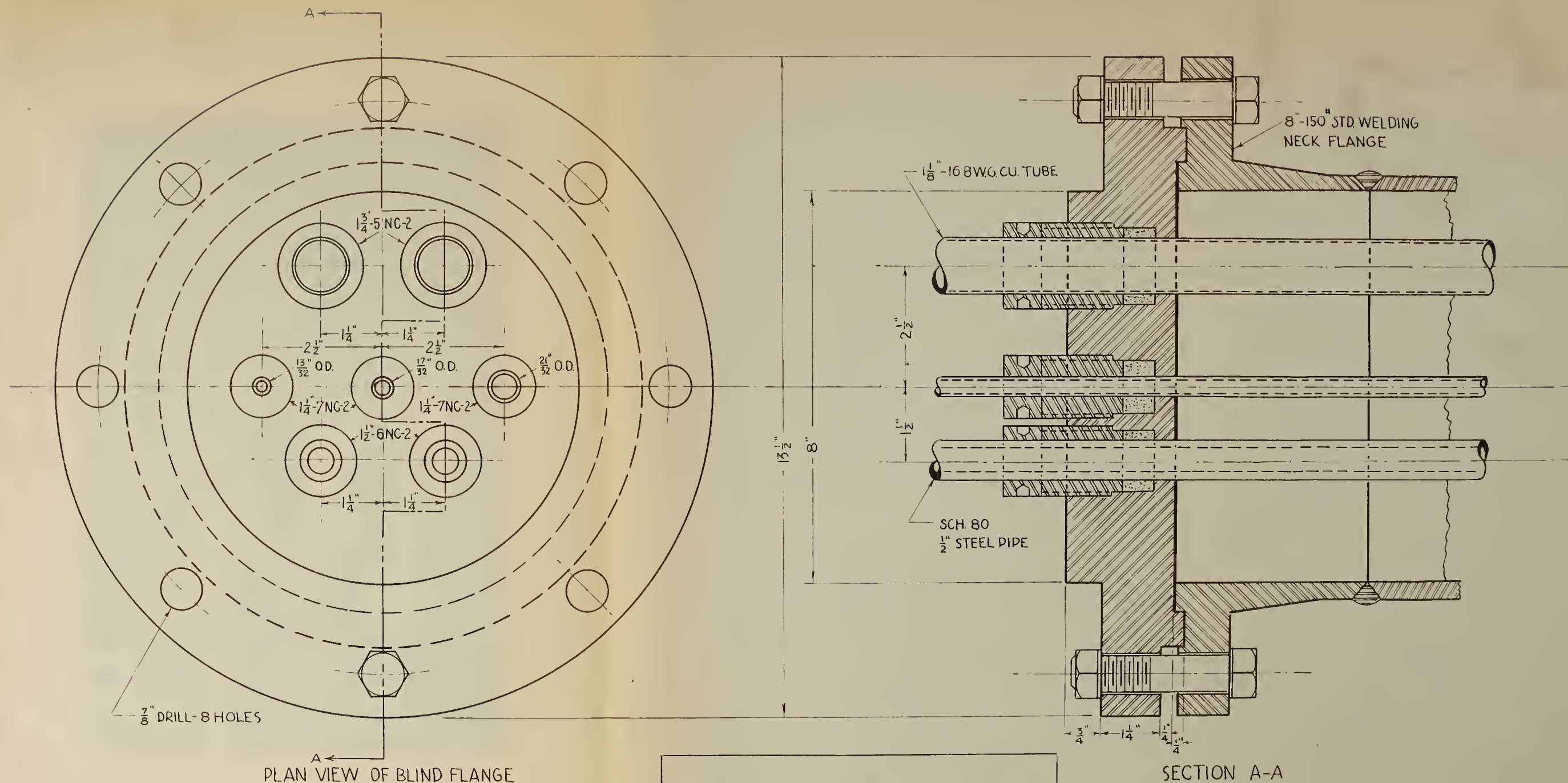


FIG.7 TYPICAL END ASSEMBLY
OF PILOT PIPELINE

SCALE - HALF SIZE
UNIVERSITY OF ALBERTA
DEPT. OF CHEMICAL AND PETROLEUM ENGINEERING
APRIL 30, 1953.

A. Yasuda



Figure 8. Equilibrium Lines and Upstream Pressure Tap
Section



Figure 9. View of Upstream Portion of Pilot Pipeline Showing Refrigeration Unit and Calming Section





Figure 10. End View of Upstream Manifold



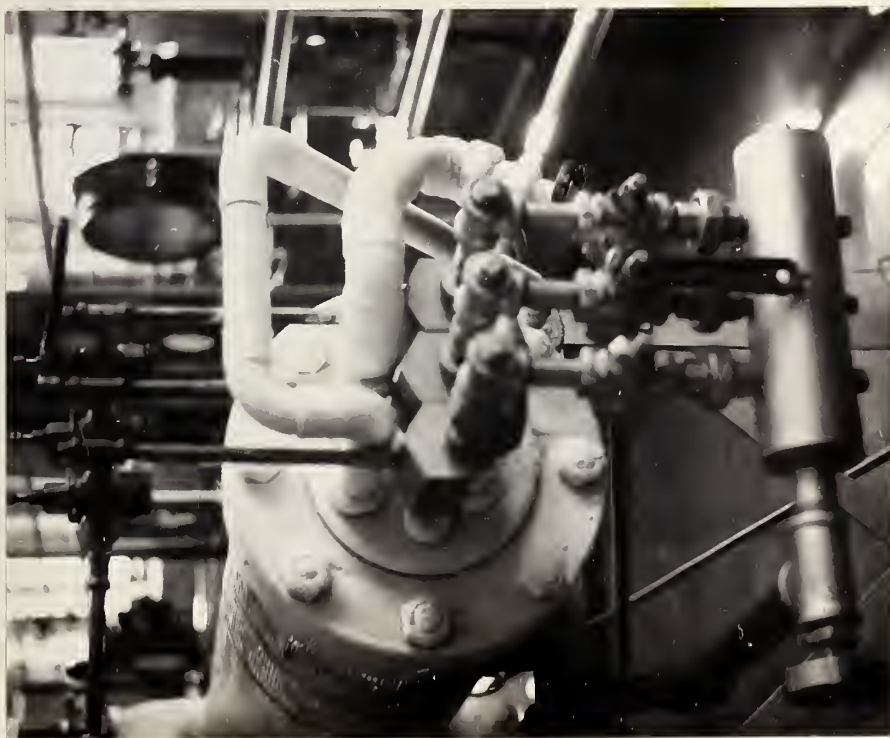


Figure 11. End View of Downstream Manifold and Pressure Taps

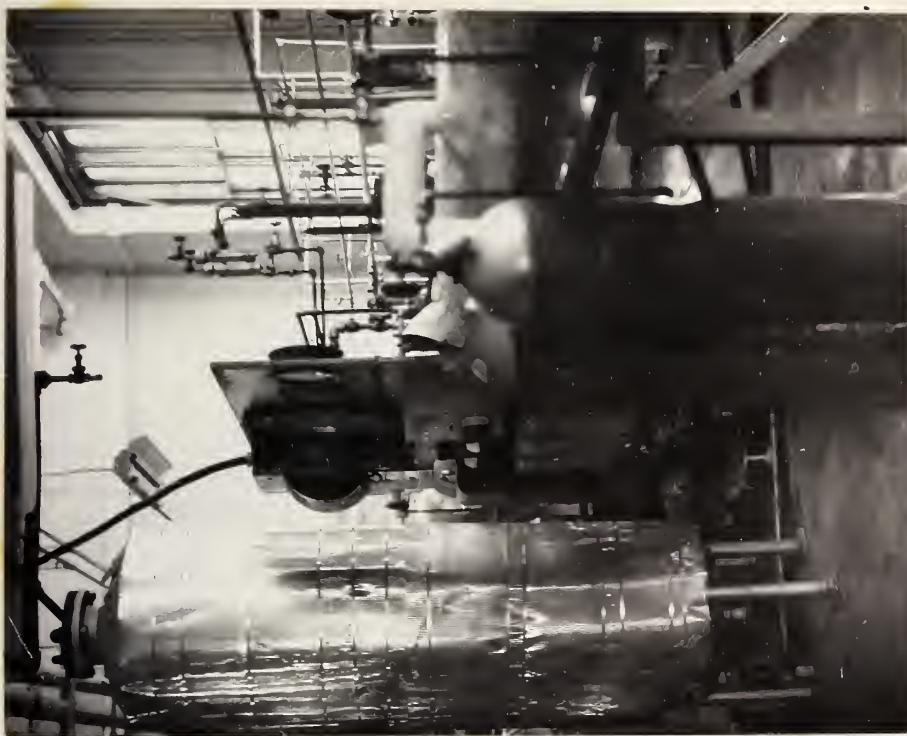
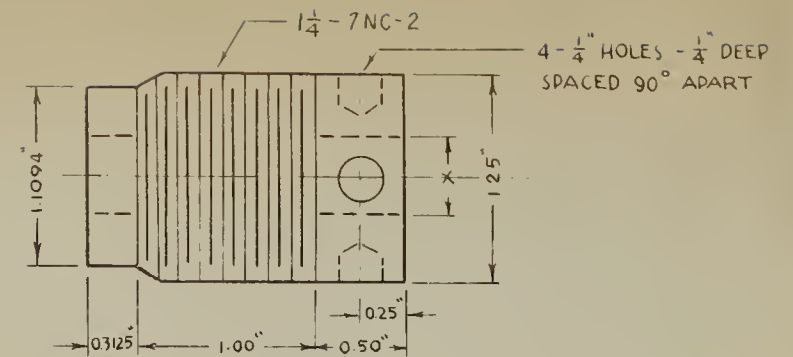
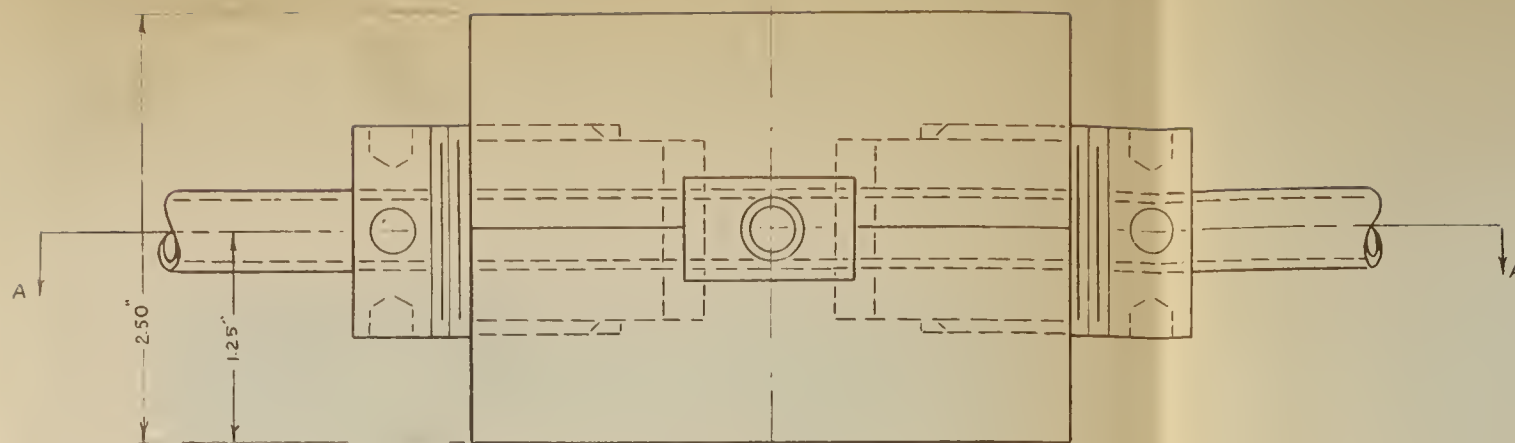


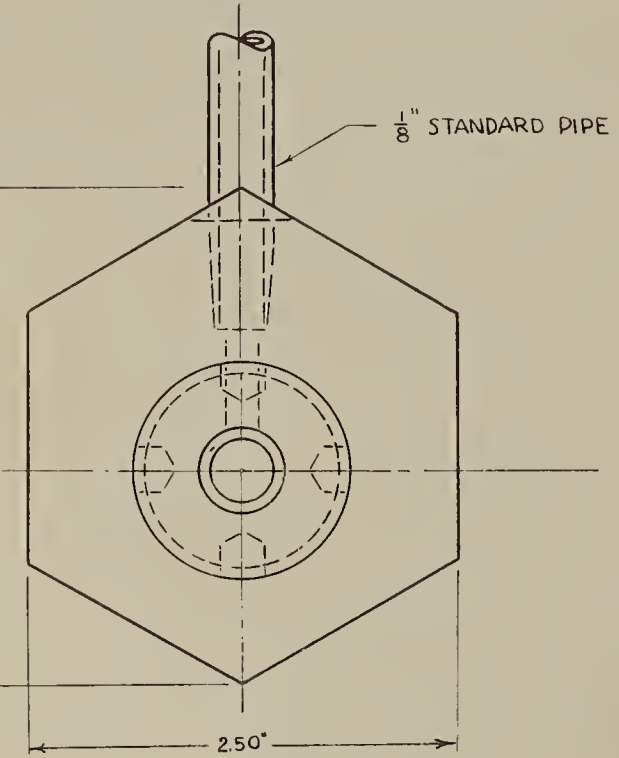
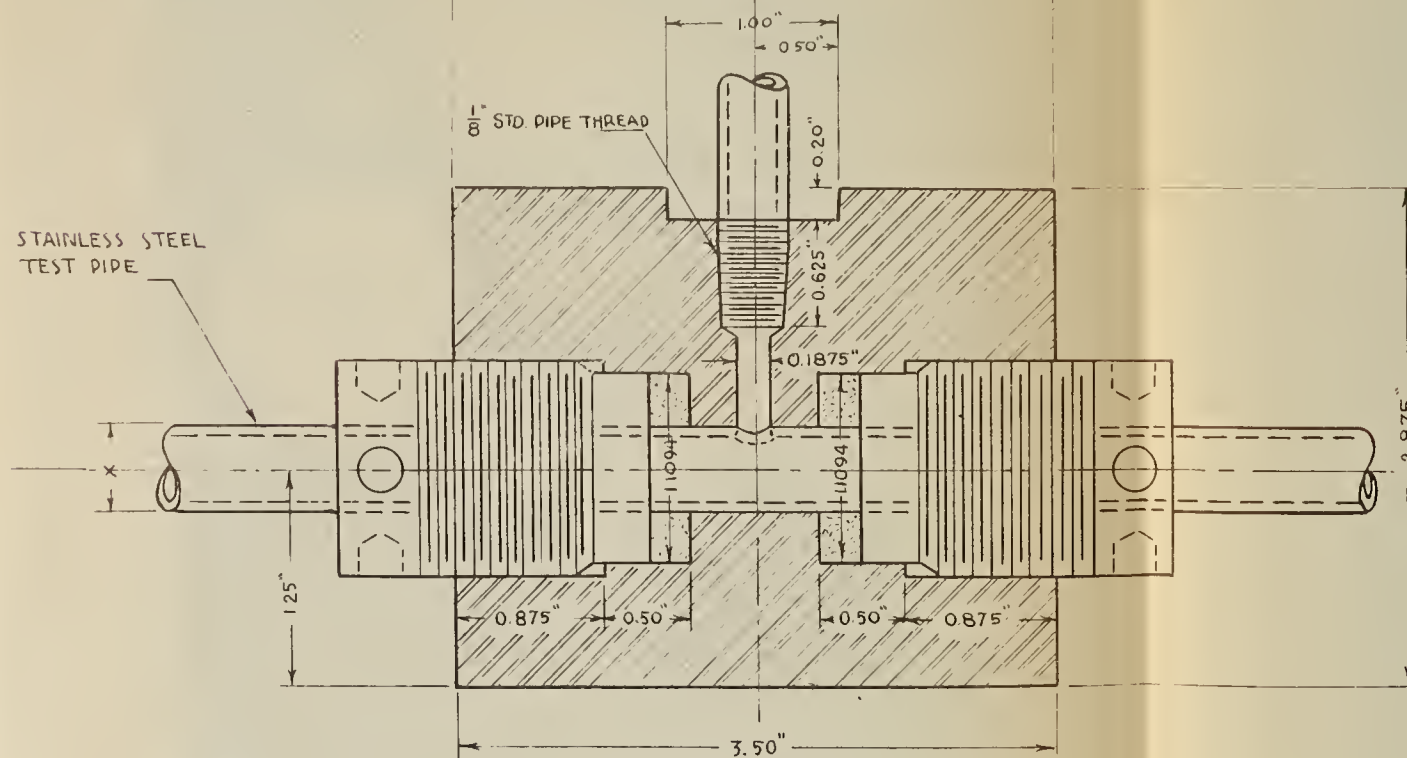
Figure 12. View of Crude Oil Measuring Tanks, Freon Storage Tanks and Instrument Panel





TOP VIEW

TYPICAL PACKING GLAND



SECTION A-A

PLAN VIEW

X = 0.375"
X = 0.500"
X = 0.625"

FIG. 13 TYPICAL PRESSURE
TAP ASSEMBLY

SCALE - FULL SIZE

UNIVERSITY OF ALBERTA
DEPT. OF CHEMICAL AND PETROLEUM ENGINEERING
APRIL 29, 1953 by A. Masuda



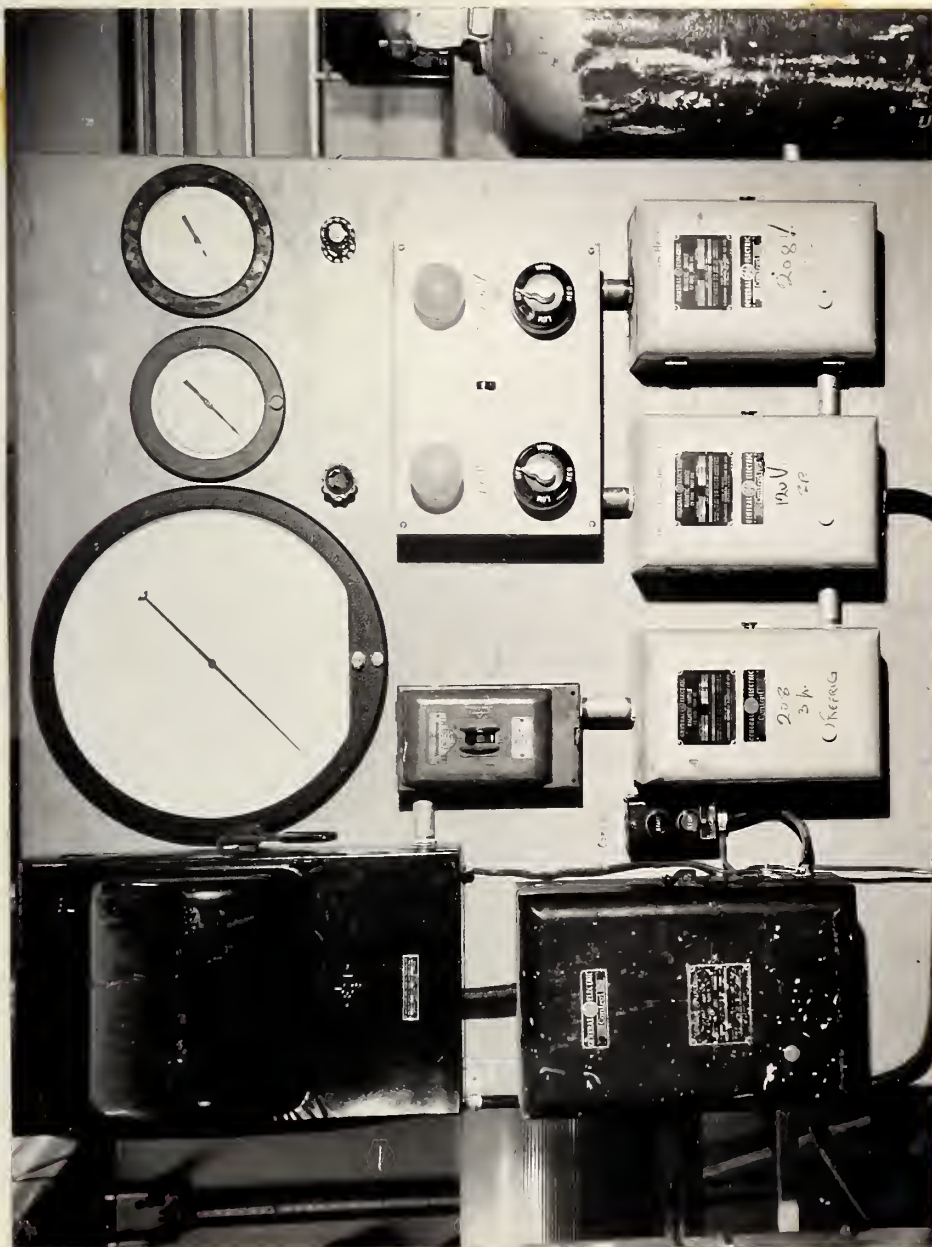


Figure 14. Instrument Panel for Pilot Pipeline



OPERATION OF THE PILOT PIPELINE

The pilot pipeline was drained of all oil used in previous tests before it was charged with new crude oil. Draining was followed by two successive flushes. In the first flush, 15 gal. of clean stove oil was circulated through the system at high velocities in order to loosen and remove any wax which may have been deposited on the walls of the test lines. This was followed by a flushing with 15 gal. of the new crude oil to be tested.

In preparation for testing, approximately 60 gals. of the crude to be tested were charged in the storage tanks. The crude oil was then circulated through the entire unit for at least one-half hour to mix any residual oil from the flushing with the charged crude. Since crude oil density data were necessary for computations, a sample of the crude in the unit was taken and densities in the temperature range of 20 to 75°F. were determined by a chain gravitometer.

The pilot pipeline, when not in use, was kept refrigerated in order to minimize loss of Freon-12 in the bath through small leaks in the shell. For the preliminary operations of flushing, charging and circulating, the refrigeration unit was cut out to enable the system to attain equilibrium at approximately 70°F.

For the first test on the new crude, the storage tank (Figure 2) was charged with the bulk of the crude oil and the by-pass valves adjusted to pressure drops which gave the desired rates of flow. Circulation of oil was maintained until an oil temperature of 75°F.



was indicated. At this temperature, the oil circulation was stopped momentarily and the tank valves adjusted for the measurement of test oil in the receiver tank. The time required to collect a pre-determined volume of crude oil was recorded. While collecting this volume of oil, upstream and downstream pressures, upstream and downstream temperatures, temperatures of storage oil, oil at the pump discharge and the final temperature of the crude in the receiver were recorded. About three readings of each of the aforementioned variables were taken during any single test to obtain average temperatures and pressures. After the test, the measured crude was transferred back into the storage tank.

For the second test, the refrigeration unit was put into operation and the oil circulated in the unit until the oil was cooled to 70°F. At 70°F., the procedure of the first test was repeated. Successive tests were made at each 5°F. drop in temperature to a low of about 20°F.

For test temperatures down to 35 or 40°F., the oil was by-passed after precooling, this resulted in cooling of the storage oil to about 40°F. It was found that 35°F. was near the minimum attainable test temperature with this arrangement, even at very low rates of flow.

In acquiring data at lower temperatures, the oil was by-passed before precooling. The resulting low rates of flow in the precool lines made possible minimum temperatures that were from 15 to 20°F. lower than by the other arrangement.



RESULTS

Pilot pipeline tests were run on the following samples:

1. Redwater crude, sample no. 1.
2. Redwater crude, sample no. 2.
3. Stettler D2-D3 blend.
4. Duhamel - Malmo - New Norway blend.
5. Leduc Woodbend blend.
6. Nisku blend.

Information on the source of samples, date received, A.P.I. gravity, and experimental tests on the crude oils is listed in Table IIB of Appendix B. In Table IIIB, the experimental density data for all crude oil samples in the temperature range 20 to 75°F. is recorded. This data is presented in Figure 15 as a plot of density vs. temperature of the crude oil.

The basic experimental data in Appendix B were obtained from pilot pipeline tests. The variables measured were:

1. temperature of storage tank oil
2. temperature of oil at pump outlet
3. temperature of receiver tank oil
4. temperature of Freon-12 bath
5. temperature of oil at test inlet
6. temperature of oil at test outlet
7. upstream pressure



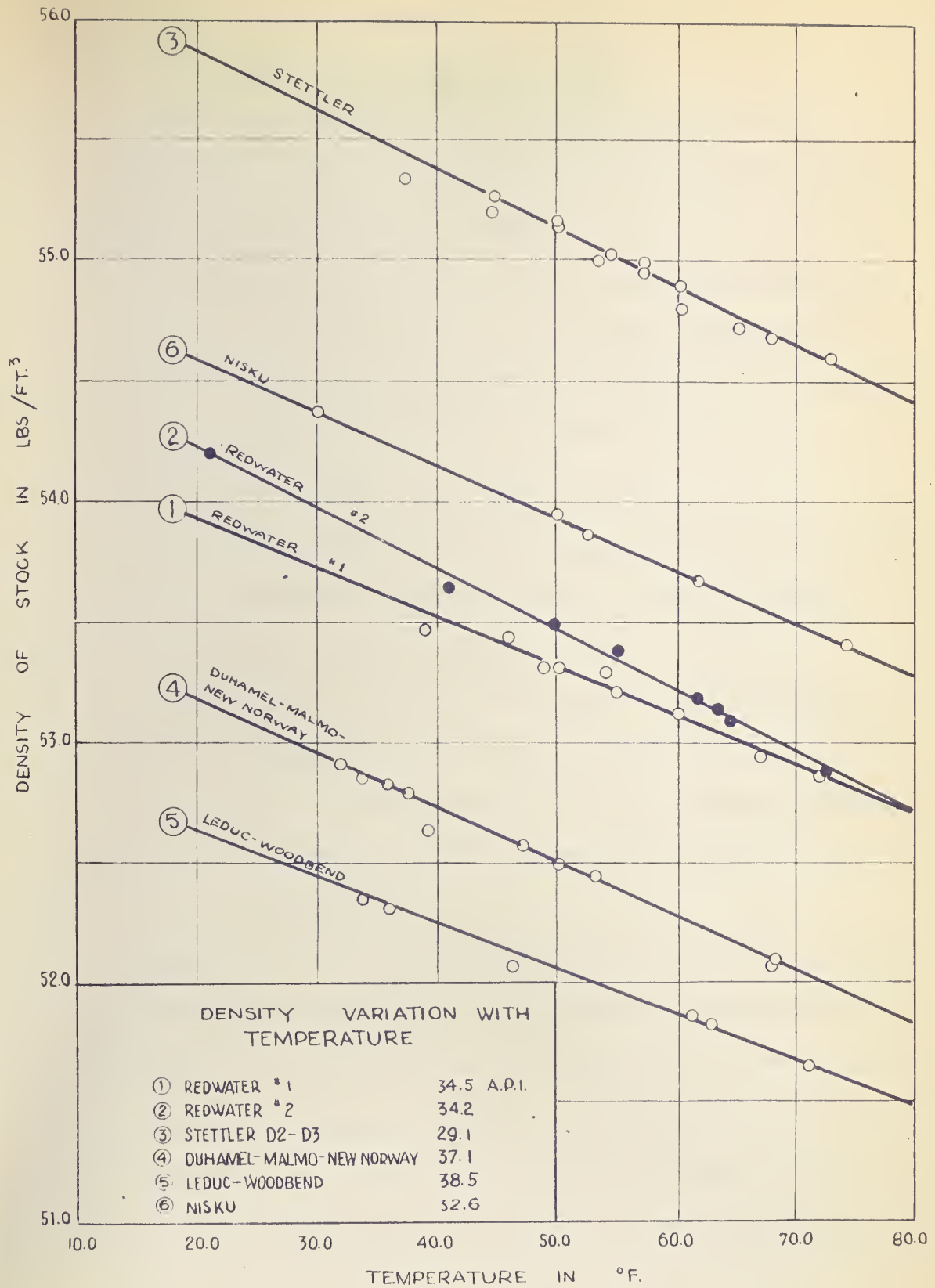


FIG. 15



8. downstream pressure
9. volume of oil collected in test
10. time for collection of measured volume of oil.

Tables IV-B to IX-B show the tabulation of the pilot pipeline data with the following modifications:

- (a) Temperature of oil at test inlet and temperature of oil at test outlet was recorded as average test temperature. The average temperature was computed by using equation (6-a) of Appendix A.

$$\text{i.e. } T_{av} = T_{out} - \frac{22.0}{59.2} (T_{out} - T_{in})$$

- (b) The pressure difference between upstream pressure and downstream pressure rather than the two pressure readings was recorded.
- (c) Instead of volume collected and time of collection, the flow rate in cubic feet per minute was reported. These flow rates were corrected to flowing temperature as shown by sample calculations in Section 1 of Appendix A.

Appendix C presents the detailed results of computations for the experimental data, Appendix B. Table I-C gives a concise summary of formulae used in computations of pipeline data. These equations are derived in Section 2 of Appendix A and their use is shown in the sample computations of Section 3, Appendix A. Tables II-C to VII-C present the detailed results of computations for the crude oils tested



by pilot pipeline and the quantities listed are:

1. average temperature of crude oil in test
2. fluid density
3. fluid velocity
4. friction factor
5. Reynolds number
6. apparent viscosity
7. shear rate at wall
8. remarks

The fluid density was obtained from Figure 15 for the particular crude oil at the average temperature of test.

Fluid velocity is given by equation (8-a) of Appendix A as:

$$V = \frac{Q'}{2.03} \times 10^2 \text{ ft/sec. for the 0.249 inch line}$$

Velocities for the 0.311 and 0.386 inch lines were computed by:

$$V = \frac{Q'}{3.17} \times 10^2 \text{ ft/sec. for the 0.311 inch line}$$

and
$$V = \frac{Q'}{4.87} \times 10^2 \text{ ft/sec. for the 0.386 inch line}$$

The friction factors were computed for fluid flow through the 0.249 inch pipe by equation (9-a) of Appendix A:

$$f = \frac{988(\Delta P)'}{V^2 \rho}$$

Equivalent friction factor equations for the other lines are:

$$f = \frac{12,35(\Delta P)'}{V^2 \rho} \quad (0.311 \text{ inch line})$$



$$f = \frac{15.32 (\Delta P')}{V^2 \rho} \quad (0.386 \text{ inch line})$$

where $\Delta P'$ is the pressure drop in lbs/in.^2

Apparent Reynolds numbers were computed as shown in Section 3 of Appendix A from the equations:

$$(N_R)_a = \frac{64}{f} \quad \text{for laminar flow}$$

$$\text{and } (N_R)_a = \frac{(0.364)^{3.77}}{f} \quad \text{for turbulent flow.}$$

The following equations were used to calculate the apparent shear rate at the wall, $\left(\frac{dv}{dr}_a\right)$:

laminar flow	turbulent flow	
$18.92 Q' \times 10^3 \text{ sec}^{-1}$	$1.231 \frac{(\Delta P')}{\mu_a} \text{ sec}^{-1}$	(0.249 inch line)
$9.74 Q' \times 10^3 \text{ sec}^{-1}$	$1.541 \frac{(\Delta P')}{\mu_a} \text{ sec}^{-1}$	(0.311 inch line)
$5.10 Q' \times 10^3 \text{ sec}^{-1}$	$1.912 \frac{(\Delta P')}{\mu_a} \text{ sec}^{-1}$	(0.386 inch line)

where Q' is in ft^3/min

and $\Delta P'$ is in lb/in.^2

Apparent viscosities, μ_a , were calculated by the use of the following equations:

laminar flow	turbulent flow	
$3.21 \times 10^{-3} \frac{(\Delta P')}{V} \frac{\text{lb}}{\text{ft. sec.}}$	$0.0208 \frac{(VQ)}{(N_R)_a} \frac{\text{lb}}{\text{ft.-sec.}}$	(0.249 inch line)
$4.99 \times 10^{-3} \frac{(\Delta P')}{V} \frac{\text{lb}}{\text{ft. sec.}}$	$0.0259 \frac{(VQ)}{(N_R)_a} \frac{\text{lb}}{\text{ft. sec.}}$	(0.311 inch line)
$7.71 \times 10^{-3} \frac{(\Delta P')}{V} \frac{\text{lb}}{\text{ft. sec.}}$	$0.0322 \frac{(VQ)}{(N_R)_a} \frac{\text{lb}}{\text{ft. sec.}}$	(0.386 inch line)



The turbulent or laminar flow of fluid was noted under the column "Remarks". Where uncertainty of flow was present, computations were made for both laminar and turbulent flow and entered in the tables.

Table VIII-C shows a comparison of the apparent viscosities obtained for Redwater samples no. 1 and no. 2 from the smoothed plots of Figures 17, 18, and 19. For sample no. 1, apparent viscosities in the range 20 to 80°F. are shown for the 0.249 inch line, the 0.386 inch line and the average of the two lines. The deviation of each from the average curve is given as a percentage. The apparent viscosity of Redwater sample no. 2 is also compared against the average apparent viscosities of sample no. 1, and the percent deviation listed in the last column.

Table IX-C presents smoothed apparent viscosity temperature correlation for all the oils tested. These values were obtained from Figures 17, 18, 19, 20, 21, 22 and 23.

Table X-C shows the conversion of apparent viscosity to kinematic and Saybolt Universal viscosities. Sample computations used in these conversions are given in Section 4 of Appendix A. Equations for the conversion of apparent viscosities are:

$$\text{Equation (18-a) of Appendix A : } k = \frac{\mu}{\rho}$$

$$\text{Equation (21-a) of Appendix A : } \mu_a = 6.72 \rho (0.0022\theta) - \frac{1.8}{\theta}$$

where k = kinematic viscosity in ft^2/sec .

θ = Saybolt universal seconds.



Appendix D shows the refrigeration studies conducted on the pilot pipeline and the context of the Appendix is:

1. a brief introduction of the purpose of this investigation
2. experimental data for refrigeration studies (Table I-D)
3. detailed outline of computations
4. presentation of results (Table II-D)
5. discussion of results.



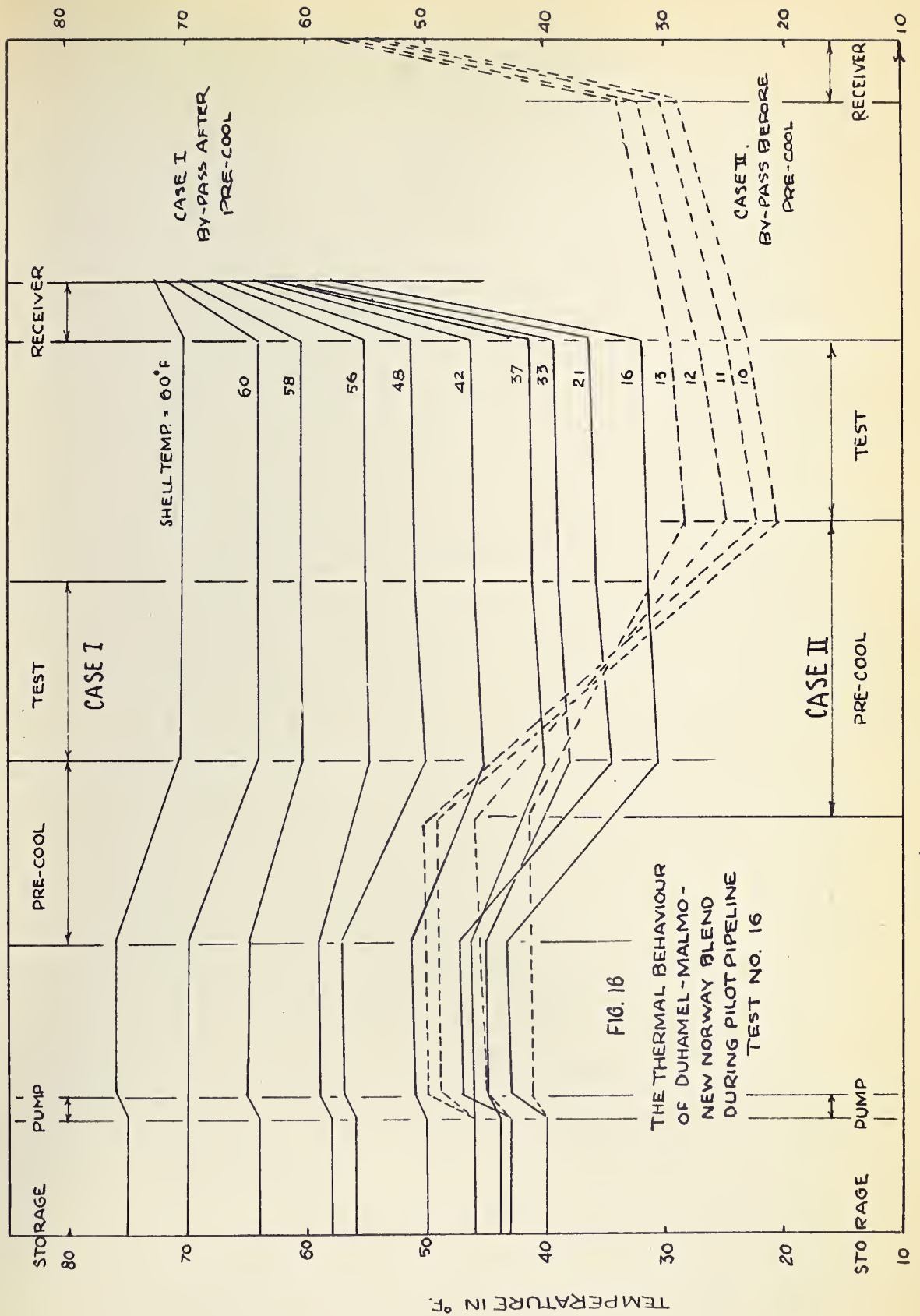
DISCUSSION OF RESULTS

A. Thermal Behaviour of Crude Oil in Test

Tests conducted on the pilot pipeline show that crude oil is subject to distinct temperature variations, depending on the particular flow circulation selected for testing. Test no. 16 on the Duhamel-Malmö-New Norway blend was selected to illustrate the temperature variations encountered during a series of tests, since a wide variation of test temperatures was obtained. The thermal behaviour of Duhamel-Malmö-New Norway blend in test no. 16 is shown in Figure 16.

For case I, where all the oil pumped, was sent through precool and then by-passed before test, the storage temperature decreased in a regular fashion for each successive run. The temperature difference in the crude oil between precool inlet and precool outlet was not very large and was usually less than 10°F. In the typical case, the crude oil was found to increase in temperature from two to three degrees in travelling through the pump, decreased to inlet test temperature through the precool, increased in the test line from a fraction of a degree to a maximum of about two degrees. The tested crude was then blended with residual crude of higher temperature in the measuring tank. The solid lines plotted on Figure 16 show the pattern obtained by using the by-pass after precooling. The lowest







test temperatures obtained by this method was about 30°F.

Where oil was by-passed before precooling (Case II), similar temperature patterns were obtained from storage tank to pump and from test inlet to measuring tank. Dissimilar thermal behaviour was due to much lower rates of flow in the precool lines as compared to rates of flow in Case I. The low rates of flow caused slightly higher temperatures in flow lines leading to the precool (a direct result of constant re-circulation, without cooling, of the bulk of the pump inlet stream to storage tank), but in the precool lines, the cooling obtained was much greater than in the previous case. Runs illustrating thermal behaviour under these conditions, are shown by the dash lines in Figure 16. Test temperatures as low as 20°F. were obtained by this method.

B. Apparent Viscosity Characteristics of Crude Oils Tested

The overall results of the experimental tests on the crude oils by the pilot pipeline may be summarized as follows:

- (a) Tests conducted on the pilot pipeline on crude oils were characterized by high apparent shear rates at the wall. Shear rates varied over a wide range, 100 to 100,000 sec^{-1} .
- (b) Apparent Reynolds numbers ranged from 61 to 26,000.
- (c) Apparent viscosity values varied only with temperature, regardless of:

- i wide variation in apparent shear rates



- ii difference in pipe diameter
- iii pattern of flow, laminar or turbulent
- iv variation of thermal history

Thus apparent viscosity values obtained by the use of the pilot pipeline indicate that the crude oil samples are Newtonian in the shear rates range studied, or that limiting values of viscosity at infinite shear for a pseudoplastic material have been obtained.

The above results show that viscosity-temperature relationships for crude oils with similar viscosity characteristics can be obtained by the pilot pipeline from a single run using one test pipe and one pattern of flow. Thermal effects were considered negligible.

The result of the experimental tests is discussed for each crude oil sample tested.

(1) Redwater Sample No. 1

The experimental data obtained for Redwater crude sample no. 1 are listed in Table IV-B. Tests 1, 2, 3, 4, 5 and 6 were tests conducted on the 0.249 inch internal diameter line, while tests 7, 8 and 9 were tests on the 0.386 inch internal diameter line. Calculated apparent viscosity temperature relationships of Table IV-B are plotted in Figure 17 for the 0.249 inch diameter line and on Figure 18 for the tests on the 0.386 inch diameter line.

Tests on the 0.249 inch line were run for pressure drop ranges of 12 psi., 22 psi., 51 psi., 58 psi., 70 psi., 97 psi., 180 psi. and 303 psi. The Reynolds number variation in this



range was from 12,950 to 96 while apparent shear rates at the wall varied from 746 to 100,000 sec.^{-1} . Turbulent flow data could not be obtained below 47°F. because of inadequate refrigeration capacity. Laminar data could not be obtained in the higher temperature ranges (70 to 80°F.) since the corresponding pressure drops were too low.

The solid curve (Figure 17) can be divided into three regions. The first region from 80 to 67°F., where reliable values were obtained for turbulent flow conditions, 67 to 47°F. where apparent viscosity data was obtained for both laminar and turbulent flow and in the region 47°F. or lower, where laminar flow conditions prevailed.

The dash lines indicate apparent viscosities computed for conditions of transitional or uncertain flow. Two sets of values were computed for transitional flow, one set assuming laminar flow, the other, turbulent flow. Similar curves were obtained for each set of transition data and as either laminar or turbulent flow became more definitely established, the dash curves approached the solid line defined by data taken under definitely laminar or turbulent conditions of flow.

The computed data plotted on arithmetic paper gave a curve that was nearly linear with temperature in the range 80 to 64°F.



Below 64°F. apparent viscosity increased rapidly with decrease in temperature. The computed points, for established patterns, also gave only one curve and the majority of data lay within experimental error of this curve. The single line relationship found between temperature and apparent viscosity indicate a Newtonian material, but due to the extreme apparent shear rates at the wall, pseudoplasticity cannot be discounted. The values obtained by the pilot pipeline may represent viscosity at infinite shear, hence the single curve relation between temperature and apparent viscosity.

The region of transition from near linear relationship between apparent viscosity and temperature to the steeply curved relationship was very indefinite. If this region of change of curvature represents the beginning of wax crystallization, waxing can be assumed to begin in the range 60 to 65°F.

The computed data of tests in the 0.386 inch line are shown in Figure 18. The apparent shear rate varied in these tests from 1470 to 10,300 sec.⁻¹. Again, the data defined a single curve indicating Newtonian behaviour within the experimental shear range.

Comparison of tests on the 0.386 and 0.249 inch lines show almost identical curves for both pipes. Near linear relationship of temperature-apparent viscosity for the 0.386 inch pipe prevails to about 63°F. In the temperature range 80 to 35°F., the deviation of the curve for the 0.386 inch line is less than 3 percent of the



curve for the 0.249 inch line. This deviation increased at lower temperatures to about 6% at 25°F. Thus, within experimental error, values can be assumed identical and pipe size disregarded as a variable affecting the value of apparent viscosity.

The temperature data taken during the runs show a wide variation in the storage tank temperatures of the crude oil under test. No effect of this variation was observed in the values of apparent viscosity. Thus thermal history effects upon the apparent viscosity of the crude seem negligible for the operating conditions of the pilot pipeline.

(2) Redwater Sample No. 2

Redwater sample no. 2 had a lower A.P.I. gravity than sample no. 1, 34.2 as compared to 34.5. Experimental data were taken on the 0.249 inch line and are tabulated in Table V-B of Appendix B. Computed results are given in Table III-C of Appendix C. A plot of the data is shown in Figure 19. The data compared favorably with those of the first Redwater sample and from 80 to 45°F., the apparent viscosities were within 5 percent of the average of the first tests taken on the 0.249 and 0.386 inch lines, (refer to Table VIII-C). At temperatures below 45°F, the deviation increases to a maximum of about 20 percent at 20°F. Behaviour of the crude indicates wax precipitation below a temperature of approximately 66°F. A comparison of the two samples is shown in Figure 24. Although slightly higher apparent viscosity values could be



expected for sample no. 2 from the specific gravity observations, this crude shows lower viscosity values in the region 30 to 55°F. No attempt was made to explain this phenomenon. Shear rates varied from 1,630 to 28,800 sec^{-1} .

(3) Stettler D2-D3 Blend

Experimental data (Table VI-B) was taken on the 0.249 inch line under conditions of laminar flow over the temperature range of 20 to 80°F. The results (Table IV-C) have been plotted as shown in Figure 20. Shear rates encountered, ranged from 6,640 to 1,260 sec^{-1} .

This was the heaviest of the crudes tested (29.1 A.P.I) and as shown on Figure 24, gave higher apparent viscosity values than any other crude oil tested. Experimental results gave a well defined curve. Near linear apparent viscosity-temperature relationship was found to about 59°F. Below 59°F the apparent viscosity of the Stettler D2-D3 blend increased rapidly with decrease in temperature.

(4) Duhamel-Malmö-New Norway Blend

The A.P.I. gravity of this stock was 37.1. Table VII-B and Table V-C show the experimental and computed data respectively. Reynolds numbers encountered (242-25,100), show that data were taken under both laminar and turbulent conditions of flow. Range of shear rates was from 1,060 to 158,000 sec^{-1} . The apparent



viscosity-temperature relationship obtained is shown in Figure 21. Near linear relationship between viscosity and temperature exists to about 58°F . Apparent viscosity ranges from 0.00224 at 80°F . to 0.01535 lb. per ft.-sec. at 20°F .

(5) Leduc-Woodbend Blend

Tables of experimental and computed data for 38.5 A.P.I. Leduc-Woodbend stock are Table VIII-B and Table VI-C, respectively. Figure 22 shows the plot of computed data. Waxing seems to have started near 50°F . Range of shear rates during these tests were 1,080 to 192,000 sec.^{-1} . Laminar and turbulent conditions of flow were used to obtain data. The apparent viscosity-temperature curve for this stock was similar to that of Duhamel-Malmo-New Norway stock except at the lower temperatures (Figure 24), where the effect of temperature on the apparent viscosity of the Leduc-Woodbend blend was much less than for the Duhamel-Malmo-New Norway blend.

(6) Nisku Blend

Experimental data for the 32.6 A.P.I. Nisku blend is given in Table IX-B and computed data in Table VII-C.

Most of the data were taken under conditions of laminar flow. Plotted data (Figure 23) shows that wax precipitation may have started at about 58°F . Below 58°F apparent viscosity increased very rapidly with decrease in temperature. Range of shear rate



encountered in laminar flow was 825 to 4,950 sec.^{-1} . The only turbulent flow data obtained was at a Reynolds number of 7,420 and a shear rate at the wall of 50,800 sec.^{-1} . Apparent viscosity values ranged from 0.0044 lb. per ft.-sec. at 80°F. to 0.0430 lb. per ft.-sec. at 20°F.

C. Generalized Effect of Crude Oil Gravity on
Apparent Viscosity.

Figure 27 shows a generalization relating the A.P.I. gravity at 60°F. to the apparent viscosity and the temperature of the crude oil. The curves show a family of lines and correlation is good to 35°F. At temperatures lower than 35°F. considerable deviation takes place. A plot of this nature can be used to approximate the viscosity-temperature relationship in pipeline computations for crude oils in the absence of actual test data. Such a plot, however, should be used only for similar base crudes and crudes suspected of anomalous behaviour should be tested.



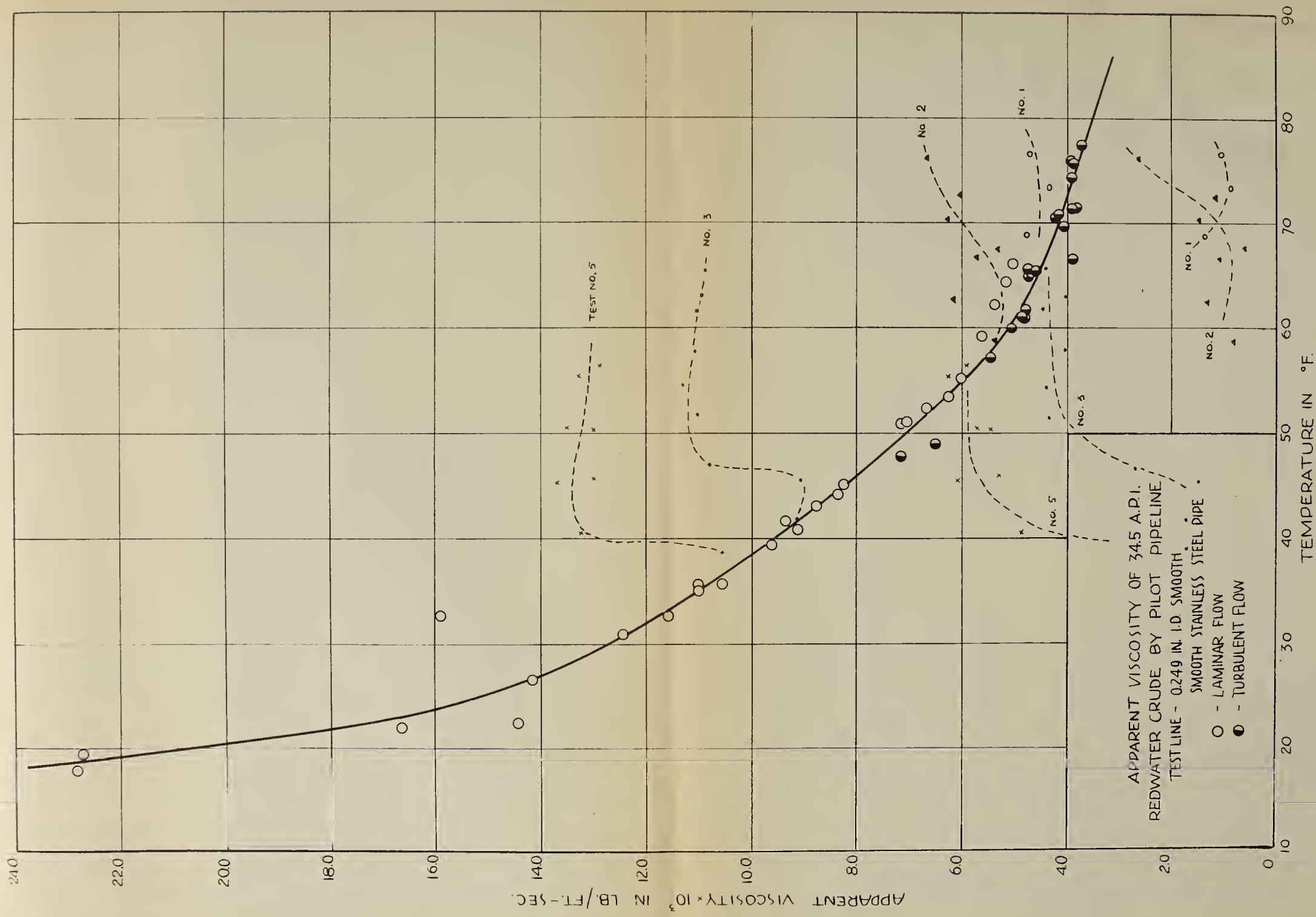


FIG. 17



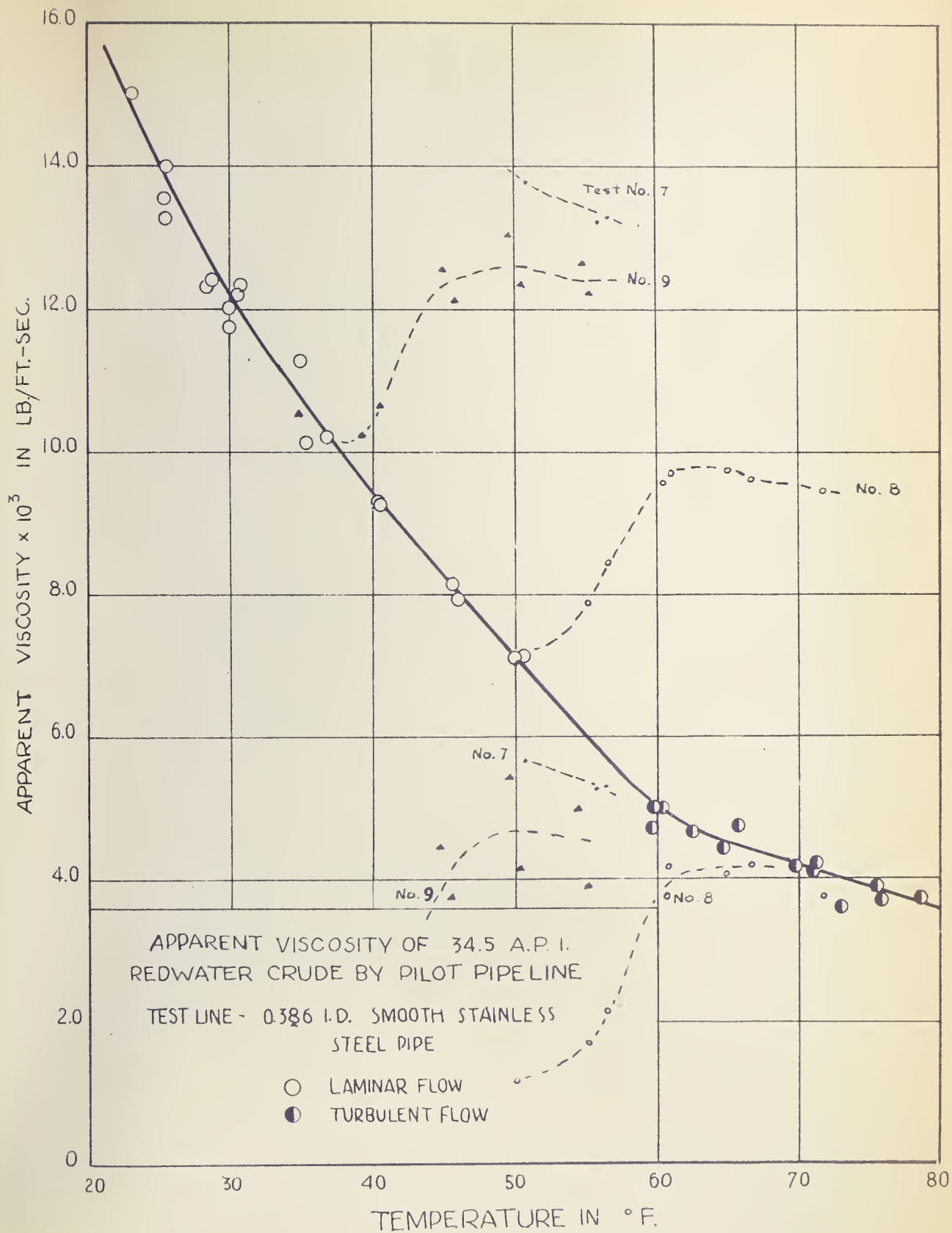


FIG. 18



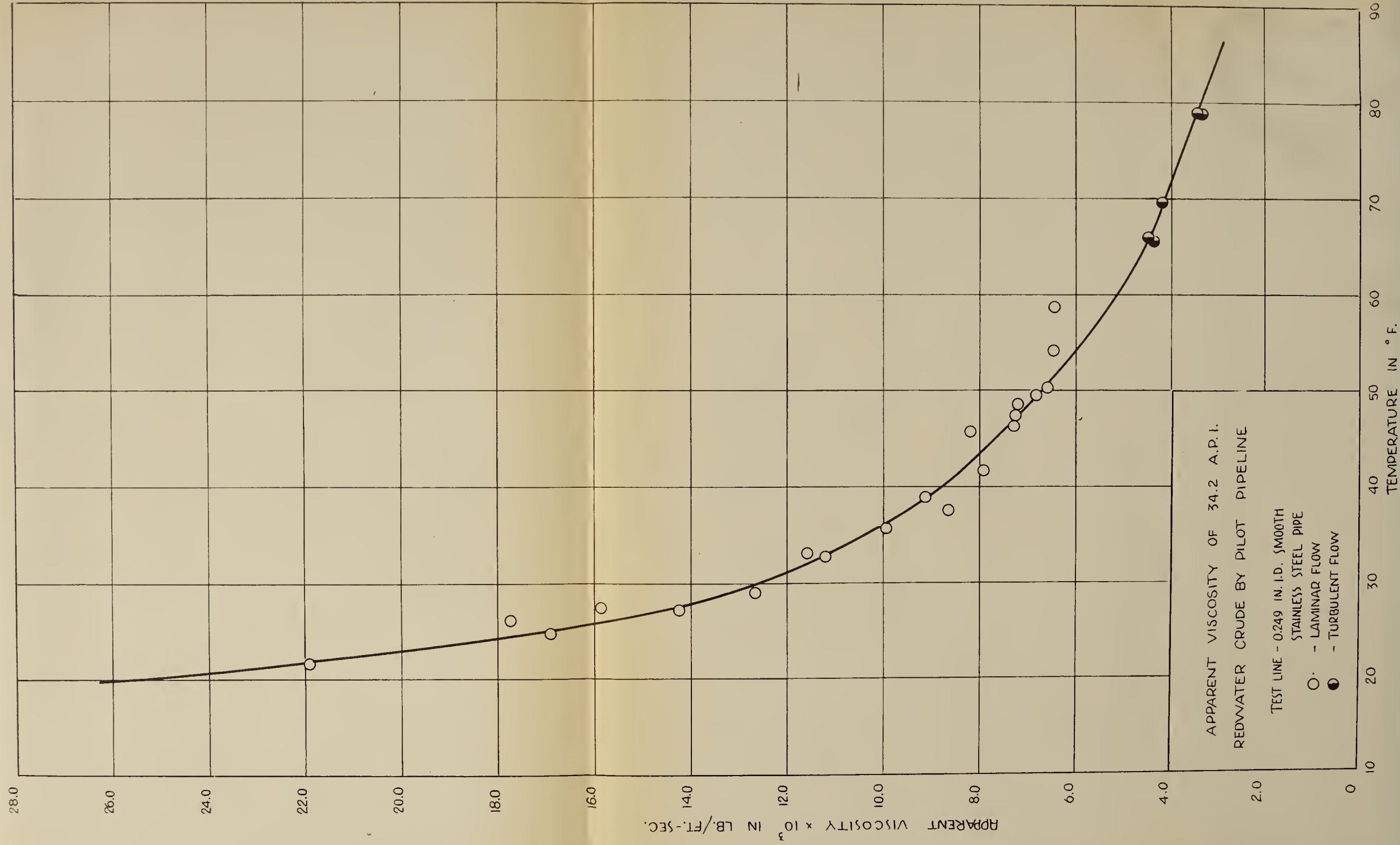


FIG. 19



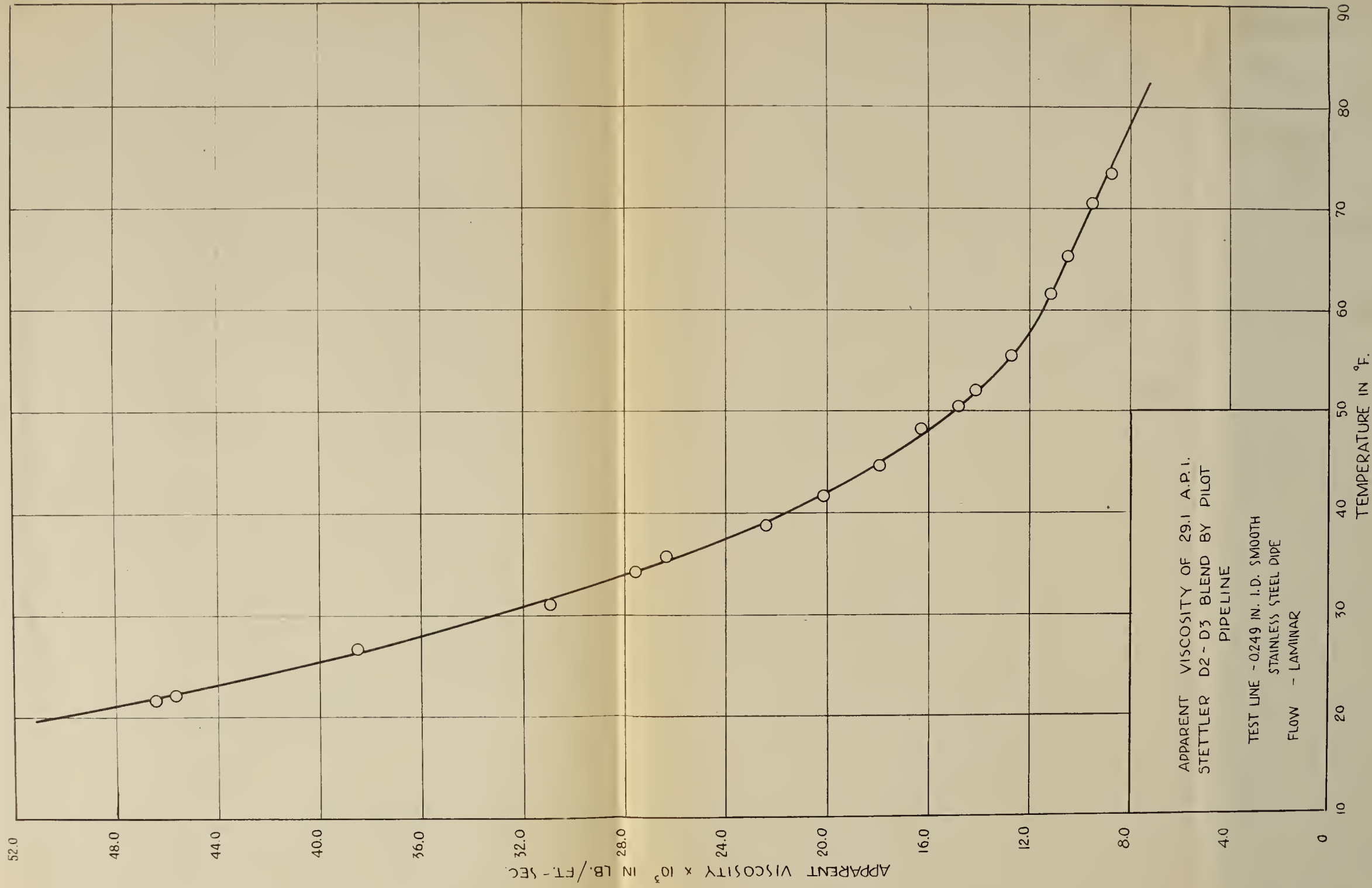


FIG. 20

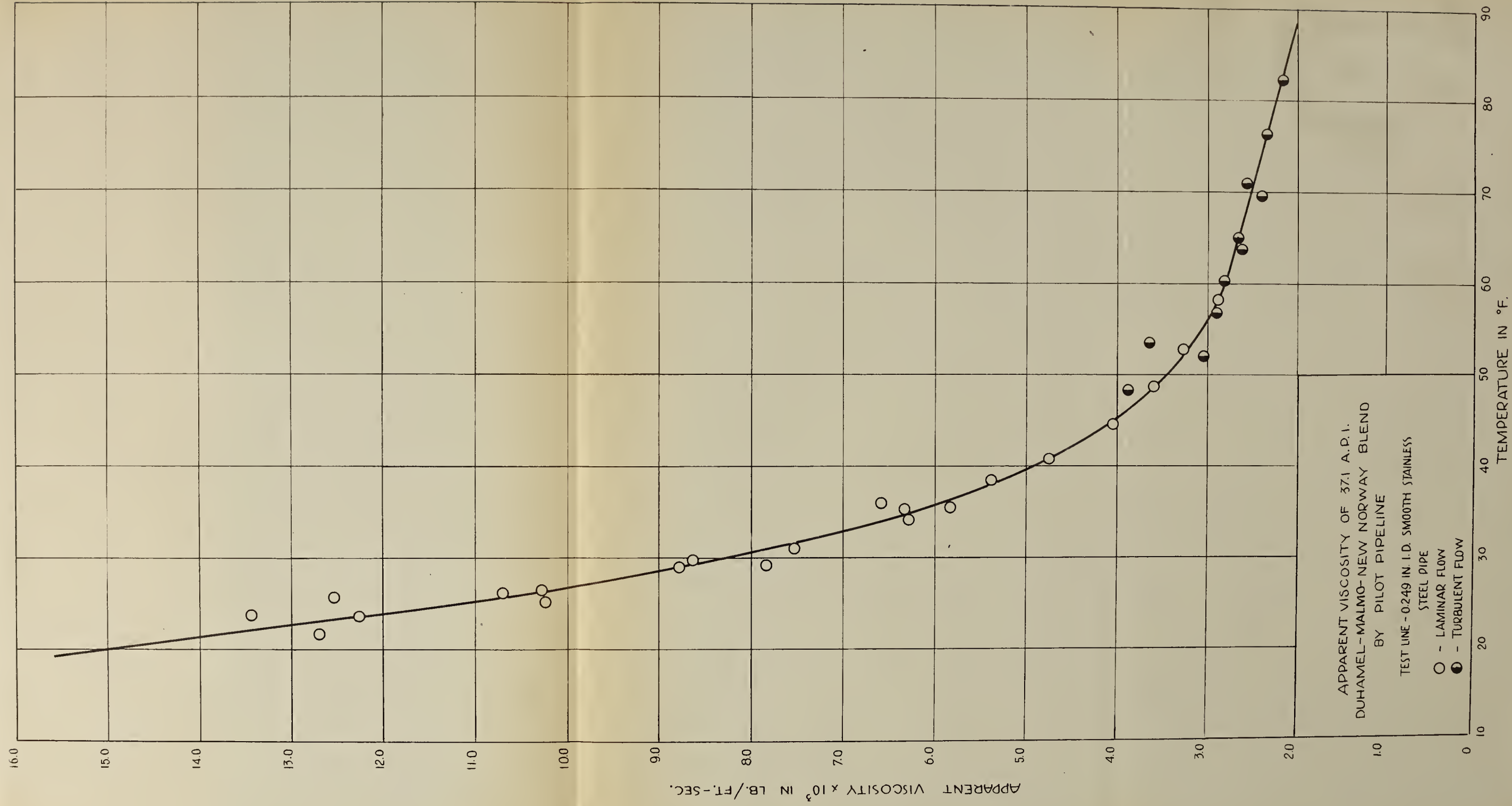


FIG. 21



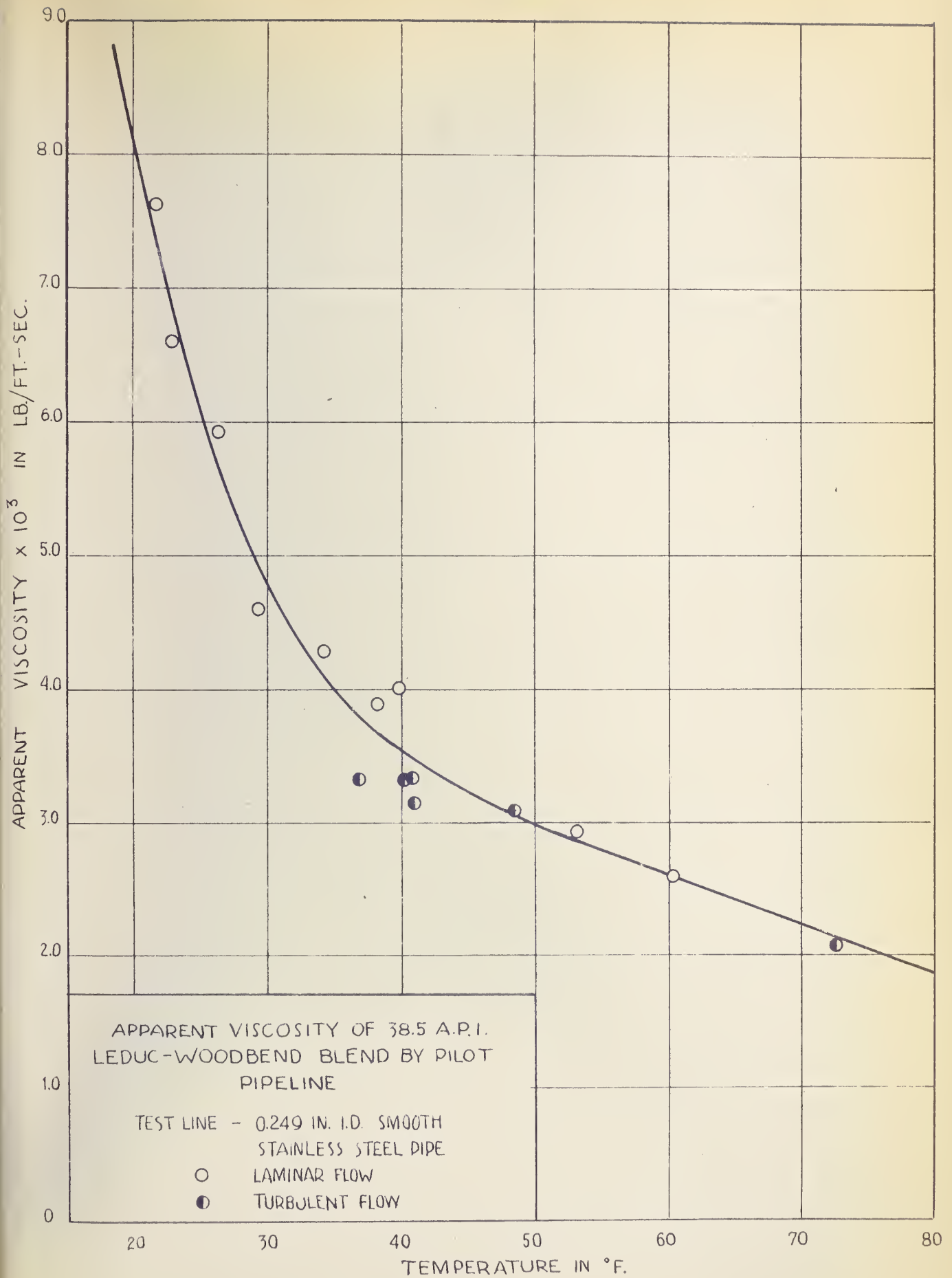


FIG. 22



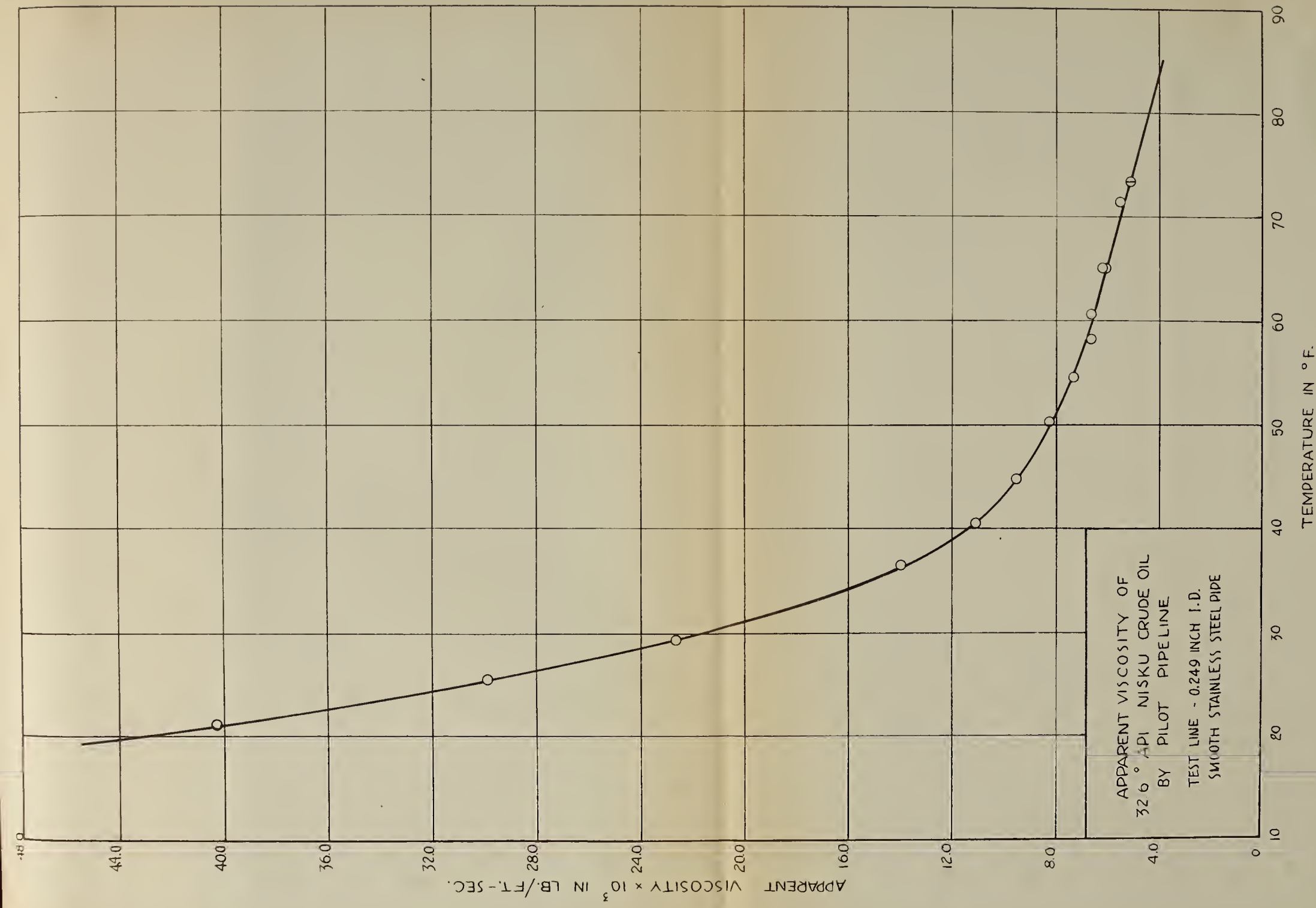


FIG. 23

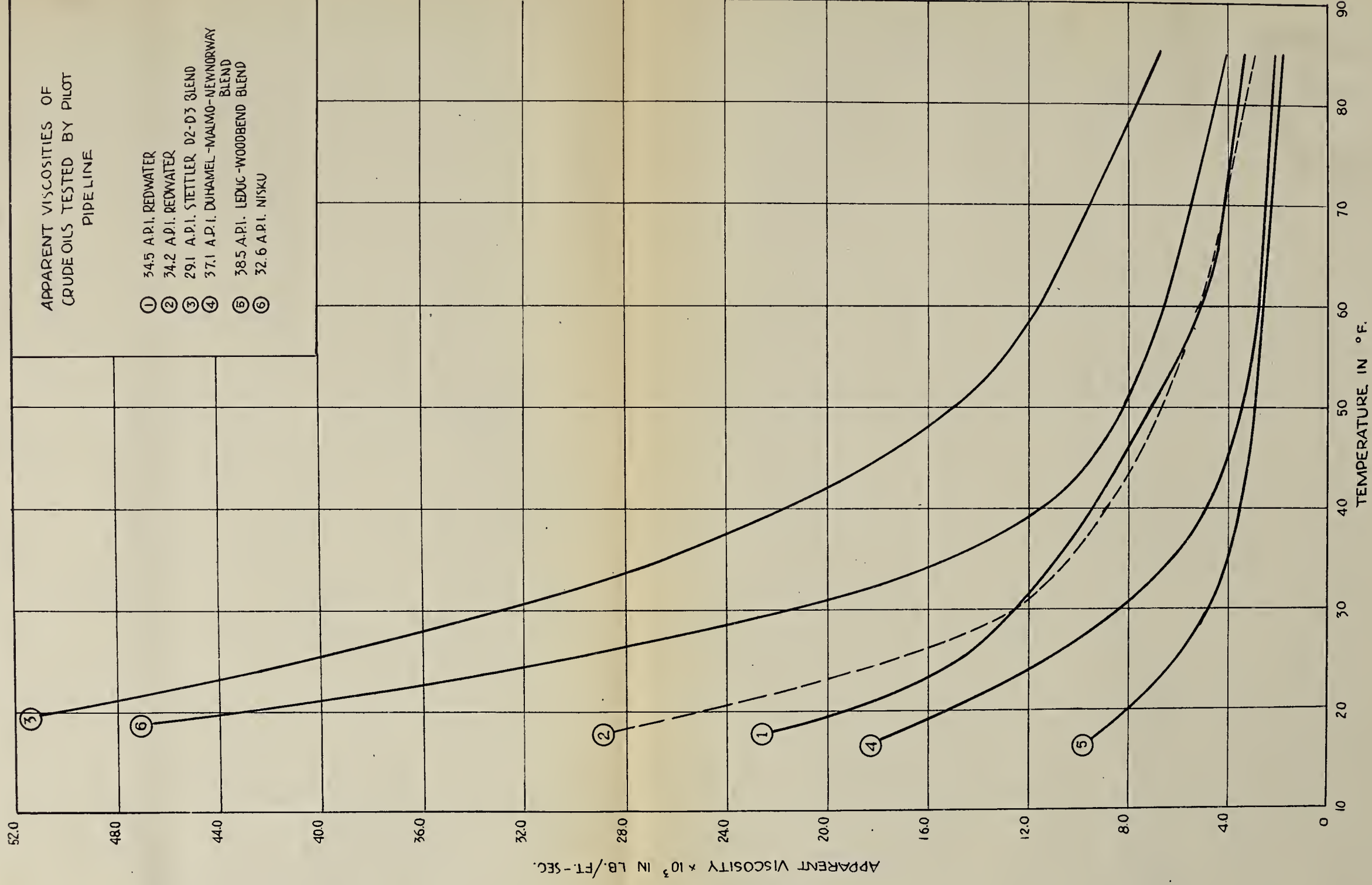


FIG. 24

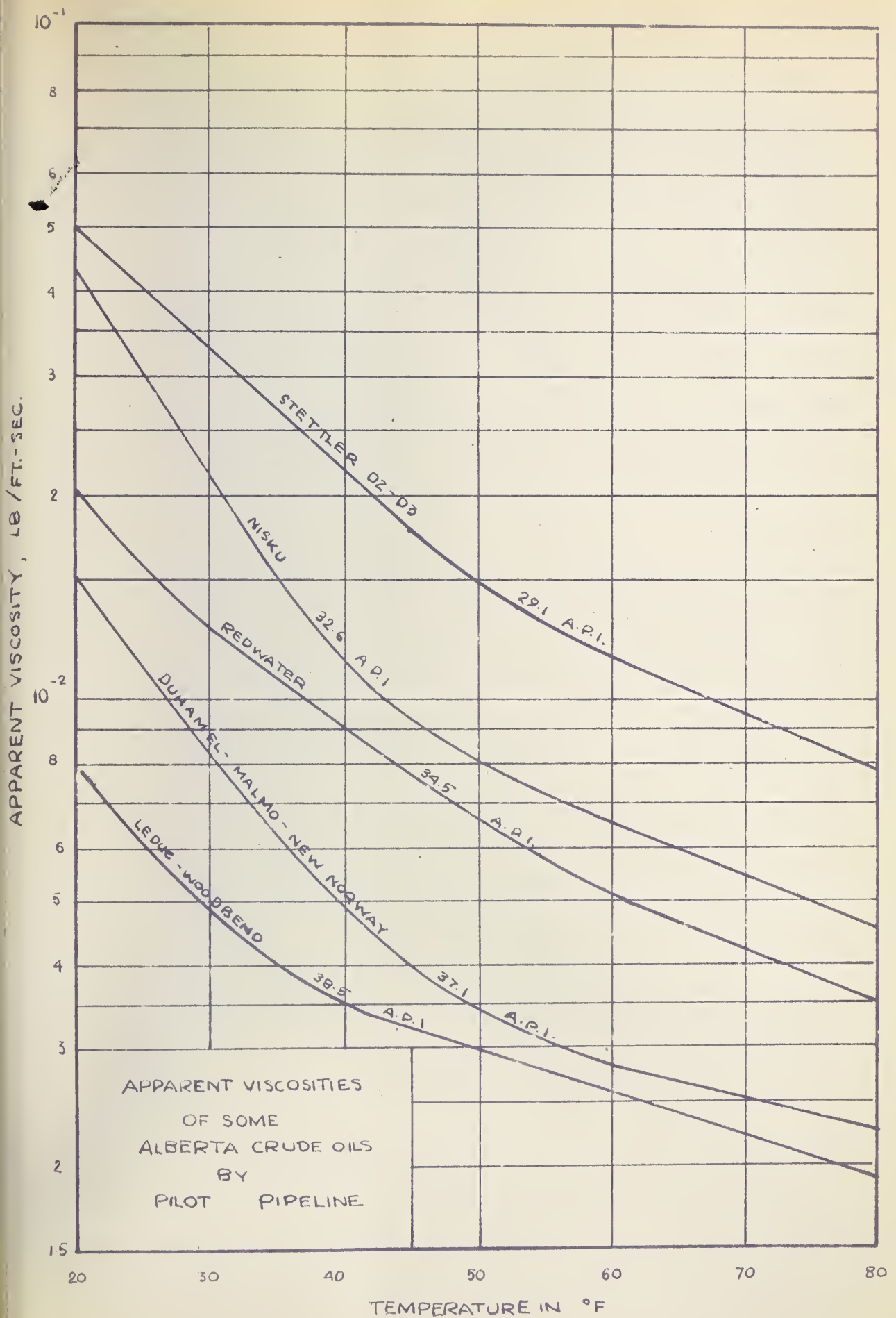


FIG. 25

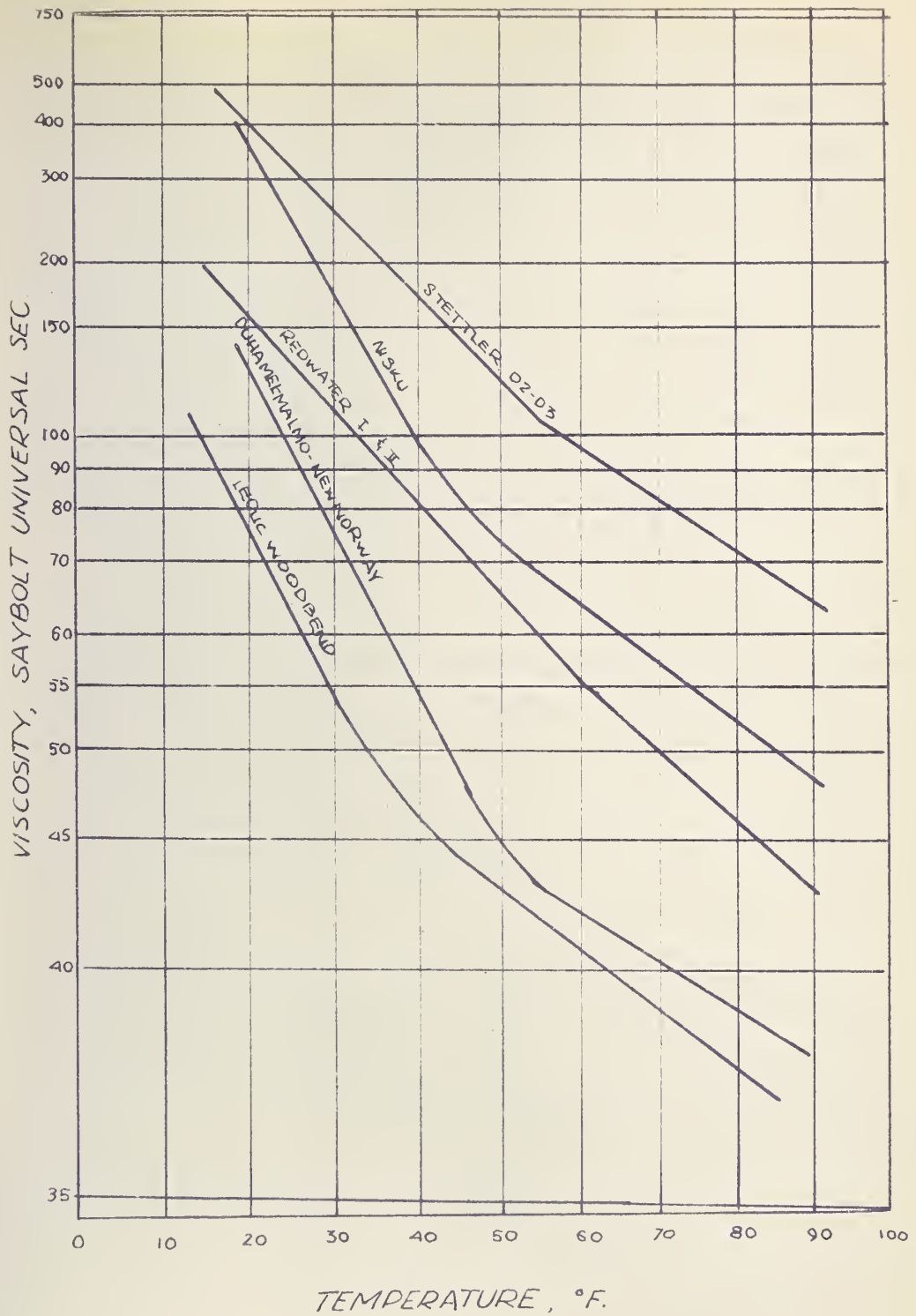


FIG. 26 Saybolt Universal Viscosities Computed from Apparent Viscosities of Pilot Pipeline Results.

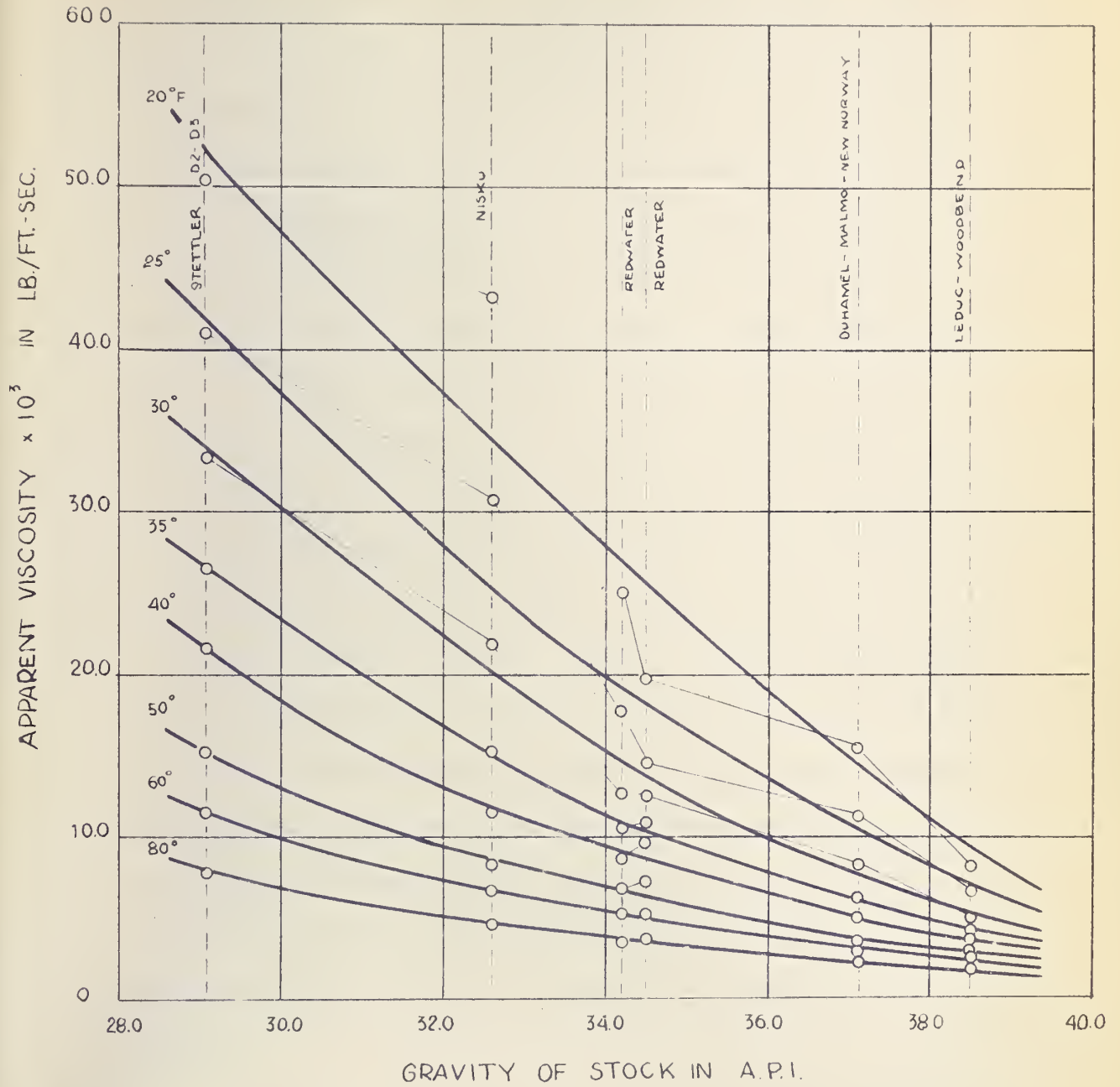


FIG. 27

GENERALIZED EFFECT OF CRUDE OIL
GRAVITY ON APPARENT VISCOSITY

CONCLUSION

The results of tests on the crude oils by means of the pilot pipeline gave a single apparent viscosity-temperature relationship for each crude oil. Factors such as pattern of flow, pipe diameter, rate of shear and thermal history were found to have negligible effect on the apparent viscosity. The crude oils tested indicated Newtonian behaviour within the apparent rate of shear range studied. These observations seem to contradict the findings of Sidjak (17) and Bauer and Ruston (5), however, the results of these previous investigators were taken from small laboratory viscosimeters in which shear rate values were very small. Maximum shear rates reported were 15 reciprocal seconds by Sidjak and 40 reciprocal seconds by Bauer and Ruston. Apparent shear rates at the pipe wall for the pipeline viscometer were usually of the order of thousands of reciprocal seconds. Hence possible pseudoplastic nature of the crude oil cannot be disregarded. Since rate of shear and pipe diameter had no effect on the apparent viscosity, values obtained could be limiting viscosity values at infinite shear for a pseudoplastic material.

The change in slope of the viscosity-temperature curve from the near linear relationship found at higher temperatures may indicate the beginnings of wax precipitation. Such zones

of change in slope of the viscosity-temperature curve were in the range 58 to 67⁰ F. for most crudes.

At the request of Interprovincial Pipe Line Co. Ltd. the pilot pipeline was constructed to duplicate the Reynolds numbers encountered in actual crude oil pipelines. Reynolds numbers in the pilot unit ranged from 61 to 26,000 and apparent rates of shear at the pipe wall ranged from 746 to 192,000 reciprocal seconds. In duplicating the high Reynolds numbers, extreme rates of shear have been introduced and for a pseudoplastic material, the majority or all viscosity data obtained from the pilot pipeline would be comparable to viscosity values at infinite shear.

Although turbulent flow at the higher Reynolds numbers could be obtained, the refrigeration was found to be inadequate in cooling the oil at the higher flow rates. As a result, a large portion of the experimental data was taken under laminar flow conditions.

In the discussion of refrigeration studies in Appendix D, it is shown that the capacity of the present refrigeration unit will not permit low temperature-high flow rate pilot pipeline studies. The need for further insulation at the flanges is pointed out. Before further research is continued, the inadequacies of the refrigeration unit should be corrected.

BIBLIOGRAPHY

- (1) Alves, G. E., Chem. Eng., 56, No. 5, p. 107 (1949).
- (2) Alves, G. E., Boucher, D. F. and Pigford, R. L., Chem. Eng., 48, No. 8, p. 385 (1952).
- (3) Anderson, L. E., Oil and Gas Journal, Dec. 8, p. 64 (1949).
- (4) Bakhmeteff, B. A., "The Mechanics of Turbulent Flow", Princeton University Press, Princeton, N. J. (1941).
- (5) Bauer, T. W. and Ruston, H. J., Memorandum "Viscosities of Excelsior and Stettler Crude Oils at Low Temperatures" Technical and Research Dept., Imperial Oil Ltd., Oct. 16, 1950.
- (6) Binder, R. C., "Fluid Mechanics" 2 ed., Prentice Hall Inc., New York (1949).
- (7) Brown, G. G., "Unit Operations" John Wiley and Sons, Inc., New York (1950).
- (8) Caldwell, D. H., and Babbitt, H. H., Ind. Eng. Chem., 33, No. 2, p. 249 (1941).
- (9) Chmilar, M. M., Report "Preliminary Tests of Pilot Pipeline Using Stove Oil and Redwater Crude Oil", Dept. of Chemical and Petroleum Engineering, University of Alberta, May, 1952.
- (10) Coulson, J. M. and Richardson, J. F., "Chemical Engineering" Vol. 1, McGraw-Hill Book Co., Inc., New York (1954).
- (11) Green, H., "Industrial Rheology and Rheological Structures" John Wiley and Sons, Inc., New York (1949).
- (12) Henderson, E. M., Report "Construction of an Oil Pipe Line Hydraulic Chart" Oklahoma Pipe Line Company, Oklahoma.
- (13) McAdams, W. H., "Heat Transmission" 2 ed., McGraw-Hill Book Co., Inc., New York (1942).
- (14) Padgett, F. W., "The Science of Petroleum" Edited by A. E. Dunston, Vol. III, p. 1941.
- (15) Perry, J. H., "Chemical Engineers' Handbook" 3 ed., McGraw-Hill Book Co., New York (1950).

- (16) Rouse, H., "Elementary Mechanics of Fluids" John Wiley and Sons, Inc., New York (1946).
- (17) Sidjak, W., "The Rheological Properties of Selected Alberta Crude Oils" M.Sc. Thesis, University of Alberta (1951).
- (18) Walker, W. H., Lewis, W. K., McAdams, W. H., and Gilliland, E. R., "Principles of Chemical Engineering" 3 ed., McGraw-Hill Book Co. Inc., New York (1937).
- (19) Weiser, H. B., "Colloid Chemistry" 2 ed., John Wiley and Sons, Inc., New York (1949).
- (20) Wilhelm, R. H., Wroughton, D. M. and Loeffel, W. F., Ind. Eng. Chem. 31, p. 622 (1939).
- (21) Winding, C. C., Baumann, G. P. and Kranich, W. L., Chem. Eng. Prog., 43, p. 527, 613 (1947).
- (22) Winning, M. D., "An Investigation of the Rheological Properties and Pipeline Flow Characteristics of Clay Slurries" M.Sc. Thesis, University of Alberta (1948).

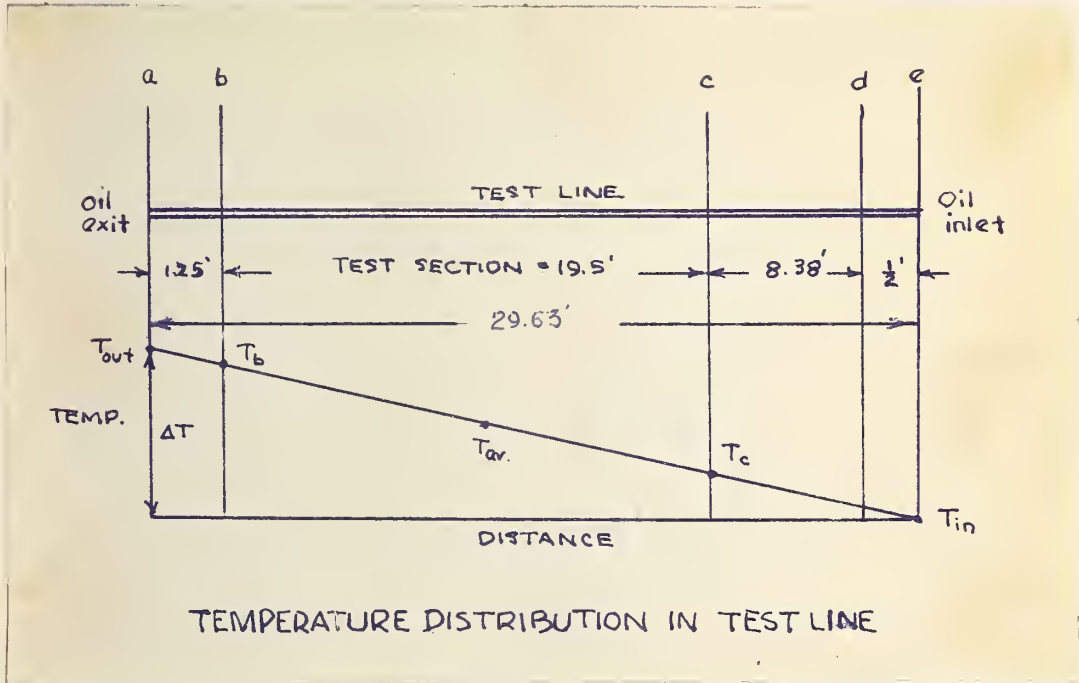
APPENDIX A

SAMPLE COMPUTATIONS OF:

- (1) EXPERIMENTAL DATA
- (2) FORMULAE USED IN COMPUTATION OF RESULTS
- (3) DETAILED RESULTS
- (4) VISCOSITY CONVERSIONS

1. Sample Computations of Experimental Data Reported in Tables
IV-B to IX-B (Appendix B).

Average Test Temperature



Test gauges provide for the measurement of temperatures at points a and e as shown by the above diagram, however T_{av} , the average test temperature of the test section between points b and c is required.

Assuming a linear temperature distribution along the whole length a-e and letting ΔT be the change in temperature, ($T_{out} - T_{in}$):

$$\Delta T = T_{out} - T_{in} \quad (1-a)$$

$$T_{av} = \frac{T_b + T_c}{2} \quad (2-a)$$

2A.

$$T_c = T_b - (\Delta T)_{\text{test}} \quad (3-a)$$

$$(\Delta T)_{\text{test}} = \frac{19.5}{29.63} (\Delta T) \quad (4-a)$$

$$T_b = T_o - \frac{1.25}{29.63} (\Delta T) \quad (5-a)$$

from equations (2-a), (3-a) and (4-a):

$$T_{\text{av}} = \frac{2T_b - \frac{19.5}{29.63} (\Delta T)}{2}$$

from equation (5-a):

$$T_{\text{av}} = T_{\text{out}} - \frac{1.25}{29.63} (\Delta T) - \frac{19.5}{2 \times 29.63} (\Delta T)$$

$$\text{whence } T_{\text{av}} = T_{\text{out}} - \frac{22.0}{59.2} (T_{\text{out}} - T_{\text{in}}) \quad (6-a)$$

Sample Computations:

A test in Stettler D2-D3 crude oil gave the following experimental data (0.249" line).

Upstream pressure^x = 30.5 psig.

Downstream pressure^x = 2.8 psig.

Test inlet temperature^x = 72.6°F.

Test exit temperature^x = 73.0°F.

Volume of crude collected = 10.40 gal.

Time for collection = 8.053 min.

Temperature of oil in receiver = 72°F.

Temperature of oil in storage = 75°F.

Temperature of oil at pump exit = 76°F .

Temperature of F-12 bath = 65°F .

^x Denotes average of three readings.

Average test temperature:

	Test in	Test out
Observed temp.	72.6°F .	73.0°F .
Corrected temp.	73.2°F .	73.6°F .

By equation (6-a):

$$T_{av} = 73.6 - \frac{22.0}{59.6} (0.4) = 73.5^{\circ}\text{F}.$$

Pressure drop across test section:

Upstream pressure = 30.5 psig.

Downstream pressure = 2.8 psig.

Pressure drop = 27.7 psig.

Flow rate:

Volume collected = 10.40 gal.

Time of collection = 8.053 min.

$$\text{Rate of flow} = \frac{10.40}{8.053} = 1.291 \text{ gal.} / \text{min.}$$

This amount was collected in the receiver at a temperature of 72°F . The rate of flow was corrected to the flow temperature of 73.5°F :

Density of crude at 72°F . = 54.59 lb./ft.³

Density of crude at 73.5°F . = 54.55 lb./ft.³

$$\text{Rate of flow at test temperature} = \frac{54.59}{54.55} \times 1.291$$

$$= 1.292 \text{ gal/min.}$$

$$\text{or rate of flow} = 1.292 \frac{\text{gal}}{\text{min}} \times \frac{\text{ft}^3}{6.24 \text{ gal}} = 0.2071 \text{ ft}^3/\text{min.}$$

2. Sample Computations: Formulae Used in Compiling the Detailed Results Reported in Table I-C of Appendix C.

Velocity:

Flow velocities were computed by the equation:

$$V = \frac{Q}{A} \quad (7-a)$$

where V = velocity in ft/sec.

Q = flow rate in ft.³/sec.

A = Internal cross-sectional area of pipe, ft.²

Equation (7-a) may be simplified for velocity computations in each pipe. For the pipe of 0.249 inch internal diameter,

$$V = \frac{(Q' \frac{\text{ft}^3}{\text{min}}) (\frac{\text{min}}{60 \text{ sec}})}{\pi (\frac{0.249}{12})^2 \text{ ft}^2} = \frac{Q'}{2.03} \times 10^2 \frac{\text{ft.}}{\text{sec.}} \quad (8-a)$$

where Q' = flow rate in ft.³/min.

Friction factor:

The Fanning equation is:

$$f = \left(\frac{\Delta P}{\rho} \right) \left(\frac{2}{V} \right) \left(\frac{L}{D} \right)$$

where f = friction factor

ΔP = pressure drop, lb/ft.²

ρ = density, lb/ft.³

V = velocity, ft/sec.

L = length of section, ft.

D = diameter, ft.

Since lengths and diameters are constant for any pipe, a simplified equation for friction factor for the 0.249 in. pipe is:

$$f = \frac{(\Delta P)' \frac{\text{lb}}{\text{in}^2} \times 2 \times 32.2 \frac{\text{lb}_m \text{ ft.}}{\text{lb}_f \text{ sec}^2} \times 19.5 \text{ ft.}}{\rho V^2 \frac{0.249 \text{ ft.}}{12} \times \frac{144 \text{ in.}^2}{\text{ft.}^2}}$$

$$= \frac{9.88 (\Delta P)'}{V^2 \rho} \quad (9-a)$$

where $(\Delta P)'$ = pressure drop in lb/in.²

Apparent Reynolds Number

In the theory, it was pointed out that friction factor could be evaluated by the use of apparent Reynolds numbers. In laminar flow, the combination of the Fanning equation and the modified Poiseuille equation gave:

$$f = 64 \left(\frac{\mu_a}{DV} \right) = \frac{64}{(N_R)_a} \quad (10-a)$$

$$\text{or } (N_R)_a = \frac{64}{f}$$

In turbulent flow a modification of the Heltzel equation gave:

$$f = \frac{0.364}{(N_R)_a^{0.265}}$$

$$\text{or } (N_R)_a = \left(\frac{0.364}{f} \right)^{3.77} \quad (11-a)$$

The Heltzel equation was chosen for friction factor calculations on the basis of Chmilar's (9) work on the pilot pipeline.

Friction factors were calculated and plotted against the Reynolds number on logarithmic scales. The range of Reynolds numbers investigated was 10,000 to 55,000. The Karman-Prandtl line (equation 12) and the Heltzel line (equation 14) were transposed on the graph. By this means, it was found that the Heltzel equation best represented the pilot pipeline data.

Apparent viscosity (laminar):

Apparent viscosities are computed by the modified Poiseuille equation:

$$\Delta P = \frac{32 \mu_a LV}{g_c D^2}$$

$$\text{or } \mu_a = \frac{D^2 \Delta P g_c}{32 LV}$$

For the 0.249 inch line, the equation reduces to:

$$\mu_a = \left(\frac{0.249^2 \times 32.2}{32 \times 19.5} \right) \frac{\Delta P'}{V} = (3.21 \times 10^{-3}) \frac{\Delta P'}{V} \frac{\text{lb}}{\text{ft. sec.}} \quad (12-a)$$

Apparent viscosity (turbulent):

The apparent viscosity in turbulent flow is derived from Reynold's number:

$$(N_{R_a}) = \frac{DV\rho}{\mu_a}$$

$$\mu_a = \frac{DV\rho}{(N_R)_a}$$

For the 0.249 inch pipe, the equation becomes :

$$\mu_a = \frac{0.249}{12} \frac{V\rho}{(N_R)_a} = \frac{0.0208}{(N_R)_a} V\rho \frac{\text{lb.}}{\text{ft. sec.}} \quad (13-a)$$

Apparent Shear rate at the wall:

The shear rate at the wall was shown by equation (20) to be:

$$-\left(\frac{dv}{dr}\right)_w = \frac{D g_c (\Delta P)}{4 L \mu}$$

This equation is valid for the laminar flow of a Newtonian fluid and in turbulent flow where a laminar sublayer exists next to the wall. The same equation, modified by the substitution of apparent viscosity is used to compute the apparent shear rate at the wall for the laminar and turbulent flow of non-Newtonian fluids. The apparent shear rate equations were only used to compare the effect of a shear rate term on the apparent viscosity and are not intended as expressions of true shear rate at the wall.

Substituting apparent viscosity for viscosity, the apparent rate of shear for a non-Newtonian is:

$$-\left(\frac{dv}{dr}\right)_a = \frac{D g_c (\Delta P)}{4 \mu_a L} \quad (14-a)$$

In laminar flow, the modified Poiseuille equation is substituted in the apparent shear rate equation:

$$-\left(\frac{dv}{dr}\right)_a = \left(\frac{D}{4\mu_a L}\right) \frac{(32\mu_a VL)}{D^2 g_c}$$

whence $-\left(\frac{dv}{dr}\right)_a = \frac{8V}{D}$

or since $V = \frac{4Q}{\pi D^2}$

$$-\left(\frac{dv}{dr}\right)_a = \frac{32Q}{\pi D^3} \quad (15-a)$$

For the pipe of 0.249 inch diameter, the equation reduces to:

$$-\left(\frac{dv}{dr}\right)_a = \frac{(32)(1.728)Q'}{\pi (0.249)^3 (60)} \times 10^3 = 18.92Q' \times 10^3 \text{sec}^{-1} \quad (16-a)$$

where $Q' = \text{flow rate in ft}^3/\text{min.}$

In turbulent flow, the apparent shear rate at the wall
(14-a) for the 0.249 inch pipe is:

$$-\left(\frac{dv}{dr}\right)_a = \frac{0.249 \times 144 \times 32.2}{12 \times 4 \times 19.5} \quad \left(\frac{\Delta P'}{\mu_a}\right) = 1.231 \frac{\Delta P'}{\mu_a} \text{sec}^{-1} \quad (17-a)$$

where ΔP is in lb/in.^2

3. Sample Computations of Detailed Results Reported in Tables II-C to VII-C Incl. of Appendix C

(a) Laminar Flow

Using the experimental data of Section 1, Appendix A:

Average test temperature = 73.5°F.

Pressure drop = 27.7 psig.

Flow rate = 1.292 gal./min.

= 0.2071 $\text{ft}^3/\text{min.}$

Density = 54.59 lb/ft.^3

Velocity:

From equation (8-a),

$$V = \left(\frac{Q'}{2.03} \times 10^2 \right) \frac{\text{ft}}{\text{sec}}$$

$$V = \frac{0.2071}{2.03} \times 10^2 = 10.20 \text{ ft/sec.}$$

Friction factor:

From equation (9-a),

$$f = \frac{9.88 (\Delta P)'}{V^2 \rho}$$

$$f = \frac{9.88 \times 27.7}{(10.20)^2 (54.59)} = 4.825 \times 10^{-2}$$

Apparent Reynolds number:

From equation (10-a),

$$\begin{aligned} (N_R)_a &= \frac{64}{f} \\ &= \frac{64}{0.0483} = 1330 \end{aligned}$$

Apparent viscosity:

From equation (12-a)

$$\begin{aligned} \mu_a &= 3.21 \times 10^{-3} \left(\frac{\Delta P'}{V} \right) \\ &= 3.21 \times 10^{-3} \left(\frac{27.7}{10.20} \right) = 0.00872 \frac{\text{lb}}{\text{ft. sec.}} \end{aligned}$$

Apparent shear rate at wall:

From equation (16-a),

$$\begin{aligned} -\left(\frac{dv}{dr}\right)_a &= 18.92 Q' \times 10^3 \\ &= 18.92 \times 10^3 (0.2071) = 3920 \text{ sec}^{-1} \end{aligned}$$

(b) Turbulent Flow

A test on Redwater sample no. 1 gave the following experimental data (0.249 inch line):

Average test temperature = 77.5°F.

Pressure drop = 303 lb/in²

Flow rate = 0.890 ft³/min.

Density = 52.8 ft/sec.

Velocity:

$$V = \frac{Q}{2.03} \times 10^2 = \frac{0.890}{2.03} \times 10^2 = 43.8 \text{ ft/sec.}$$

Friction factor:

$$f = 9.88 \frac{\Delta P}{V^2 \rho} = \frac{9.88 \times 303}{(43.8)^2 \times 52.8} = 0.0295$$

Apparent Reynolds number:

by equation (11-a)

$$\begin{aligned} (N_R)_a &= \left(\frac{0.364}{f} \right)^{3.77} \\ &= \left(\frac{0.364}{0.0295} \right)^{3.77} = 12,950 \end{aligned}$$

Apparent viscosity:

by equation (13-a),

$$\mu_a = 0.0208 \frac{V \rho}{(N_R)_a} = \frac{0.0208 \times 43.8 \times 52.8}{12,950}$$

$$= 0.00371 \frac{\text{lb}}{\text{ft. sec.}}$$

Apparent shear rate at wall:

by equation (17-a),

11A.

$$\begin{aligned}
 - \left(\frac{dv}{dr} \right)_a &= 1.231 \left(\frac{\Delta P}{r_a} \right) \\
 &= 1.231 \left(\frac{303}{0.00371} \right) \\
 &= 100,000 \text{ sec}^{-1}
 \end{aligned}$$

4. Sample Computations for Viscosity Conversions Reported in
Table X-C, Appendix C.

Kinematic Viscosity:

The kinematic viscosity of a fluid is defined by the equation:

$$k = \frac{\mu}{\rho} \quad (18-a)$$

where μ = viscosity in lb/ft-sec.

ρ = density in lb/ft.³

and k = kinematic viscosity in $\frac{\text{ft}^2}{\text{sec.}}$

From Table IX-C, the average apparent viscosity of Redwater crude oil, sample no. 1 is 19.72×10^{-3} lb/ft.-sec. at 20°C., the density at this temperature is 53.93 lb/ft.³

$$\begin{aligned}
 \text{Kinematic viscosity, } k &= \frac{19.72 \times 10^{-3}}{53.93} \\
 &= 3.66 \times 10^{-4} \text{ ft}^2/\text{sec.}
 \end{aligned}$$

Saybolt Universal viscosity:

The relationship of Saybolt Universal viscosity to kinematic viscosity is given in Perry (15) as:

$$k = \left(A\theta - \frac{B}{\theta} \right) \frac{\text{cm}^2}{\text{sec}} \quad (\text{stokes}) \quad (19-a)$$

where $A = 0.0022$

$B = 1.80$

θ = efflux time in sec (Saybolt Universal)

This equation is valid for other efflux-type viscometers, with change in values of the constants A and B. Substituting apparent viscosity in equation (19-a) one obtains:

$$\mu_a = \rho \left(0.0022 - \frac{1.80}{\theta} \right) \text{ poise} \quad (20-a)$$

converting to English units:

$$\mu_a = 6.72 \rho \left(0.0022 \theta - \frac{1.8}{\theta} \right) \frac{\text{lb}}{\text{ft-sec}} \quad (21-a)$$

Equation (21-a) is most convenient in the form

$$k = 6.72 \left(0.0022\theta - \frac{1.8}{\theta} \right) \frac{\text{ft}^2}{\text{sec.}} \quad (22-a)$$

where the values of kinematic viscosity (k) can be computed for selected efflux times (θ). Plots of this relationship are available and values of Saybolt Universal seconds given in Table X-C of Appendix C are taken from such a plot for the corresponding kinematic viscosity.

APPENDIX B

EXPERIMENTAL DATA OF PILOT PIPELINE.

1 B

TABLE I-B

Test Line Dimensions of the Pilot Pipeline.

Pipe size:

Nominal outer diameter, in.	$\frac{3}{8}$	$\frac{1}{2}$	$\frac{5}{8}$
Internal diameter, in.	0.249	0.311	0.386
Cross-sectional area, ft. ²	3.38×10^{-4}	5.28×10^{-4}	8.12×10^{-4}
Test length, ft.	19.5	19.5	19.5

TABLE 11-B.

Record of Crude Oils Tested.

Crude.	Date Received.	A.P.I. Gravity.	Test Numbers.	Remarks.
Redwater, Sample No.1.	Apr.7/52	34.5	1 to 9	Received from I.P.L. by M. Chmilar.
Redwater, Sample No.2.	Feb.5/53	34.2	10,11,12.	Obtained from I.P.L. from Redwater. gathering line.
Stettler D2-D3 Blend	Feb.23/53	29.1	13	Pipeline sample obtained by Canadian Gulf Oil Co.
Duhamel-Malmo- New Norway Blend.	Feb.26/53	37.1	14 to 17	Sample obtained by Canadian Gulf Oil Co.
Leduc-Woodbend Blend	Apr.20/53	38.5	18	Obtained from I.P.L.
Nisku Blend.	Apr.22/53	32.6	19	Obtained by I.P.L. at Nisku and is mainly Campbell crude.

TABLE III-B

Density Determinations by Chain Gravitometer.

Crude	Temp.		Density.	
	°F.	gm/ml.	lb/ft. ³	
Redwater, sample no.1.	39.0	0.8564	53.47	
	54.0	0.8534	53.28	
	49.0	0.8539	53.31	
	55.0	0.8521	53.20	
	60.0	0.8508	53.12	
	67.0	0.8480	52.94	
	46.0	0.8559	53.43	
	50.0	0.8538	53.30	
	87.0	0.8408	52.49	
	72.0	0.8466	52.85	
Redwater, sample no.2.	72.5	0.8469	52.87	
	64.4	0.8504	53.09	
	63.6	0.8510	53.13	
	60.8	0.8519	53.18	
	55.0	0.8550	53.38	
	49.8	0.8567	53.48	
	41.0	0.8592	53.64	
	21.0	0.8682	54.20	
Stettler D2-D3 blend.	73.0	0.8475	54.59	
	60.4	0.8780	54.81	
	65.3	0.8765	54.72	
	68.0	0.8759	54.68	
	37.4	0.8865	55.34	
	44.8	0.8853	55.27	
	50.0	0.8838	55.17	
	53.6	0.8811	55.00	
	57.2	0.8802	54.95	
	60.4	0.8795	54.90	
	44.6	0.8844	55.21	
	50.0	0.8832	55.14	
	54.5	0.8818	55.05	
	57.2	0.8808	54.99	

Crude	Temp.		Density.
	°F.	gm/ml.	lb/ft. ³
Duhamel-Malmo-New Norway blend.	68.0	0.8340	52.07
	68.2	0.8343	52.09
	39.2	0.8429	52.63
	47.3	0.8418	52.56
	50.3	0.8408	52.49
	53.2	0.8400	52.44
	32.0	0.8474	52.91
	33.8	0.8466	52.86
	35.9	0.8462	52.83
	37.8	0.8455	52.79
Leduc-Woodbend blend.	71.6	0.8271	51.64
	63.0	0.8300	51.82
	61.2	0.8304	51.85
	46.4	0.8340	52.07
	36.0	0.8378	52.31
	33.8	0.8385	52.35
Nisku blend.	74.3	0.8553	53.40
	61.7	0.8596	53.67
	52.7	0.8627	53.86
	50.0	0.8640	53.94
	30.2	0.8708	54.37

Table IV-B

Experimental Data of Pilot Pipeline Tests for
Redwater Sample No. 1.

Tests in 0.249 inch line, 1 to 6 inclusive.

Tests in 0.386 inch line, 7 to 9 inclusive.

Test No.	Temperatures in deg.F.				Pressure drop.	Flow rate.
	storage.	pump exit	receiver.	shell.	test average	lb/in ² ft ³ /min.
1	76	76	76	76	76.5	12.00 0.1675
	78	80	75	67	68.8	11.75 0.1600
	78	79	72	58	64.5	11.95 0.1510
	76	77	70	49	59.3	12.18 0.1393
	76	76	65	38	52.4	12.47 0.1220
	73	73	61	30	41.8	12.95 0.0905
	75	75	60	26	32.8	13.10 0.0538
	75	74	58	19	17.9	13.75 0.0394
	75	75	57	18	19.4	13.55 0.0402
	82	82	58	22	43.1	12.78 0.0950
	78	80	60	33	62.3	11.90 0.1440
	74	75	62	48	66.2	11.85 0.1540
	76	76	67	68	73.2	11.53 0.1700
2	75	77	73	75	76.0	20.2 0.1970
	78	80	74	63	70.1	20.9 0.215
	77	79	73	52	66.7	19.85 0.224
	76	76	71	42	62.6	19.33 0.222
	72	73	67	32	55.3	20.0 0.200
	69	70	65	25	51.0	20.5 0.1873
	67	68	60	20	45.2	21.0 0.1667
	65	66	59	18	40.9	21.4 0.1530
	61	63	56	13	35.7	22.0 0.1366
	59	59	54	11	31.0	22.9 0.1200
	56	57	50	9	26.7	23.3 0.1075
	47	50	62	11	22.0	23.8 0.0942
	56	60	54	23	22.6	23.5 0.1073
	56	59	51	41	39.5	22.2 0.1523
	57	60	48	44	44.3	21.3 0.1680
	57	59	52	30	51.1	21.2 0.213
	59	60	55	54	58.8	20.5 0.237
	65	66	58	68	67.5	20.4 0.252
	66.	67	62		72.5	21.8 0.236

Test No.	Temperatures in deg.F.				Pressure drop.	Flow rate.
	storage.	pump exit.	Receiver.	Shell.	test average	lb/in ² ft. ³ /min.
3	75	76	75	73	75.8	50.7 0.318
	73	75	72	30	62.8	52.6 0.314
	69	70	67	21	57.5	53.7 0.317
	63	64	64	18	51.5	54.0 0.320
	56	57	65	15	45.2	48.7 0.351
	51	53	61	11	41.4	49.7 0.353
	56	58	61	12	46.7	51.9 0.336
	59	60	59	15	54.2	55.0 0.318
	62	64	58	22	61.6	53.4 0.317
	65	66	60	38	65.2	52.6 0.316
	68	69	62	65	70.9	51.6 0.316
	70	72	65	73	74.5	51.3 0.317
4	78	80	72	37	71.5	57.4 0.340
	74	77	70	25	66.6	58.4 0.338
5	74	76	68	58	71.5	68.0 0.370
	76	78	68	51	65.5	68.2 0.364
	71	72	65	35	61.0	69.2 0.364
	68	69	64	26	56.4	70.5 0.365
	61	63	62	22	50.2	73.7 0.370
			60	15	45.8	74.5 0.374
	47	53	55	12	38.6	67.2 0.416
	44	45	50	11	35.7	68.8 0.408
	41	43	48	8	32.8	70.5 0.397
	44	45	51	9	35.1	70.1 0.416
	45	46	48	10	40.4	78.8 0.388
	48	50	47	19	45.3	80.4 0.383
	51	52	48	29	50.4	79.2 0.383
	55	56	50	44	55.3	76.9 0.378
	60	61	54	58	61.8	73.4 0.378
	63	64	58	64	65.8	72.3 0.375
	66	68	60	69	69.7	71.1 0.380
6	72	80	65	58	77.5	303 0.890
	81	85	69	59	75.8	165 0.624
	77	78	70	52	70.7	169 0.623
	72	75	66	42	65.4	174 0.623
	65	71	71	32	60.0	182 0.632
	73	75	65	20	65.0	97.2 0.445
	70	71	65	16	61.2	67.0 0.357
	68	70	62	12	55.7	42.8 0.283
	66	68	60	10	57.3	96.9 0.435
	65	67	60	9	57.1	68.7 0.360

Test No.	Temperatures in deg.F.				Pressure drop		Flow rate.
	Storage.	pump exit.	receiver.	shell	test average	lb/in ²	
	61	62	58	6	49.7	44.7	0.301
	60	62	56	6	53.6	190	0.625
	59	60	55	6	51.6	70.1	0.359
	59	61	55	5	52.6	101	0.437
	55	57	54	6	45.0	44.3	0.328
	57	60	54	6	49.0	190	0.621
	56	57	53	6	46.3	73.5	0.370
	55	57	51	7	48.5	103	0.439
	54	58	57	9	43.4	48.6	0.344
	56	60	55	9	47.8	192	0.618
	57	60	55	9	49.2	146	0.535
7	77	78	73	65	78.7	19.50	0.605
	77	78	74	65	75.5	19.55	0.602
	73	75	74	51	69.8	19.85	0.599
	71	72	71	42	64.7	20.0	0.598
	67	67	66	34	59.8	20.45	0.594
	63	62	64	30	55.8	20.8	0.593
	57	58	63	17	50.7	22.1	0.604
	58	60	67	13	56.3	21.0	0.594
	62	65	65	18	60.3	20.4	0.591
	67	68	65	34	65.7	19.93	0.591
	71	73	66		71.2	19.72	0.597
	76	78	71	75	75.9	19.57	0.604
8	76	75	76	61	73.0	10.28	0.420
	71	72	72	59	66.7	10.73	0.420
	65	66	65	47	61.0	10.96	0.424
	60	60	62	38	55.3	9.26	0.440
	58	58	60	29	50.0	8.36	0.442
	55	56	59	24	46.0	8.88	0.420
	50	52	56	19	40.6	9.64	0.392
	46	48	55	17	36.9	10.05	0.370
	45	46	49	12	30.8	10.83	0.330
	39	41	48	10	25.4	11.44	0.296
	37	40	54	8	23.1	11.59	0.288
	39	41	50	8	25.6	11.20	0.301
	41	41	45	10	30.0	10.65	0.333
	45	45	47	18	35.3	10.09	0.374
	45	47	45	25	40.3	9.96	0.403
	48	50	47	37	45.6	8.99	0.413
	50	52	50	48	50.4	8.60	0.454
	56	58	55	57	56.6	10.05	0.448
	61	62	58	59	60.7	11.09	0.435
	65	66	61	62	65.0	11.20	0.432
	68	69	63	74	71.9	10.88	0.431

Test No.	Temperatures in deg.F.				Pressure drop		Flow rate.
	storage.	pump exit.	receiver.	shell	test average	lb/in. ²	
9	70	71	70	69	71.0	18.82	0.582
	68	69	69	63	62.5	18.83	0.573
	68	68	67	59	59.8	18.82	0.570
	65	66	65	52	54.7	19.18	0.570
	61	61	62	41	49.7	20.00	0.576
	55	56	59	32	44.9	19.65	0.590
	52	52	55	21	40.4	17.47	0.618
	46	47	53	18	35.0	17.65	0.590
	44	44	51	13	30.6	18.20	0.562
	42	43	55	12	28.9	18.43	0.559
	36	37	58	8	25.5	18.85	0.534
	39	39	54	8	28.4	18.30	0.559
	40	40	49	8	30.0	17.83	0.570
	41	42	44	15	34.7	17.13	0.615
	44	45	45	29	39.4	17.13	0.613
	47	48	46	43	45.8	19.35	0.599
	50	51	50	51	50.4	19.45	0.591
	54	55	52	57	55.1	19.20	0.593

TABLE V-B

Experimental Data of Pilot Pipeline Tests
for Redwater Sample No.2. in 3/8 Inch Line.

Test No.	Temperature in deg.F.				Pressure drop		Flow rate.
	storage	pump exit	receiver	shell	test average	lb/in. ²	
10	81	81	72	62	79.0	73.9	0.400
	80	81	74	63	78.9	35.2	0.262
	79	80	75	64	78.5	25.7	0.223
	80	81	74	59	68.7	21.3	0.201
	80	80	74	54	67.9	35.9	0.260
	79	80	72	47	64.8	76.7	0.396
	79	78	70	42	62.0	21.5	0.212
	76	76	71	38	61.6	36.5	0.262

Test No.	Temperatures in deg. F.				Pressure	Flow	
	storage	pump exit	receiver.	shell test average	drop lb/in. ²	rate ft. ³ /min.	
	76	75	66	34	61.7	77.1	0.396
	71	71	65	25	54.2	23.5	0.237
	68	69	63	23	54.6	36.8	0.266
	65	65	60	18	48.6	25.2	0.228
	65	65	59	19	50.4	40.4	0.283
	63	61	58	17	47.4	23.0	0.207
	58	59	58	16	41.8	16.52	0.1363
	58	59	56	16	37.5	12.84	0.0971
11	50	51	60	28	49.5	23.7	0.227
	45	49	60	26	46.2	24.1	0.215
	47	48	56	24	39.0	24.9	0.1780
	51	50	52	23	33.1	22.8	0.1282
	52	53	51	21	27.5	23.1	0.0953
	54	52	50	18	26.2	23.4	0.0860
12	76	81	73	32	66.0	287.3	0.837
	73	74	72	59	69.7	135.2	0.548
	70	70	71	58	65.6	137.9	0.550
	62	63	66	55	58.7	23.6	0.238
	60		65	52	54.9	22.7	0.245
	55		63	43	50.3	23.2	0.229
	46		58	35	45.7	39.0	0.310
	40		56	25	38.5	48.5	0.346
	42		52	25	35.6	50.3	0.329
	45		50	18	32.8	43.5	0.253
	46		47	15	29.0	33.1	0.1616
	46		46	13	27.2	33.4	0.1529
	46		45	11	21.7	29.4	0.0874
	46		44	10	24.9	31.9	0.1230

TABLE VI-B

Experimental Data of Pilot Pipeline Tests
for Stettler D2 - D3 Blend in 0.249 Inch Line.

Test No.	Temperatures in deg.F.					Pressure drop lb/in. ²	Flow rate ft. ³ /min.
	storage	pump exit	receiver	shell	test average		
13	75	76	72	65	73.5	27.7	0.2071
	73	74	71	63	70.6	51.3	0.3507
	70	70	71	57	65.2	55.2	0.3445
	62	64	68	53	61.6	58.6	0.3427
	59	60	66	43	55.5	62.9	0.3233
	53	56	60	37	50.5	65.7	0.2889
	56	58	57	26	48.3	66.2	0.2658
	59	60	57	23	44.8	49.7	0.1810
	60	61	56	18	41.8	51.1	0.1656
	60	61	56	17	35.8	43.3	0.1072
	59	60	53	11	38.9	58.3	0.1698
	59	59	53	11	34.3	52.8	0.1252
	59	60	51	10	31.1	49.8	0.1049
	60	60	51	10	26.7	49.0	0.08304
	60	61	50	10	22.2	47.0	0.06704
	61	62	48	9	21.8	47.4	0.06654
	56	54	49	18	52.0	64.2	0.2969

TABLE VII-B

Experimental Data of Pilot Pipeline Tests
for Duhamel-Malmö - New Norway Blend in 0.249 Inch Line

Test No.	Temperatures in deg.F.					Pressure drop lb/in. ²	Flow rate ft. ³ /min.
	storage	pump exit	receiver	shell	test average		
14	74	75	73	63	76.2	301.8	0.9584
	73	73	75	65	69.7	98.6	0.5008
	68	68	72	61	65.0	84.3	0.4477
	63	63	68	57	60.2	96.8	0.4827
	60	60	67	52	56.8	82.5	0.4378
	56	60	63	47	52.0	61.5	0.3668
	50	53	60	43	48.3	62.8	0.3676
	48	51	59	39	44.2	63.7	0.3671
	45	48	51	34	39.9	73.6	0.3923
	48	50	51	23	37.9	56.2	0.3336

Test No.	Temperatures in deg.F.					Pressure	Flow
	storage	pump exit	receiver	shell	test average	drop lb/in. ²	rate ft. ³ /min.
	47	48	50	18	34.1	20.0	0.2077
	38	43	52	24	34.9	69.2	0.3751
	43	48	50	20	29.1	16.01	0.1334
	44	48	51	10	25.2	15.76	0.09956
	46	48	51	8	25.7	19.04	0.1337
	45	42	49	9	36.0	22.02	0.2181
	40	41	45	23	41.7	22.94	0.2148
15	74	75	71	55	63.7	41.1	0.2983
	46	46	48	27	35.5	12.72	0.1420
	49	49	55	29	29.8	12.85	0.0970
	46	46	49	24	26.5	12.53	0.0793
	48	48	50	18	23.8	12.40	0.0600
	58	60	58	28	53.5	306.0	0.8960
	54	56	61	40	48.2	158.3	0.6090
16	75	76	73	60	70.7	8.74	0.1313
	70	70	72	60	64.3	8.90	0.1335
	64	65	71	58	60.5	9.97	0.1428
	58	59	68	56	55.1	10.74	0.1504
	56	57	66	48	50.6	10.33	0.1509
	50	51	64	42	45.6	10.10	0.1530
	46	46	63	37	40.8	7.56	0.1036
	44	45	62	33	38.4	6.78	0.0819
	43	47	61	21	35.2	6.77	0.0695
	40	43	60	16	31.0	7.80	0.0675
	40	41	58	13	29.0	9.37	0.0695
	43	45	57	12	26.2	10.52	0.0640
	46	50	55	11	23.7	10.64	0.0565
	46	49	54	10	21.7	10.89	0.0558
17	76	78	73	69	77.3	6.78	0.1180
	76	81	76	70	82.2	329.6	1.023
	68	67	76	64	67.2	5.500	0.1174
	68	73	74	63	71.0	326.0	0.9967
	63	62	71	59	58.1	4.685	0.1056
	57	57	70	54	52.8	5.153	0.1027
	54	52	65	48	48.7	5.181	0.09386
	48	49	64	44	44.7	5.355	0.08610
	48	49	61	40	41.6	128.9	0.5426

TABLE VIII-B.

Experimental Data of Pilot Pipeline Test for
Leduc-Woodbend Blend in 0.249 Inch Line.

Test No.	Temperature in deg.F.				Pressure drop	Flow rate	
	storage	pump exit	receiver	shell test average			
18	71	78	72	59	72.7	323.9	1.020
	74	76	72	67	73.8	3.368	0.03663
	66	69	73	67	65.6	4.016	0.09878
	60	64	72	62	60.3	3.176	0.08001
	54	54	69		53.1	3.346	0.07440
	38	40	59	41	39.8	3.998	0.06491
	38	39	50	37	38.3	4.663	0.07808
	35	36	50	36	34.2	5.145	0.07839
	37	38	54	35	29.4	5.384	0.07629
	35	38	51	32	21.7	6.700	0.05723
	43	47	51	22	22.9	9.405	0.09291
	48	50	50	21	26.5	7.436	0.08174
	43	43	48	20	36.9	195.8	0.7063
	42	50	45	22	40.9	363.4	1.0183
	49	55	50	32	48.4	292.2	0.9012
	42	49	55	31	40.1	289.8	0.8868
	40	51	51	30	40.8	466.9	1.166

TABLE IX-B.

Experimental Data of Pilot Pipeline Test
for Nisku Blend in 0.249 Inch Line.

Test No.	Temperature in deg. F.					Pressure drop	Flow rate
	storage	pump exit	receiver	shell	test average	lb./in. ²	ft. ³ /min.
19	72	76	74	58	73.6	207.4	0.6803
	71	72	68	66	73.7	18.88	0.2214
	66	67	68	63	65.2	19.34	0.2092
	60	61	68	58	59.2	19.96	0.1975

Test No.	Temperatures in deg. F.				Pressure drop	Flow rate	
	storage	pump exit	receiver.	shell test average			
56		57	67	52	54.7	20.66	0.1845
51		52	64	46	50.3	21.41	0.1718
48		49	63	35	44.8	22.75	0.1559
43		48	60	34	40.6	21.46	0.1263
48		50	60	30	36.5	56.0	0.2610
51		54	58	31	29.3	30.5	0.08701
52		57	57	27	25.5	27.4	0.05986
54		59	56	24	21.2	26.9	0.04357
70		73	59	61	71.5	10.28	0.1220
66		67	63	62	65.1	10.94	0.1161
62		65	65	56	60.7	11.48	0.1133

APPENDIX C

DETAILED RESULTS OF COMPUTATIONS OF PILOT
PIPELINE TESTS.

TABLE I-C.

Summary of Formulae Used in Computations

Reported in Section 2 (Appendix A).

Internal pipe diameter, in.	0.249	0.311	0.386
Velocity, ft/sec.	$\frac{Q' \times 10^2}{2.03}$	$\frac{Q' \times 10^2}{3.17}$	$\frac{Q' \times 10^2}{4.87}$
Friction factor.	$\frac{9.88 \Delta P'}{V^2 \rho}$	$\frac{12.35 \Delta P'}{V^2 \rho}$	$\frac{15.32 \Delta P'}{V^2 \rho}$
Apparent Reynolds number,			
laminar	$\frac{64}{f}$	$\frac{64}{f}$	$\frac{64}{f}$
turbulent	$\left(\frac{0.364}{f}\right)^{3.77}$	$\left(\frac{0.364}{f}\right)^{3.77}$	$\left(\frac{0.364}{f}\right)^{3.77}$
Apparent viscosity, lb/ft-sec.			
laminar	$3.21 \times 10^{-3} \frac{(\Delta P')}{(V)}$	$4.99 \times 10^{-3} \frac{(\Delta P')}{(V)}$	$7.71 \times 10^{-3} \frac{(\Delta P')}{(V)}$
turbulent	$0.0208 \frac{(V \rho)}{(N_R)_a}$	$0.0259 \frac{(V \rho)}{(N_R)_a}$	$0.0322 \frac{(V \rho)}{(N_R)_a}$
Apparent shear rate at wall, sec. ⁻¹			
laminar.	18.92×10^3	9.74×10^3	5.10×10^3
turbulent	$1.231 \frac{(\Delta P')}{(\mu_a)}$	$1.541 \frac{(\Delta P')}{(\mu_a)}$	$1.912 \frac{(\Delta P')}{(\mu_a)}$

Note: Units of symbols used in the above equations are:-

 Q' = flow rate, ft³/min. $\Delta P'$ = pressure drop, lbs/in.² ρ = density, lb/ft.³ V = velocity, ft/sec.

TABLE 11-C.

Detailed Results of Computations for Pilot Pipeline Tests
on Redwater Sample No. 1.

Test No.	Average temp.	Density lb./ft ³	Velocity ft/sec	Friction factor	Reynolds no.	Apparent viscosity lb/ft-sec	Shear rate @ wall	Remarks
-	°F	lb./ft ³	ft/sec	x10 ²	x10 ⁻³	x10 ⁺³	x10 ⁻³ sec ⁻¹	
1	76.5	52.8	8.25	3.30	8.45	1.07	13.8	flow uncertain assume turbulent
	76.5	52.8	8.25	3.30	1.94	4.67	3.17	flow uncertain assume laminar
	68.8	52.9	7.88	3.54	6.55	1.32	11.0	flow uncertain assume turbulent
	68.8	52.9	7.88	3.55	1.81	4.79	3.03	flow uncertain assume laminar
	64.5	53.0	7.44	4.04	1.58	5.16	2.86	flow laminar
	59.3	53.1	6.96	4.68	1.37	5.61	2.64	flow laminar
	52.4	53.3	6.00	6.53	0.980	6.67	2.31	flow laminar
	41.8	53.5	4.45	12.10	0.529	9.35	1.71	flow laminar
	32.8	53.6	2.65	34.4	0.186	15.88	1.02	flow laminar
	17.9	53.9	1.94	67.0	0.096	22.8	0.746	flow laminar
	19.4	53.9	1.98	63.4	0.099	22.7	0.761	flow laminar
	43.1	53.4	4.67	10.84	0.590	8.77	1.80	flow laminar
	62.3	53.1	7.09	4.41	1.45	5.39	2.73	flow laminar
	66.2	53.0	7.58	3.86	1.66	5.02	2.92	flow laminar
	73.2	52.8	8.37	3.08	11.00	0.835	17.0	flow uncertain assume turbulent
	73.2	52.8	8.37	3.08	2.08	4.42	3.22	flow uncertain assume laminar

Test No.	Average temp.	Density	Velocity	Friction factor	Reynolds no.	Apparent viscosity	Shear rate @ wall	Remarks
-	°F	lb./ft ³	ft/sec	x10 ²	x10 ⁻³	x10 ⁺³ lb/ft-sec	x10 ⁻³ sec ⁻¹	
				-	-			
2	76.0	52.8	9.70	4.02	4.06	2.62	9.51	flow uncertain assume turbulent
	76.0	52.8	9.70	4.02	1.59	6.71	3.73	flow uncertain assume laminar
	70.1	52.9	10.60	3.48	6.96	1.49	14.02	flow uncertain assume turbulent
	70.1	52.9	10.60	3.48	1.84	6.33	4.07	flow uncertain assume laminar
	66.7	53.0	11.03	3.03	11.7	1.04	23.4	flow uncertain assume turbulent
	66.7	53.0	11.03	3.03	2.11	5.75	4.24	flow uncertain assume laminar
	62.6	53.0	10.93	3.28	8.74	1.38	17.2	flow uncertain assume turbulent
	62.6	53.0	10.93	3.28	1.95	6.17	4.20	flow uncertain assume laminar
	55.3	53.2	9.85	3.83	1.67	6.60	3.78	flow laminar
	51.0	53.3	9.22	4.47	1.43	7.15	3.54	flow laminar
	45.2	53.4	8.20	5.78	1.11	8.22	3.16	flow laminar
	40.9	53.5	7.54	6.95	0.921	9.10	2.90	flow laminar
	35.7	53.6	6.73	8.96	0.714	10.53	2.59	flow laminar
	31.0	53.7	5.91	12.03	0.532	12.42	2.27	flow laminar
	26.7	53.8	5.29	15.30	0.418	14.15	2.04	flow laminar
	22.0	53.9	4.59	20.8	0.380	16.63	1.78	flow laminar
	22.6	53.0	5.23	15.80	0.405	14.42	2.03	flow laminar
	39.5	53.5	7.42	7.45	0.859	9.60	2.88	flow laminar
	44.3	53.4	8.19	5.89	1.09	8.36	3.18	flow laminar
	51.1	53.3	10.40	3.79	1.69	6.54	4.03	flow laminar
	58.8	53.1	11.55	2.82	1.54	0.83	30.3	flow uncertain assume turbulent

Test No.	Average temp.	Density	Velocity	Friction factor	Reynolds no.	Apparent viscosity	Shear rate @ wall	Remarks
-	°F	lb./ft ³	ft/sec	x10 ²	x10 ⁻³	x10 ⁺³	x10 ⁻³	
				-	-	lb/ft-sec	sec ⁻¹	
	58.8	53.1	11.55	2.82	2.27	5.70	4.48	flow uncertain assume laminar
	67.5	52.9	12.28	2.52	23.6	0.57	44.0	flow uncertain assume turbulent
	67.5	52.9	12.28	2.52	2.54	5.33	4.77	flow uncertain assume laminar
	72.5	52.8	11.50	3.09	10.92	1.15	23.3	flow uncertain assume turbulent
	72.5	52.8	11.50	3.09	2.07	6.08	4.46	flow uncertain assume laminar
3	75.8	52.8	15.65	3.94	4.39	3.91	16.0	flow turbulent
	62.8	53.0	15.45	4.10	3.76	4.01	16.1	flow uncertain assume turbulent
	62.8	53.0	15.45	4.10	1.56	10.93	5.94	flow uncertain assume laminar
	57.5	53.2	15.62	4.09	3.70	4.01	16.5	flow uncertain assume turbulent
	57.5	53.2	15.62	4.09	1.56	11.03	6.00	flow uncertain assume laminar
	51.5	53.3	15.75	4.03	4.01	4.35	15.3	flow uncertain assume turbulent
	51.5	53.3	15.75	4.03	1.58	11.00	6.05	flow uncertain assume laminar
	45.2	53.4	17.30	3.02	11.95	1.48	40.5	flow uncertain assume turbulent
	45.2	53.4	17.30	3.02	2.08	9.05	6.64	flow uncertain assume laminar
	41.4	53.5	17.38	3.04	11.63	1.66	36.8	flow uncertain assume turbulent

Test No.	Average temp.	Density	Velocity	Friction factor	Reynolds no.	Apparent viscosity	Shear rate @ wall	Remarks
-	°F	lb./ft ³	ft/sec	x10 ²	x10 ⁻³	x10 ⁺³ lb/ft-sec	x10 ⁻³ sec ⁻¹	
				-	-			
	41.4	53.5	17.38	3.04	2.11	9.18	6.68	flow uncertain assume laminar
	46.7	53.4	16.54	3.50	6.83	2.69	21.4	flow uncertain assume turbulent
	46.7	53.4	16.54	3.50	1.83	10.8	6.36	flow uncertain assume laminar
	54.2	53.2	15.65	4.05	3.94	4.40	15.2	flow uncertain assume turbulent
	54.2	53.2	15.65	4.05	1.58	11.29	6.02	flow uncertain assume laminar
	61.6	53.1	15.60	4.08	3.81	4.52	16.8	flow uncertain assume turbulent
	61.6	53.1	15.60	4.08	1.57	11.00	6.00	flow uncertain assume laminar
	65.2	53.0	15.55	4.07	3.88	4.42	18.2	flow uncertain assume turbulent
	65.2	53.0	15.55	4.07	1.57	10.86	5.98	flow uncertain assume laminar
	70.9	52.9	15.55	4.00	4.13	4.14	15.3	flow turbulent
	74.5	52.8	15.60	3.94	4.39	3.91	16.2	flow turbulent
4	71.5	52.9	16.75	3.83	4.85	3.81	18.6	flow turbulent
	66.6	53.0	16.65	3.86	4.72	3.89	18.5	flow turbulent
5	71.5	52.9	18.20	3.78	5.11	3.92	31.40	flow turbulent
	65.5	53.0	17.91	3.96	4.30	4.60	18.28	flow turbulent
	61.0	53.1	17.91	4.00	4.12	4.80	17.80	flow turbulent
	56.4	53.2	17.55	4.25	3.28	5.93	14.6	flow uncertain assume turbulent

Test No.	Average temp.	Density	Velocity	Friction factor	Reynolds no.	Apparent viscosity	Shear rate @ wall	Remarks
-	°F	lb./ft ³	ft/sec	x10 ²	x10 ⁻³	x10 ⁺³ lb/ft-sec	x10 ⁻³ sec ⁻¹	
	56.4	53.2	17.55	4.25	1.51	12.9	6.91	flow uncertain assume laminar
	50.2	53.3	18.20	4.12	3.69	5.47	16.6	flow uncertain assume turbulent
	50.2	53.3	18.20	4.12	1.55	13.00	7.00	flow uncertain assume laminar
	45.8	53.4	18.40	4.08	3.81	5.36	17.1	flow uncertain assume turbulent
	45.8	53.4	18.40	4.08	1.57	13.00	7.80	flow uncertain assume laminar
	38.6	53.5	20.5	2.95	12.95	1.76	47.0	flow uncertain assume turbulent
	38.6	53.5	20.5	2.95	2.17	10.52	7.89	flow uncertain assume laminar
	35.7	53.6	20.1	3.14	2.04	11.00	7.74	flow laminar
	32.8	53.6	19.55	3.40	1.88	11.59	7.51	flow laminar
	35.1	53.6	20.5	3.08	2.08	11.00	7.89	flow laminar
	40.4	53.5	19.10	3.98	4.20	4.85	20.0	flow uncertain assume turbulent
	40.4	53.5	19.10	3.98	1.61	13.26	7.35	flow uncertain assume laminar
	45.3	53.4	18.85	4.19	3.47	6.03	16.4	flow uncertain assume turbulent
	45.3	53.4	18.85	4.19	1.53	13.70	7.25	flow uncertain assume laminar
	50.4	53.3	18.85	4.13	3.65	5.72	17.1	flow uncertain assume turbulent
	50.4	53.3	18.85	4.13	1.55	13.50	7.25	flow uncertain assume laminar

Test No.	Average temp.	Density	Velocity	Friction factor	Reynolds no.	Apparent viscosity	Shear rate @ wall	Remarks
-	°F	lb./ft ³	ft/sec	x10 ²	x10 ⁻³	x10 ⁺³ lb/ft-sec	x10 ⁻³ sec-l	
	55.3	53.2	18.60	4.25	3.28	6.28	15.1	flow uncertain assume turbulent
	55.3	53.2	18.60	4.25	15.1	13.3	7.15	flow uncertain assume laminar
	61.8	53.1	18.60	3.95	4.32	4.76	19.0	flow turbulent
	65.8	53.0	18.46	3.96	4.30	4.72	18.9	flow turbulent
	69.7	52.9	18.70	3.79	5.05	4.07	21.5	flow turbulent
6	77.5	52.8	43.8	2.95	12.95	3.71	100.0	flow turbulent
	75.8	52.8	30.7	3.28	8.74	3.86	52.0	flow turbulent
	70.7	52.9	30.7	3.35	8.02	4.21	49.4	flow turbulent
	65.4	53.0	30.7	3.44	7.24	4.68	45.7	flow turbulent
	60.0	53.1	31.1	3.50	6.82	5.04	44.5	flow turbulent
	65.0	53.0	21.9	3.78	5.11	4.72	25.3	flow turbulent
	61.2	53.1	17.58	4.03	4.01	4.84	17.3	flow turbulent
	55.7	53.2	13.93	4.10	3.76	4.10	12.9	flow uncertain assume turbulent
	55.7	53.2	13.93	4.10	1.56	9.87	5.35	flow uncertain assume laminar
	57.3	53.2	21.4	3.94	4.37	5.42	22.0	flow turbulent
	57.1	53.2	17.73	4.13	3.65	4.73	17.9	flow uncertain assume turbulent
	57.1	53.2	17.73	4.13	1.55	12.44	6.81	flow uncertain assume laminar
	49.7	53.3	14.82	3.76	5.23	3.14	17.5	flow uncertain assume turbulent
	49.7	53.3	14.82	3.76	1.70	9.69	5.70	flow uncertain assume laminar
	53.6	53.2	30.8	3.72	5.44	6.27	37.3	flow turbulent
	51.6	53.3	17.70	4.15	3.61	5.43	15.9	flow uncertain assume turbulent

Test No.	Average temp.	Density	Velocity	Friction factor	Reynolds no.	Apparent viscosity	Shear rate @ wall	Remarks
-	°F	lb./ft ³	ft/sec	x10 ²	x10 ⁻³	x10 ⁺³	x10 ⁻³	
				-	-	lb/ft-sec	sec ⁻¹	
	51.6	53.3	17.70	4.15	1.54	12.72	6.80	flow uncertain assume laminar
	52.6	53.3	21.5	4.05	3.94	6.05	20.5	flow uncertain assume turbulent
	52.6	53.3	21.5	4.05	1.58	15.09	8.27	flow uncertain assume laminar
	45.0	53.4	16.15	3.14	10.30	1.74	31.4	flow uncertain assume turbulent
	45.0	53.4	16.15	3.14	2.04	8.81	6.21	flow uncertain assume laminar
	49.0	53.3	30.6	3.76	5.23	6.49	36.0	flow turbulent
	46.3	53.4	18.22	4.10	3.76	5.39	16.8	flow uncertain assume turbulent
	46.3	53.4	18.22	4.10	1.56	12.95	7.00	flow uncertain assume laminar
	48.5	53.3	21.6	4.10	3.76	6.37	19.9	flow uncertain assume turbulent
	48.5	53.3	21.6	4.10	1.56	15.10	8.30	flow uncertain assume laminar
	43.4	53.4	16.93	3.14	10.3	1.83	32.7	flow uncertain assume turbulent
	43.4	53.4	16.93	3.14	2.04	9.22	6.51	flow uncertain assume laminar
	47.8	53.3	30.4	3.86	4.74	7.16	32.9	flow turbulent
	49.2	53.3	26.3	3.92	4.46	6.52	27.6	flow uncertain assume turbulent
	49.2	53.3	26.3	3.92	1.63	17.8	10.10	flow uncertain assume laminar

(Transition data of test No. 6 omitted from graph because of wide pressure drop variations)

Test No.	Average temp.	Density	Velocity	Friction factor	Reynolds No.	Apparent Viscosity	Shear rate @ wall	Remarks
-	of	lb/ft ³	ft/sec	x10 ²	x10 ⁻³	lb/ft-sec	x10 ⁻³ sec-1	
	61.0	53.1	8.71	4.16	1.54	9.70	2.16	flow uncertain assume laminar
	55.3	53.2	9.04	3.26	9.25	1.68	10.5	flow uncertain assume turbulent
	55.3	53.2	9.04	3.26	1.96	7.90	2.24	flow uncertain assume laminar
	50.0	53.3	9.08	2.92	13.55	1.15	13.9	flow uncertain assume turbulent
	50.0	53.3	9.08	2.92	2.19	7.10	2.26	flow uncertain assume laminar
	46.0	53.4	8.62	3.44	1.56	7.95	2.14	flow laminar
	40.6	53.5	8.05	4.27	1.50	9.24	2.00	flow laminar
	36.9	53.6	7.60	4.97	1.29	10.20	1.89	flow laminar
	30.8	53.7	6.78	6.88	0.930	12.32	1.69	flow laminar
	25.4	53.8	6.06	8.88	0.720	14.55	1.51	flow laminar
	23.1	53.8	5.91	9.45	0.677	15.10	1.47	flow laminar
	25.6	53.8	6.17	8.38	0.763	14.00	1.54	flow laminar
	30.0	53.7	6.84	6.50	0.984	12.00	1.70	flow laminar
	35.3	53.6	7.68	4.89	1.310	10.12	1.91	flow laminar
	40.3	53.5	8.26	4.19	1.530	9.30	2.06	flow laminar
	45.5	53.4	8.48	3.59	1.780	8.17	2.11	flow laminar
	50.4	53.3	9.32	2.88	2.22	7.11	2.32	flow laminar
	56.6	53.2	9.20	3.42	7.36	2.14	8.98	flow uncertain assume turbulent
	56.6	53.2	9.20	3.42	1.870	8.43	2.29	flow uncertain assume laminar
	60.7	53.1	8.93	4.01	4.06	3.76	5.63	flow uncertain assume turbulent

Test No.	Average Temp.	Density	Velocity	Friction factor	Reynolds No.	Apparent Viscosity	shear rate @ wall	Remarks
-	°F	lb/ft ³	ft/sec	x10 ²	x10 ⁻³	lb/ft-sec	x10 ⁻³ sec-l	
	60.7	53.1	8.93	4.01	1.595	9.58	2.22	Flow uncertain Assume laminar
	65.0	53.0	8.87	4.12	3.69	4.10	5.22	Flow uncertain Assume turbulent
	65.0	53.0	8.87	4.12	1.553	9.75	2.21	Flow uncertain Assume laminar
	71.9	52.9	8.85	4.03	3.99	3.78	5.50	Flow uncertain Assume turbulent
	71.9	52.9	8.85	4.03	1.590	9.48	2.20	Flow uncertain Assume laminar
9	71.0	52.9	11.95	3.82	4.93	4.13	8.71	Flow turbulent
	62.5	53.0	11.75	3.94	4.34	4.63	7.77	Flow turbulent
	59.8	53.1	11.70	3.96	4.25	4.71	7.64	Flow turbulent
	54.7	53.2	11.70	4.03	4.01	5.00	7.34	Flow uncertain Assume turbulent
	54.7	53.2	11.70	4.03	1.60	12.62	2.91	Flow uncertain Assume laminar
	49.7	53.3	11.82	4.10	3.74	5.43	7.03	Flow uncertain Assume turbulent
	49.7	53.3	11.82	4.10	1.56	13.04	2.94	Flow uncertain Assume laminar
	44.9	53.4	12.10	3.86	4.72	4.41	8.53	Flow uncertain Assume turbulent
	44.9	53.4	12.10	3.86	1.66	12.55	3.01	Flow uncertain Assume laminar
	40.4	53.5	12.68	3.11	10.66	2.05	16.3	Flow uncertain Assume turbulent
	40.4	53.5	12.68	3.11	2.05	10.65	3.15	Flow uncertain Assume laminar

LC

TABLE III-C

Detailed Results of Computations for Pilot Pipeline Tests on Redwater
Sample No. 2. (Results in Uncertain Flow Region are Omitted from Graph).

Test No.	Average temp.	Density lb/ft ³	Velocity ft/sec.	Friction factor	Reynolds no.	Apparent viscosity	Shear rate @ wall	Remarks
	°F			x10 ²	x10 ⁻³	x10 ³ lb/ft.sec.	x10 ⁻³ sec ⁻¹	
10				-	-			
	79.0	52.7	19.70	3.58	6.23	3.46	26.2	flow turbulent
	78.9	52.7	12.90	3.97	4.23	3.34	13.0	flow turbulent
	78.5	52.7	10.98	4.01	4.08	2.94	10.8	flow uncertain
								assume turbulent
	78.5	52.7	10.98	4.01	1.595	7.51	4.22	flow uncertain
	68.7	53.0	9.90	4.05	3.95	2.76	9.53	assume laminar
	68.7	53.0	9.90	4.05	1.58	6.91	3.80	flow uncertain
								assume turbulent
	67.9	53.0	12.80	4.08	3.81	3.70	11.9	assume laminar
								flow uncertain
	67.9	53.0	12.80	4.08	1.54	9.01	4.92	assume turbulent
								flow uncertain
	64.8	53.1	19.50	3.75	5.27	4.09	23.0	assume laminar
	64.8	53.1	19.50	3.75	1.71	12.63	7.50	flow uncertain
	62.0	53.1	10.43	3.67	5.70	2.02	13.1	assume laminar
	62.0	53.1	10.43	3.67	1.74	6.33	4.01	flow uncertain
	61.6	53.1	12.90	4.09	3.79	3.76	12.0	assume laminar
								flow uncertain
								assume turbulent

Test No.	Average temp.	Density	Velocity	Friction factor	Reynolds no.	Apparent viscosity	Shear rate @ wall	Remarks
	°F	lb/ft ³	ft/sec.	x10 ²	x10 ⁻³	x10 ³	x10 ⁻³	
				-	-	lb/ft.sec.	sec ⁻¹	
	61.6	53.1	12.90	4.09	1.56	9.09	4.96	flow uncertain assume laminar
	61.7	53.1	19.50	3.77	5.15	4.18	22.7	flow uncertain assume turbulent
	61.7	53.1	19.50	3.77	1.66	12.70	7.49	flow uncertain assume laminar
	54.2	53.3	11.67	3.20	2.00	6.47	4.48	flow laminar
	54.6	53.3	13.10	3.96	4.30	3.78	12.00	flow uncertain assume turbulent
	54.6	53.3	13.10	3.96	1.615	9.02	5.03	flow uncertain assume laminar
	48.6	53.5	11.22	3.69	1.73	7.21	4.31	flow uncertain assume turbulent
	50.4	53.4	13.93	3.85	4.76	3.25	15.20	flow uncertain assume laminar
	50.4	53.4	13.93	3.85	1.66	9.31	5.35	flow laminar
	47.4	53.5	10.20	4.07	1.57	7.24	3.92	flow laminar
	41.8	53.6	6.71	6.75	0.948	7.91	2.58	flow laminar
	37.5	53.8	4.78	10.30	0.621	8.63	1.84	flow laminar
	49.5	53.4	11.17	3.51	1.82	6.81	4.30	flow laminar
	46.2	53.5	10.60	3.98	1.72	7.30	4.07	flow laminar
	39.0	53.7	8.76	5.97	1.07	9.13	3.37	flow laminar
	33.1	53.9	6.32	10.45	0.606	11.58	2.43	flow laminar
	27.5	54.2	4.69	19.15	0.334	15.82	1.81	flow laminar
	26.2	54.3	4.23	23.80	0.269	17.75	1.63	flow laminar

Test No.	Average temp.	Density	Velocity	Friction factor	Reynolds no.	Apparent viscosity	Shear rate @ wall	Remarks
	$^{\circ}\text{F}$	lb/ft^3	ft/sec.	$\times 10^2$	$\times 10^{-3}$	$\times 10^3$	$\times 10^{-3}$	
				-	-	lb/ft. sec.^{-1}	sec^{-1}	
12	66.0	53.0	41.23	3.151	10.14	4.48	78.8	flow turbulent
	69.7	52.9	26.99	3.467	7.080	4.20	39.6	flow turbulent
	65.6	53.0	27.09	3.502	6.803	4.39	38.6	flow turbulent
	58.7	53.2	11.72	3.190	2.006	6.47	4.50	flow laminar
	54.9	53.3	12.07	2.888	14.10	0.95	29.4	flow uncertain
								assume turbulent
	54.9	53.3	12.07	2.888	2.216	6.04	4.64	flow uncertain
								assume laminar
	50.3	53.4	11.28	3.374	1.897	6.60	4.33	flow laminar
	45.7	53.5	15.27	3.088	2.073	8.20	5.87	flow laminar
	38.5	53.7	17.04	3.073	11.00	1.73	34.5	flow uncertain
								assume turbulent
	38.5	53.7	17.04	3.073	2.183	9.14	6.55	flow uncertain
								assume laminar
	35.6	53.8	16.21	3.575	1.821	9.96	6.22	flow laminar
	32.8	53.9	12.46	5.135	1.246	11.21	4.84	flow laminar
	29.0	54.0	7.96	9.558	0.670	13.35	3.06	flow laminar
	27.2	54.0	7.53	10.78	0.594	14.24	2.89	flow laminar
	21.7	54.1	4.31	28.90	0.221	21.90	1.65	flow laminar
	24.9	54.1	6.06	15.87	0.403	16.90	2.33	flow laminar

TABLE IV-C.

Detailed Results of Computation for Pilot Pipeline
Tests on Stettler D2-D3 Blend.

Test No.	Average Temp. ° F	Density lb/ft ³	Velocity ft/sec	Friction factor x10 ²	Reynolds No. x10 ⁻³	Apparent Viscosity x10 ³ lb/ft.sec	Shear rate @ wall x10 ⁻³ sec ⁻¹	Remarks
13	73.5	54.55	10.20	4.825	1.326	8.72	3.92	flow laminar
	70.6	54.62	17.28	3.107	2.060	9.53	6.64	flow laminar
	65.2	54.75	16.97	3.459	1.850	10.44	6.52	flow laminar
	61.6	54.84	16.88	3.705	1.727	11.14	6.48	flow laminar
	55.5	54.99	15.93	4.454	1.437	12.67	6.12	flow laminar
	50.5	55.11	14.23	5.817	1.100	14.82	5.47	flow laminar
	48.3	55.17	13.09	6.920	0.925	16.23	5.03	flow laminar
	44.8	55.25	8.916	11.18	0.573	17.89	3.43	flow laminar
	41.8	55.33	8.157	13.71	0.467	20.11	3.13	flow laminar
	35.8	55.47	5.281	27.65	0.232	26.32	2.03	flow laminar
	38.9	55.40	8.364	14.86	0.431	22.37	3.21	flow laminar
	34.3	55.51	6.167	24.72	0.259	27.48	2.37	flow laminar
	31.1	55.59	5.167	33.15	0.193	30.94	1.99	flow laminar
	26.7	55.70	4.091	51.92	0.123	38.45	1.57	flow laminar
	22.2	55.81	3.302	76.32	0.0838	45.69	1.27	flow laminar
	21.8	55.82	3.278	78.04	0.0820	46.42	1.26	flow laminar
	52.0	55.07	14.63	5.382	1.190	14.09	5.62	flow laminar

TABLE V-C.

Detailed Results of Computations of Pilot Pipeline
Tests on Duhamel-Malmö - New Norway Blend.
(Uncertain flow results omitted from graph)

Test No.	Average Temp.	Density	Velocity	Friction factor	Reynolds No.	Apparent Viscosity	Shear rate @ wall	Remarks
	°F	lb/ft ³	ft/sec	x10 ²	x10 ⁻³	x10 ³ lb/ft.sec.	x10 ⁻³ sec ⁻¹	
14	76.2	51.90	47.21	2.577	21.68	2.35	158.0	flow turbulent
	69.7	52.05	24.67	3.075	11.13	2.40	50.4	flow turbulent
	65.0	52.15	22.05	3.285	8.67	2.76	37.6	flow turbulent
	60.2	52.26	23.78	3.236	9.183	2.82	42.2	flow turbulent
	56.8	52.34	21.57	3.247	8.099	2.90	35.0	flow turbulent
	52.0	52.45	18.07	3.548	6.486	3.04	24.9	flow turbulent
	48.3	52.53	18.11	3.601	6.134	3.23	23.9	flow uncertain
	48.3	52.53	18.11	3.601	1.780	11.12	6.96	assume turbulent
	44.2	52.62	18.08	3.659	5.774	3.43	22.8	flow uncertain
	44.2	52.62	18.08	3.659	1.750	11.30	6.95	assume laminar
	39.9	52.72	19.32	3.695	5.567	3.81	23.8	flow uncertain
	39.9	52.72	19.32	3.695	1.730	12.22	7.42	assume turbulent
	37.9	52.77	16.43	3.899	4.545	3.97	17.1	flow uncertain
	37.9	52.77	16.43	3.899	1.640	10.98	6.31	assume laminar

Test No.	Average temp.	Density	Velocity	Friction factor	Reynolds no.	Apparent viscosity	Shear rate @ wall	Remarks
	$^{\circ}\text{F}$	lb/ft^3	ft/sec.	$\times 10^2$	$\times 10^{-3}$	$\times 10^3$	$\times 10^{-3}$	
				-	-	lb/ft. sec.	sec^{-1}	
	34.1	52.85	10.23	3.575	1.790	6.28	3.93	flow laminar
	34.9	52.84	18.48	3.789	5.063	4.01	22.1	flow uncertain assume turbulent
	34.9	52.84	18.48	3.789	1.690	12.02	7.10	flow uncertain assume laminar
	29.1	52.97	6.571	6.92	0.925	7.82	2.52	flow laminar
	25.2	53.06	4.904	12.20	0.525	10.32	1.88	flow laminar
	25.7	53.05	6.586	8.17	0.783	12.53	2.53	flow laminar
	36.0	52.81	10.74	3.57	1.791	6.58	4.13	flow laminar
	41.7	52.68	10.58	3.85	5.580	2.08	13.6	flow uncertain assume turbulent
	41.7	52.68	10.58	3.85	1.664	6.96	4.06	flow uncertain assume laminar
15	63.7	52.19	14.69	3.61	6.12	2.61	19.4	flow turbulent
	35.5	52.82	7.01	4.84	1.32	5.83	2.69	flow laminar
	29.8	52.95	4.78	10.60	0.603	8.63	1.84	flow laminar
	26.5	53.03	3.91	15.27	0.419	10.29	1.50	flow laminar
	23.8	53.09	2.96	25.8	0.248	13.44	1.14	flow laminar
	53.5	52.41	44.2	2.96	1.26	3.64	10.0	flow laminar
	48.2	52.53	30.0	3.31	0.844	3.88	50.2	flow laminar
16	70.7	52.03	6.48	3.95	4.36	1.61	6.68	flow uncertain assume turbulent
	70.7	52.03	6.48	3.95	1.62	4.33	2.48	flow uncertain assume laminar
	64.3	52.17	6.59	3.87	4.68	1.53	7.15	flow uncertain assume turbulent

Test No.	Average temp.	Density	Velocity	Friction factor	Reynolds no.	Apparent viscosity	Shear rate @ wall	Remarks
	°F	lb/ft ³	ft/sec.	x10 ²	x10 ⁻³	x10 ³	x10 ⁻³	
				-	-	lb/ft.sec.	sec ⁻¹	
	64.3	52.17	6.59	3.87	1.65	4.33	2.53	flow uncertain assume laminar
	60.5	52.26	7.05	3.79	5.04	1.52	8.08	flow uncertain assume turbulent
	60.5	52.26	7.05	3.79	1.69	4.54	2.71	flow uncertain assume laminar
	55.1	52.38	7.42	3.68	5.67	1.43	9.30	flow uncertain assume turbulent
	55.1	52.38	7.42	3.68	1.74	4.65	2.85	flow uncertain assume laminar
	50.6	52.46	7.45	3.50	6.84	1.19	10.7	flow uncertain assume turbulent
	50.6	52.46	7.45	3.50	1.83	4.45	2.86	flow uncertain assume laminar
	45.6	52.60	7.55	3.33	8.22	1.01	12.3	flow uncertain assume turbulent
	45.6	52.60	7.55	3.33	1.92	4.30	2.90	flow uncertain assume laminar
	40.8	52.70	5.11	5.43	1.18	4.75	1.96	flow laminar
	38.4	52.78	4.03	7.83	1.82	5.39	1.55	flow laminar
	35.2	52.83	3.43	10.70	0.596	6.33	1.32	flow laminar
	31.0	52.93	3.33	13.13	0.487	7.52	1.29	flow laminar
	29.0	52.97	3.43	14.80	0.432	8.77	1.32	flow laminar
	26.2	53.04	3.16	19.49	0.329	10.70	1.21	flow laminar
	23.7	53.09	2.79	20.00	0.313	12.25	1.07	flow laminar
	21.7	53.14	2.75	26.4	0.242	12.70	1.06	flow laminar

Test No.	Average temp.	Density	Velocity	Friction factor	Reynolds no.	Apparent viscosity	Shear rate @ wall	Remarks
	$^{\circ}\text{F}$	lb/ft^3	ft/sec.	$\times 10^2$	$\times 10^{-3}$	$\times 10^3$	$\times 10^{-3}$	
				-	-	lb/ft. sec.	sec^{-1}	
17	77.8	51.85	5.82	3.82	5.46	1.15	10.8	flow uncertain assume turbulent
	77.8	51.85	5.82	3.82	1.68	5.51	2.23	flow uncertain assume laminar
	82.2	51.76	50.39	2.43	25.1	2.16	188.0	flow turbulent
	67.2	52.11	5.80	3.10	10.7	0.59	14.1	flow uncertain assume turbulent
	67.2	52.11	5.80	3.10	2.06	3.75	2.22	flow uncertain assume laminar
	71.0	52.02	49.10	2.57	21.9	2.57	156.0	flow turbulent
	58.1	52.31	5.202	3.27	1.96	2.89	2.00	flow laminar
	52.8	52.43	5.059	3.80	1.69	3.27	1.94	flow laminar
	48.7	52.52	4.624	4.56	1.40	3.60	1.78	flow laminar
	44.7	52.61	4.241	5.59	1.15	4.05	1.63	flow laminar
	41.6	52.69	26.73	3.38	7.76	3.78	42.0	flow uncertain assume turbulent
	41.6	52.69	26.73	3.38	1.89	15.48	10.3	flow uncertain assume laminar

TABLE VI-C.

Detailed Results of Computations for Pilot Pipeline
Tests on Leduc-Woodbend Blend
(Uncertain flow results omitted from graph)

Test No.	Average temp.	Density	Velocity	Friction factor	Reynolds no.	Apparent viscosity	Shear rate @ wall	Remarks
	$^{\circ}\text{F}$	lb/ft ³	ft/sec.	x10 ²	x10 ⁻³	x10 ³	x10 ⁻³	
				-	-	lb/ft.sec.	sec ⁻¹	
18	72.7	51.62	50.25	2.46	26.0	2.07	192.0	flow turbulent
	73.8	51.60	4.267	3.34	8.16	0.56	7.18	flow uncertain
	73.8	51.60	4.267	3.34	1.86	2.46	1.64	assume turbulent
	65.6	51.75	4.866	3.24	9.05	0.55	8.99	assume laminar
	65.6	51.75	4.866	3.24	1.98	2.65	1.87	flow uncertain
	60.3	51.85	3.941	3.90	1.64	2.89	1.51	assume laminar
	53.1	51.99	3.665	4.74	1.35	2.93	1.41	flow laminar
	39.8	52.25	3.197	7.40	0.865	4.01	1.23	flow laminar
	38.3	52.27	3.846	5.96	1.07	3.89	1.48	flow laminar
	34.2	52.35	3.861	6.51	0.983	4.28	1.48	flow laminar
	29.4	52.45	3.758	7.18	0.892	4.60	1.44	flow laminar
	21.7	52.60	2.819	15.84	0.416	7.63	1.08	flow laminar
	22.9	52.57	4.577	8.44	0.759	6.60	1.76	flow laminar
	26.5	52.50	4.027	8.63	0.742	5.93	1.55	flow laminar
	36.9	52.30	34.79	3.06	11.4	3.33	72.4	flow turbulent
	40.9	52.22	50.16	2.73	17.4	3.14	142.0	flow turbulent
	48.4	52.13	44.39	2.81	15.6	3.08	116.0	flow turbulent
	40.1	52.24	43.68	2.87	14.4	3.30	108.0	flow turbulent
	40.8	52.23	57.44	2.68	18.8	3.32	114.0	flow turbulent

TABLE VII-C.

Detailed Results of Computations for Pilot Pipeline
Tests on Nisku Blend.
(Uncertain flow results omitted from graph)

Test No.	Average temp.	Density	Velocity	Friction factor	Reynolds no.	Apparent viscosity	Shear rate @ wall	Remarks
	$^{\circ}\text{F}$	lb/ft ³	ft/sec.	x10 ²	x10 ⁻³	x10 ³ lb/ft.sec.	x10 ⁻³ sec ⁻¹	
19	73.6	53.42	33.51	3.42	7.42	5.02	50.8	flow turbulent
	73.7	53.42	10.91	2.93	13.3	0.92	25.2	flow uncertain
	73.7	53.42	10.91	2.93	2.18	5.56	4.18	assume turbulent
	65.2	53.60	10.31	3.35	1.91	6.02	3.96	flow uncertain
	59.2	53.75	9.729	3.88	1.65	6.59	3.72	assume laminar
	54.7	53.83	9.088	4.89	1.39	7.30	3.49	flow laminar
	50.3	53.93	8.463	5.48	1.17	8.12	3.25	flow laminar
	44.8	54.04	7.680	7.05	0.908	9.51	2.95	flow laminar
	40.6	54.14	6.222	10.12	0.632	11.07	2.39	flow laminar
	36.5	54.23	12.86	6.17	1.04	13.98	4.95	flow laminar
	29.3	54.39	4.286	30.16	0.212	22.84	1.65	flow laminar
	25.5	54.47	2.949	57.15	0.112	29.84	1.12	flow laminar
	21.2	54.57	2.146	105.8	0.0605	40.24	0.825	flow laminar
	71.5	53.46	6.010	5.16	1.24	5.49	2.31	flow laminar
	65.1	53.60	5.670	6.27	1.02	6.19	2.22	flow laminar
	60.7	53.70	5.581	6.78	0.944	6.60	2.15	flow laminar

TABLE VIII-C.

Apparent Viscosity Comparisons for Redwater
Crudes. (Values from Figures 17, 18 and 19)

Temp.	Sample No. 1				Sample No. 2			
	Apparent Viscosity		Deviation from Average		Apparent Viscosity		Deviation from Av. of No. 1	
	$\frac{\text{lb.}}{\text{ft. sec.}}$	$\frac{\text{lb.}}{\text{ft. sec.}}$	$\frac{\text{lb.}}{\text{ft. sec.}}$	%	$\frac{\text{lb.}}{\text{ft. sec.}}$	%		
20	0.249"	0.386"	Average					
25	$\frac{\text{lb.}}{\text{ft. sec.}}$	$\frac{\text{lb.}}{\text{ft. sec.}}$	$\frac{\text{lb.}}{\text{ft. sec.}}$					
30	20.30x10 ⁻³	14.13x10 ⁻³	19.72x10 ⁻³	+ 2.9	25.10x10 ⁻³		27.3	
35	15.00	12.25	14.57	2.9	17.60		20.9	
40	12.72	10.74	12.49	1.9	12.60		0.9	
45	10.99	9.43	10.87	1.2	10.41		-4.2	
50	9.56	8.22	9.50	0.7	8.86		-6.8	
55	8.27	7.08	8.25	0.3	7.67		-7.0	
60	7.09	6.01	7.09	0.1	6.70		-5.5	
65	6.00	5.02	6.01	0.8	5.93		-1.3	
70	5.08	4.45	5.05	0.6	5.20		3.0	
75	4.53	4.22	4.49	0.9	4.56		1.6	
80	4.20	3.90	4.21	0.2	4.15		-1.4	
	3.83	3.60	3.87	0.9	3.77		-2.6	
	3.51		3.56	1.3	3.38		-5.1	

TABLE IX-C.

Summary of Apparent Viscosity Correlations.

(Average values of Redwater sample No. 1. from Table VIII-C, apparent viscosities of other crudes from Figures 19, 20, 21, 22 and 23).

Temperature °F	OR	Apparent Viscosities in $\frac{\text{lb}}{\text{ft-sec.}} \times 10^3$				Duhamel- Malmo - New Norway	Leduc - Woodbend	Nisku.
		Redwater Sample No. 1 (average)	Redwater Sample No. 2	Stettler D2-D3				
20	480	19.72	25.10	50.20	15.35	8.08	43.10	
25	485	14.57	17.60	40.90	11.18	6.06	30.64	
30	490	12.49	12.60	33.10	8.21	4.87	21.70	
35	495	10.87	10.41	26.40	6.20	4.00	15.20	
40	500	9.50	8.86	21.60	4.93	3.54	11.40	
45	505	8.25	7.67	17.80	4.00	3.23	9.43	
50	510	7.09	6.70	15.08	3.44	2.98	8.20	
55	515	6.01	5.93	12.90	3.05	2.79	7.22	
60	520	5.05	5.20	11.48	2.81	2.60	6.55	
65	525	4.49	4.56	10.49	2.67	2.42	6.04	
70	530	4.21	4.15	9.50	2.53	2.24	5.56	
75	535	3.87	3.77	8.60	2.38	2.05	5.04	
80	540	3.56	3.38	7.70	2.24	1.87	4.55	

TABLE X-C.

Conversion of Apparent Viscosity to Kinematic and Saybolt Universal Viscosities
(Computations shown in section 4 of Appendix A)

Redwater Sample No.1.			Redwater Sample No.2			Stettler D2-D3 Blend.			
Temperature	Kinematic viscosity		Saybolt Universal	Kinematic viscosity		Saybolt Universal	Kinematic viscosity		Saybolt Universal
	°F	°R	ft ² /sec.	sec.	ft ² /sec	sec	ft ² /sec	sec.	
20	480		3.66x10 ⁻⁴	159	4.63x10 ⁻⁴	203	8.98x10 ⁻⁴	395	
25	485		2.71	119	3.26	143	7.35	320	
30	490		2.32	104	2.34	105	5.95	257	
35	495		2.03	93	1.94	90	4.75	208	
40	500		1.78	84	1.65	79	3.90	171	
45	505		1.55	75	1.43	71	3.22	140	
50	510		1.33	67	1.25	65	2.74	120	
55	515		1.13	60	1.11	60	2.34	105	
60	520		0.951	55	0.977	56	2.11	97	
65	525		0.848	52	0.860	54	1.91	89	
70	530		0.795	50	0.784	50	1.74	83	
75	535		0.733	48	0.714	47	1.58	77	
80	540		0.675	46	0.640	45	1.42	70	

Temperature		Duhamel-Malmö-New Norway			Leduc-Woodbend			Nisku.		
°F	°F	Kinematic viscosity	Saybolt Universal	sec.	Kinematic viscosity	Saybolt Universal	sec	Kinematic viscosity	Saybolt Universal	sec
20	480	2.88×10^{-4}		126	1.54×10^{-4}		75	7.88×10^{-4}		345
25	485	2.10	96		1.15	61		5.62		249
30	490	1.55	76		0.929	53		3.99		174
35	495	1.17	62		0.765	49		2.80		123
40	500	0.935	64		0.678	46		2.10		96
45	505	0.760	49		0.619	44		1.74		82
50	510	0.655	45		0.572	43		1.52		75
55	515	0.581	43		0.537	42		1.34		68
60	520	0.537	42		0.500	41		1.22		64
65	525	0.512	41		0.467	40		1.13		60
70	530	0.487	40		0.433	39		1.04		57
75	535	0.459	39.5		0.397	38		0.944		54
80	540	0.432	39		0.363	37		0.854		52

APPENDIX D

REFRIGERATION STUDIES

Refrigeration Studies Conducted on the Pilot Pipeline

To determine whether more insulation, larger surface area of heat transfer in the precool bath, an auxiliary precool refrigeration unit or a refrigeration unit of greater capacity is required to give the desired lowering in oil temperature at the higher rates of flow, an investigation was made of the refrigeration capacity of the existing unit at various rates of crude oil flow through the 0.386 inch internal diameter test line. The flow rates used were:

- Test I Zero flow through test line, maximum flow through by-pass (18.86 g.p.m.)
- Test II Small flow through test line (5.64 g.p.m.) bulk of flow through by-pass.
- Test III Medium flow through test line (8.35 g.p.m.) moderate flow through by-pass.
- Test IV Large flow through test line (12.71 g.p.m.), small flow through by-pass.

For each case, the by-pass valve was adjusted for the desired rate of crude oil flow through the test line, the remaining portion of the crude oil pumped, was by-passed to storage without cooling. The oil was allowed to circulate through the storage tank, refrigerated shell and receiver and data of Table I-D, Appendix D, taken after equilibrium conditions were obtained.

TABLE 1-D

Experimental Data for Refrigeration Studies on the Pilot Pipeline

(Refer to Figure 1-D)

Test ^x	Symbol	Units	I	II	III	IV
Compressor:						
F-12, suction press.	P ₁	psig.	1.5	1.5	3.0	3.0
discharge press.	P ₂	psig.	95	115	120	122
discharge temp.	T ₂	°F.	97	162	172	192
Power input	K _c	Kw.	2.05	2.08	2.26	2.22
Condenser:						
Water, inlet temp.	T ₃	°F.	60	60	62	62
exit temp.	T ₄	°F.	68.6	76	84.6	84.6
flow rate	Q _w	lb/sec.	0.343	0.351	0.372	0.382
F-12, exit temp.	T ₅	°F	64	66	76	72
Shell:						
Oil, precool inlet temp.	T ₆	°F	-	37	50	71.5
test line inlet temp.	T ₇	°F	-	29.8	41.6	68.0
test line exit temp.	T ₈	°F	-	30.4	42.7	69.0
test line inlet press.	P ₇	psig.	-	39.0	91.0	174.0
test line exit press.	P ₈	psig.	-	4.2	6.9	15.8
test flow rate	Q _T	g.p.m.	0	5.64	8.35	12.71
by-pass flow rate	Q _B	g.p.m.	18.86	-	-	-
Bath temp.	T _S	°F.	1.0	11.5	28.5	56.5
Average vapour barrier surface temp.	T _A	°F.	57	60.1	60.9	65.6
Average flange surface temp.	T _F	°F.	25	28	40	59
Room temp.	T _R	°F.	77.1	78.1	73.0	72.5
Barometric press.	P _B	psia.	13.7	13.7	13.7	13.6

^x 0.386 inch internal diameter line used in all tests^z Redwater crude oil, 34.5 A.P.I. in test.

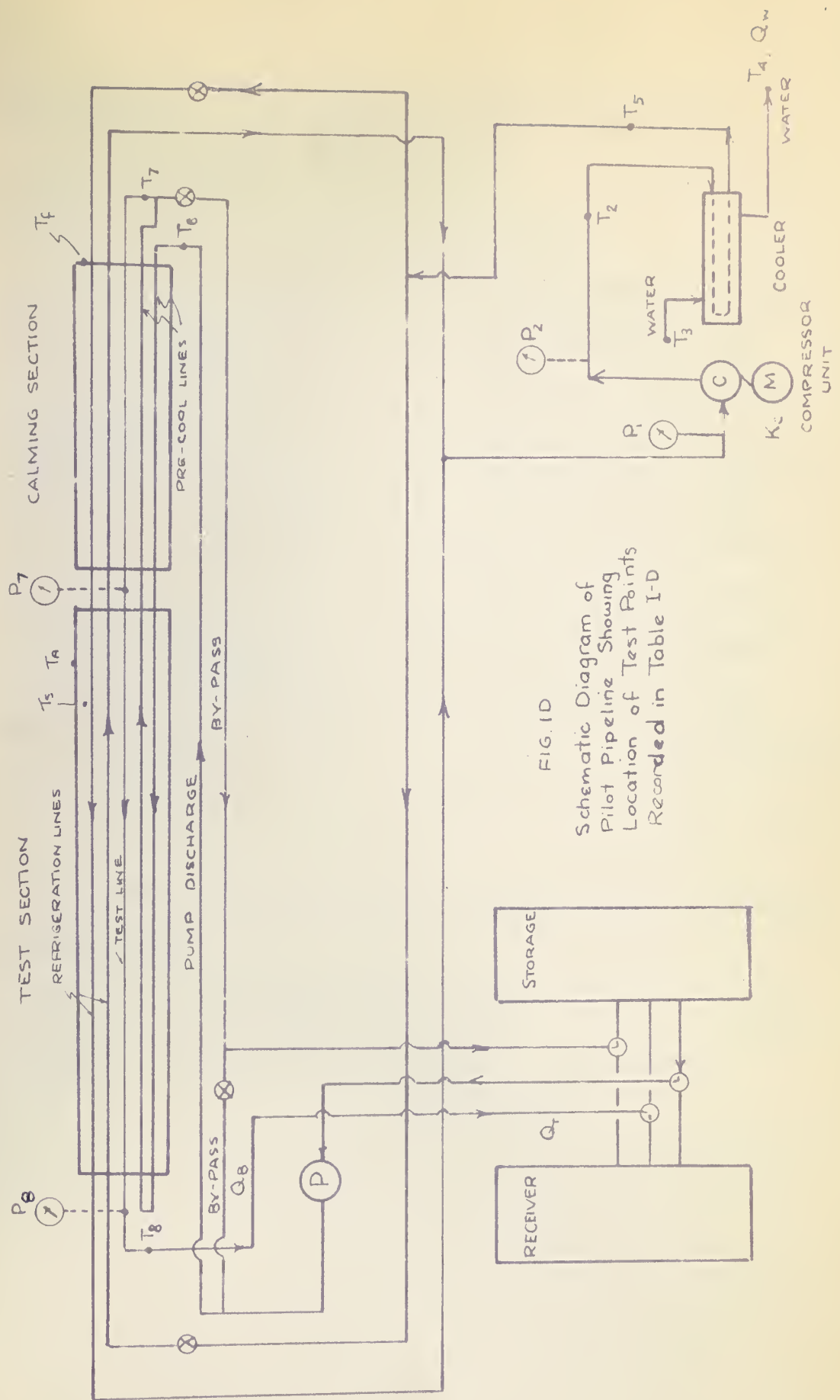


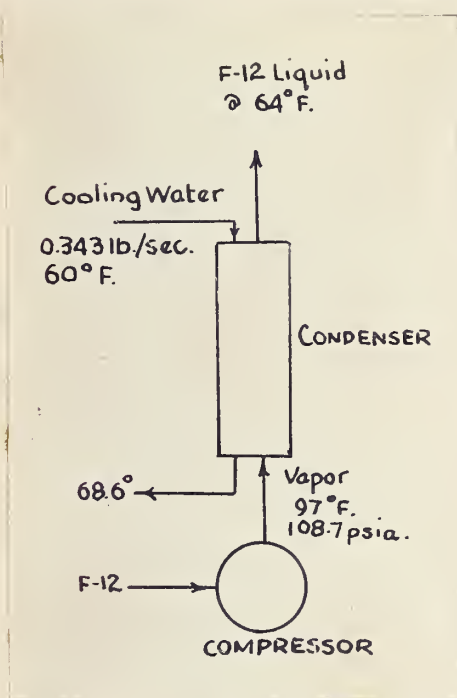
FIG. 1D

Schematic Diagram of
Pilot Pipeline Showing
Location of Test Points
Recorded in Table I-D

Detailed Outline of Computations Used in Refrigeration Studies

A. By Heat Balance Method.

(a) Condenser:



Data (Test I):

F-12 enters condenser as vapor,

temperature, $T_2 = 97^\circ\text{F}$.

pressure, $P_2 = 95$ psig.

F-12 leaves condenser as liquid,

temperature, $T_5 = 64^\circ\text{F}$.

Cooling water leaves condenser,

temperature, $T_4 = 68.6^\circ\text{F}$.

Cooling water enters condenser,

temperature, $T_3 = 60^\circ\text{F}$.

rate, $Q_w = 0.343$ lb./sec.

Atmospheric pressure = 13.7 psia.

The amount of F-12 circulated is found by a simple heat balance around the condenser:

$$q_c - Q_w C_p (\Delta T)_w = Q_F (\Delta H)_F \quad (\text{I-d})$$

where $(\Delta T)_w = T_4 - T_3 =$ change in temperature of
cooling water

$(\Delta H)_F =$ enthalpy change of F-12 or the enthalpy
of F-12 vapor at temperature T_2 and
pressure P_2 , minus the saturated liquid
enthalpy of F-12 at temperature T_5 .

Q_F = mass rate of flow of F-12

C_p = specific heat of water

and q_c = heat loss to the surroundings by the condenser.

The heat gained by the cooling water (q_w) is:

$$q_w = Q_F C_p (\Delta T)_w = (0.343 \frac{\text{lb.}}{\text{sec}}) (1.0 \frac{\text{Btu.}}{\text{lb.}^\circ\text{F.}}) (68.6 - 60)^\circ\text{F} \\ = 2.95 \text{ Btu/sec.}$$

The enthalpy (h_g) of F-12 superheated vapor at 97°F and 108.7 psia. from Perry (15) is 87.99 Btu/lb. The enthalpy (h_f) of F-12 liquid at 64°F , assuming saturation, is 22.50 Btu/lb.

$$\text{Hence } (\Delta H)_F = h_g - h_f = (87.99 - 22.50) \text{ Btu/lb.} \\ = 65.49 \text{ Btu/lb.}$$

Assuming adiabatic operation, $q_c = 0$, thus from equation (1-d):

$$2.95 = 65.49 Q_F$$

$$\text{or } Q_F = 0.0450 \text{ lb./sec.}$$

which is the rate of F-12 flow through the refrigeration unit for Case I.

The mass rate of flow of F-12 may also be computed by considering the volume displacement of the compressor. Two cylinders of $2\frac{1}{2}$ inch diameter with a $3\frac{1}{2}$ inch stroke are driven at the rate of 650 cycles per minute.

$$\text{The theoretical volume displaced per min} = \frac{\pi D^2 S}{2} \times 650 \quad (2-d)$$

where D = diameter of cylinder

S = length of stroke

Substituting values in equation (2-d):

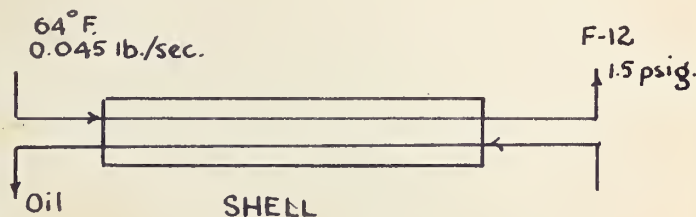
$$\begin{aligned} \text{theoretical displacement} &= \frac{\pi (2.5)^2 (3.5) (650)}{2 (1728)} \\ &= 12.84 \text{ ft}^3/\text{min}. \end{aligned}$$

Assuming F-12 to enter the compressor as saturated vapor, (2.490 ft³/lb.), at the suction pressure of 1.5 psig., or 15.2 psia., the capacity of the refrigeration unit is:

$$\frac{(12.84 \text{ ft}^3/\text{min})}{(2.490 \text{ ft}^3/\text{lb}) (60 \text{ sec}/\text{min})} = 0.0860 \text{ lb}/\text{sec}.$$

The flow of 0.0860 lb/sec. is much higher than the flow rate of 0.0450 lb/sec. calculated by the heat balance method, however, the flow rate of 0.0860 lb/sec. does not account for the volumetric efficiency of the compressor nor possible superheating of inlet vapors.

(b) Shell



Data: F-12 enters expansion line at temperature,

$$T_5 = 64^\circ\text{F}$$

F-12 expands in line at suction pressure,

$$P_1 = 1.5 \text{ psig}$$

No oil flow through test line

$$\text{Shell temperature, } T_S = 1.0^\circ \text{F}$$

Assumptions:

1. Saturated F-12 liquid enters expansion line at 64°F .
2. Saturated F-12 vapor enters compressor at 15.2 psia.
3. Flow of F-12 is distributed equally in each line.

From Perry (15):

Saturated liquid enthalpy of F-12 at $64^\circ \text{F} = 22.50 \text{ Btu/lb.}$

Saturated vapor enthalpy of F-12 at 15.2 psia = 75.84 Btu/lb.

Therefore change in enthalpy, $(\Delta H)_F = 53.34 \text{ Btu/lb.}$

By a simple heat balance around the shell, the heat gained by F-12 in evaporating at 15.2 psia equals the heat transferred through the shell plus the heat transfer from the flow of crude oil in the test line under equilibrium conditions:

$$q_s + q_o = Q_F (\Delta H)_F \quad (3-d)$$

where q_s = heat transfer through shell plus losses in refrigeration capacity.

q_o = net heat transfer from oil, defined by the thermodynamic flow equation.

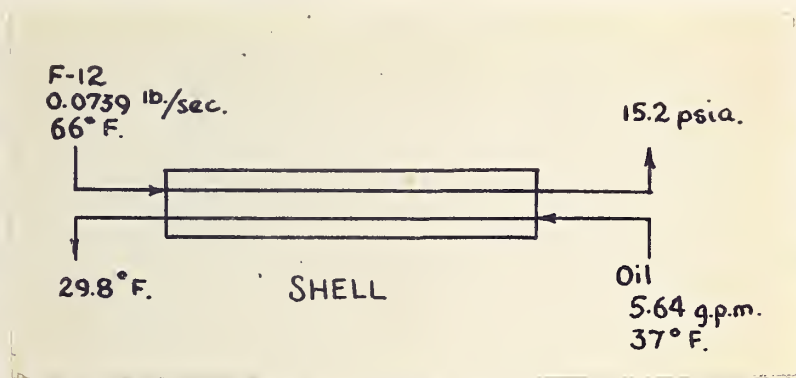
$(\Delta H)_F$ = change in F-12 enthalpy.

For Case I, where there is no oil flow, substitution of values in equation (3-d) gives:

$$\begin{aligned} q_s &= 0.0450 (53.34) \text{ Btu/sec.} \\ &= 2.4 \text{ Btu/sec. or } 8,640 \text{ Btu/hr.} \end{aligned}$$

Thus 8,640 Btu/hr is transferred into the shell in maintaining the shell at a temperature of 1.0°F. Actually some of this heat is transferred through the external piping and may be considered as losses in the refrigeration capacity. No estimation of losses was attempted.

(c) Sample computations for case of oil flow through test line.



The heat transferred (q_o) from the oil may be calculated by the thermodynamic flow equation:

$$Q_T \left[\Delta U + \Delta(PV) + \frac{\Delta V^2}{2 g_c} + \frac{\Delta xg}{g_c} \right] = - Q_T w_s - q_o$$

Where: Q_T = mass rate of flow of oil

$\Delta U = \int C_v dT$ = change in internal energy, U .

P = Pressure

V = specific volume

V = velocity

x = height above datum

q_o = net heat transferred, positive
when heat is transferred from oil stream.

w_s = shaft work

C_v = specific heat of oil

T = temperature

g = acceleration due to gravity

g_c = conversion factor

Since there is no shaft work done on the oil in the precool and test lines, $w_s = 0$. The change in potential energy is small and is assumed negligible. The change in specific volume and specific heat of the oil is assumed negligible. The equation becomes:

$$q_o = -Q_T \left[C_v \Delta T + \Delta P + \frac{\Delta V^2}{2 g_c} \right] \quad (4-d)$$

Data: (Test II)

Oil enters precool at temperature, $T_6 = 37.0^\circ\text{F}$

Oil enters test line at pressure, $P_7 = 39.0$ psig.

Oil enters test line at temperature, $T_7 = 29.8^\circ\text{F}$

Oil exits test line at temperature, $T_8 = 30.4^\circ\text{F}$

Oil exits test line at pressure, $P_8 = 4.2$ psig.

Rate of flow of oil, $Q_T = 5.64$ gal/min.

Density of oil:

$$\text{at } 37.0^\circ\text{F} = 53.6 \text{ lbs/ft}^3$$

$$30.4^\circ\text{F} = 53.7 \text{ lbs/ft}^3$$

$$29.8^\circ\text{F} = 53.7 \text{ lbs/ft}^3$$

Apparent viscosity of oil:

$$\text{at } 37.0^{\circ}\text{F} = 0.0102 \text{ lb/ft. sec.}$$

$$30.4^{\circ}\text{F} = 0.0121 \text{ lb/ft. sec.}$$

$$29.8^{\circ}\text{F} = 0.0123 \text{ lb/ft. sec.}$$

F-12 enters expansion line at temperature,

$$T_5 = 66^{\circ}\text{F}$$

F-12 expands in line at suction pressure,

$$P_1 = 1.5 \text{ psig.}$$

Calculated rate of flow of F-12, $Q_F = 0.0739 \text{ lb/sec.}$

Cross-sectional area of test line 0.000812 ft.^2

From Perry (15):

Specific heat of oil, $C_v = 0.41 \text{ Btu/lb.}^{\circ}\text{F.}$

Internal diameter of precool line = 0.622 inches

Cross sectional area of precool line = 0.00211 ft.^2

Assumptions:

1. F-12 enters expansion valve as saturated liquid.
2. F-12 enters compressor as saturated vapor.

From a heat balance around the shell, the heat gained in evaporating F-12 (q_F), is equal to sum of heat transferred from the oil (q_O), the heat transferred through the shell plus the heat transferred through the external piping (q_s), or:

$$q_F = q_s + q_O \quad (5-d)$$

$$\text{but } q_F = Q_F (\Delta H)_F$$

$$\text{and } q_O = - Q_T \left[C_v (\Delta T) + v(\Delta P) + \frac{\Delta V^2}{2 g_c} \right]$$

Substituting values in equation (4-d):

$$- Q_T C_v \Delta T = \frac{(5.64 \times 53.7 \times 60 \text{ lb})}{6.24 \text{ hr.}} (0.41 \frac{\text{Btu}}{\text{lb}^\circ\text{F}}) (37.0 - 30.4) ^\circ\text{F}$$

$$= 7880 \text{ Btu/hr.}$$

The pressure drop in ΔP , of equation (4-d) is the pressure drop from precool inlet to test outlet. This includes 55 feet of $\frac{1}{2}$ inch precool pipe, 8 feet of 0.386 inch internal diameter calming section and 19.5 feet of 0.386 inch internal diameter test section. Obstructions to flow in the precool section are five 90° elbows, three tees and one sudden contraction. Equivalent lengths for these obstructions are from Brown (7):

5 - 90° elbows	=	5 x 1.5 ft.	=	7.5 feet
3 - tees	=	3 x 3.5 ft.	=	10.5 feet
1 sudden contraction	=	0.6 ft.	=	<u>0.6 feet</u>
Total equivalent length of obstructions			=	18.6 feet
Length of $\frac{1}{2}$ inch precool pipe			=	<u>55.0 feet</u>
Total equivalent length of $\frac{1}{2}$ inch pipe			=	73.6 feet

The velocity of the oil in the $\frac{1}{2}$ inch precool line is:

$$V = \left(\frac{5.64 \text{ ft.}^3}{6.24 \times 60 \text{ sec.}} \right) \left(\frac{1}{0.00211 \text{ ft.}^2} \right) = 7.14 \text{ ft./sec.}$$

The maximum Reynolds number in the $\frac{1}{2}$ inch pipe will be:

$$\left(\frac{DV}{\mu} \right)_a = \frac{(0.622) (7.14) (53.7)}{(12) (0.0102)} = 1950$$

The pressure drop in laminar flow for the $\frac{1}{2}$ inch pipe is calculated using the modified Poiseuille equation, that is:

$$\Delta P = \frac{32LV\mu_a}{g_c D^2}$$

Substituting values:

$$\Delta P = \frac{32 (73.6) (7.14) (0.0113)}{(32.2) (0.622)^2} = 15.3 \text{ lb/in.}^2$$

The pressure drop in the test section is:

$$P_7 - P_8 = 39.0 - 4.2 = 34.8 \text{ lb/in.}^2$$

The pressure drop in the 8 foot calming section is:

$$\frac{8}{19.5} \times 34.8 \frac{\text{lbs.}}{\text{in.}^2} = 14.3 \text{ lb/in.}^2$$

The total change in pressure in the precool and test lines is - 64.4 psig. The product of the specific volume and the pressure drop becomes:

$$\begin{aligned} - Q_T \bar{v}(\Delta P) &= \left(\frac{5.64 \times 60 \times 53.7}{6.24} \frac{\text{lb.}}{\text{hr.}} \right) \left(\frac{\text{ft.}^3}{53.7 \text{ lb.}} \right) (64.4 \times 144 \frac{\text{lb.}}{\text{ft.}^2}) \left(\frac{\text{Btu}}{778 \text{ lb.ft}} \right) \\ &= 646 \text{ Btu/hr.} \end{aligned}$$

The kinetic energy term, $\frac{\Delta V^2}{2 g_c}$ may be computed:

velocity in $\frac{1}{2}$ inch precool line = 7.14 ft/sec.

$$\begin{aligned} \text{velocity in test line} &= \frac{5.64}{8.12 \times 10^{-4} \times 6.24 \times 60} \\ &= 18.6 \text{ ft./sec.} \end{aligned}$$

$$- Q_T \left(\frac{\Delta V^2}{2 g_c} \right) = - 2920 \left(\frac{18.6^2 - 7.1^2}{2 \times 32.2} \right) \frac{1}{778} = - 17.2 \text{ Btu/hr.}$$

and the total heat transferred from the oil is:

$$q_o = (7,880 \pm 646 - 17.2) \frac{\text{Btu}}{\text{hr}} = 8,509 \text{ Btu/hr.}$$

From Perry (15):

$$h_g \text{ at } 15.2 \text{ psia} = 75.84 \text{ Btu./lb.}$$

$$h_f \text{ at } 66^\circ\text{F} = 23.00 \text{ Btu/lb.}$$

$$\text{hence } (\Delta H)_f = 52.84 \text{ Btu./lb.}$$

$$\text{Thus } q_F = 0.0739 (52.8) \text{ Btu/sec.} = 3.90 \text{ Btu/sec. or } 16,250 \text{ Btu/hr.}$$

Finally the heat transfer through the shell from the surroundings is:

$$q_s = (16,250 - 8509) \text{ Btu/hr.}$$

$$= 7,741 \text{ Btu/hr.}$$

In a similar manner, the heat transfer through the shell was computed for each test and tabulated in Table II-D, Appendix D.

(d) Total Energy Balance

From the results of the preceding computations, an overall energy balance may be written around the refrigeration unit. Consider the system to include the refrigeration lines, compressor, motor, condenser and shell. Then the energy balance is given by:

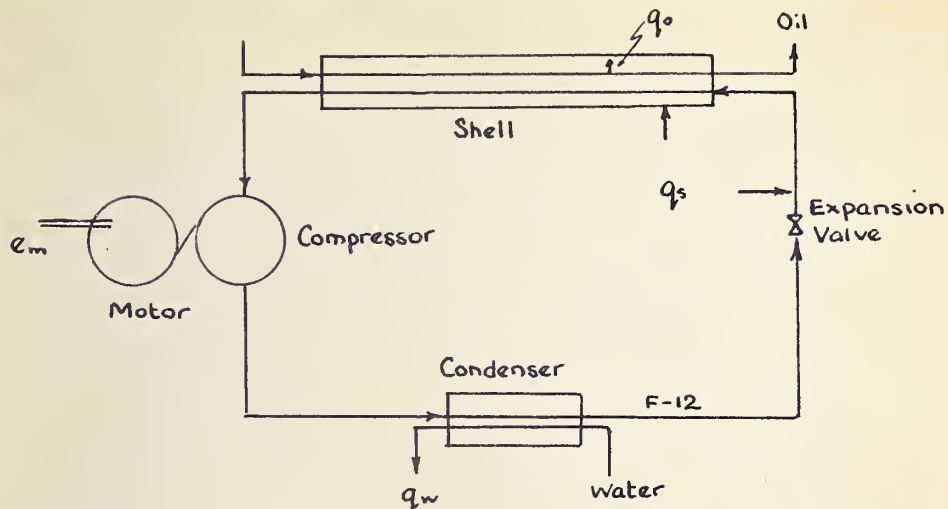
$$q_w = q_s \pm q_o \pm e_m$$

where q_w is the heat energy transferred from the system by the water

q_s is the heat energy transferred into the system through the shell and the external piping, equation (3-d).

q_o is the heat energy transferred into the system by the oil, equation (5-d)

and e_m is the electrical energy supplied to the system.



From condenser cooling water requirements (part a):

$$q_w = (2.95 \text{ Btu/sec.}) (3600 \text{ sec./hr.}) = 10,600 \text{ Btu/hr.}$$

From total energy balance:

$$q_s = 8640 \text{ Btu/hr.}$$

$$q_o = 0$$

$$e_m = 2.05 (0.75) \text{ Kw} (3413 \text{ Btu/Kw.hr.}) = 5250 \text{ Btu/hr.}$$

(assuming 75% efficiency of motor and compressor unit)

$$q_w = q_s + q_o + e_m = 13,890 \text{ Btu/hr.}$$

For each test, the energy output at the condenser may be computed by the total energy balance and compared to the sensible heat gained by the water at the condenser.

In the compression of F-12 vapors, the compressor was assumed to operate in a reversible adiabatic manner (constant entropy process). In actual practice, consideration of entropies at compressor inlet and exit conditions showed that the process could not be adiabatic. In Case I, the entropies of F-12 vapor for the inlet condition of 15.2 psia. and -20°F and the exit condition of 108.7 psia and 97°F , were 0.1727 Btu/lb. $^{\circ}\text{F}$. and 0.1694 Btu/lb. $^{\circ}\text{F}$ respectively. The heat rejected, neglecting irreversibilities is approximately:

$$\frac{557 + 440}{2} (-0.0033) = -1.65 \text{ Btu/lb.}$$

At the F-12 flow rate of 0.0450 lb/sec., the heat rejected is:

$$0.0450 (3600) (1.65) = 267 \text{ Btu/hr.}$$

The heat expelled at the condenser by the total energy balance is decreased by the amount of heat rejected by the compressor, that is, the total energy balance becomes:

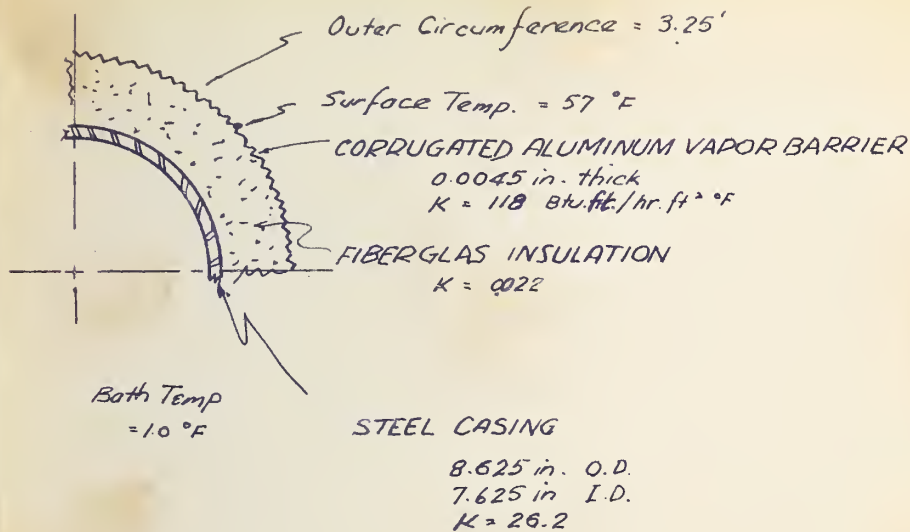
$$q_u = q_s + q_o + e_m - q_r$$

where q_r = heat rejected at compressor.

For Case I, the heat expelled at the condenser becomes 13,620 Btu/hr. In general heat effects at the compressor could become quite large when operating at higher pressures and flow rates.

B. Heat Transfer Through Shell by Method of Overall Resistance Coefficient

Data: as shown on following sketch:



Casing length between flanges:

Calming section	6 ft. 5 in.
Test section	17 ft. $10\frac{1}{2}$ in.
Total Casing	24 ft. $3\frac{1}{2}$ in.

Inner wall temperature estimated at 2.0 °F.

Thermoconductivity values from McAdams (13).

The conduction of heat through several bodies in series is given in Perry (15) as follows:

$$q = \frac{\sum \Delta t}{R_T} \quad (6-d)$$

where q = heat transferred through the composite wall

Δt = the sum of the individual temperature drops
across each material

R_T = the sum of the individual resistances R_1, R_2 etc.

The resistance R is defined as:

$$R = \frac{l}{KA} \quad (7-d)$$

where l = thickness of heat conducting material

K = thermal conductivity of material

A = cross-sectional area perpendicular to the
direction of heat flow.

Substituting values and computing the individual resistances
per foot of pipe:

(a) Steel casing

$$R_s = \frac{l_s}{K_s A_s} = \frac{(0.50/12) \text{ ft.}}{(26.2 \frac{\text{Btu}}{\text{hr. ft.}^2 \text{ } ^\circ\text{F}}) (2.16 \frac{\text{ft.}^2}{\text{ft.}})} \\ = 0.000733 \text{ hr. } ^\circ\text{F. ft.}/\text{Btu.}$$

where A_s = log mean area per foot of pipe

$$= \frac{\pi(D_o - D_i)}{\ln \frac{D_o}{D_i}} = \frac{\pi(1.0)}{12 \ln \frac{8.625}{7.625}} \text{ ft}^2/\text{ft.} \quad (8-d) \\ = 2.16 \text{ ft.}^2/\text{ft.}$$

(b) Fiberglass insulation

$$R_I = \frac{l_I}{K_I A_I} = \left(\frac{3.62/2}{12 \times 0.022 \times 2.71} \right) \frac{\text{hr. } ^\circ\text{F. ft.}}{\text{Btu.}} \\ = 2.53 \text{ hr. } ^\circ\text{F. ft.}/\text{Btu.}$$

By equation (8-d) the log mean

$$\text{area } A_I = \frac{\pi (12.25 - 8.625)}{12 \ln \frac{12.25}{8.625}} \text{ ft.}^2/\text{ft.}$$

$$= 2.71 \text{ ft.}^2/\text{ft.}$$

where outer diameter of insulation $D_I = \frac{3.25}{\pi}$ (12) in.

$$= 12.25 \text{ in.}$$

and inner diameter of insulation = 8.625 in.

(c) Aluminum vapor barrier

$$R_a = \frac{l_a}{K_a A_a} = \left(\frac{0.0045}{12 \times 118 \times 3.25} \right) \frac{\text{hr. } ^\circ\text{F. ft.}}{\text{Btu.}}$$

$$= 0.000,00098 \frac{\text{hr. ft. } ^\circ\text{F.}}{\text{Btu.}}$$

$$\text{whence } R_T = (0.000733 + 2.53) \frac{\text{hr. } ^\circ\text{F. ft.}}{\text{Btu.}}$$

$$= 2.53 \frac{\text{hr. } ^\circ\text{F. ft.}}{\text{Btu.}}$$

$$q = \frac{(57.0 - 2.0) ^\circ\text{F.}}{2.53 \frac{\text{hr. } ^\circ\text{F. ft.}}{\text{Btu.}}} \quad (24.29 \text{ ft})$$

$$= 527 \text{ Btu/hr.}$$

The heat transfer through the end flanges were computed on a log mean area based on the area exposed to the cooling bath and the outside area of the flange face:

$$A_{lm} = \frac{A_2 - A_1}{\ln \frac{A_2}{A_1}}$$

where A_2 = outer area

A_1 = inner area

$$\text{hence } A_{lm} = \frac{\pi(13.5^2 - 7.63^2)}{4 \times 144 \ln \frac{13.5^2}{7.63^2}}$$

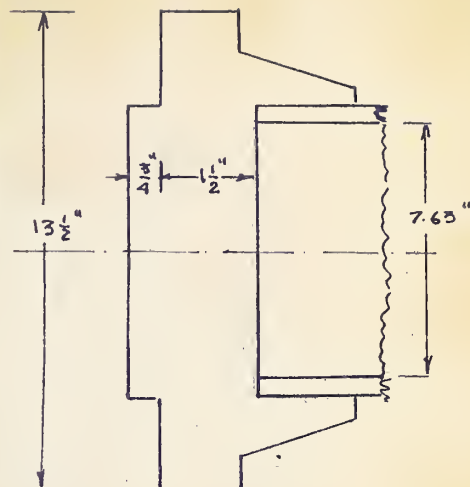
$$= 0.601 \text{ ft.}^2$$

Letting q be the heat transfer,

$$q = KA \frac{\Delta t}{X}$$

$$\frac{(26.2 \times 0.601 \times 23)}{2.25/12} \frac{\text{Btu}}{\text{hr.}}$$

$$= 1930 \frac{\text{Btu}}{\text{hr.}}$$



The unit is provided with two exposed dead end flanges and two partially insulated inner flanges (Fig. 8). Estimating the heat transfer through the insulated flange to be one-third of the exposed flange, the total heat transfer through the shell is estimated as 5,677 Btu/hr.

Heat transfer through casing 527 Btu/hr.

Heat transfer through exposed
flanges,

$$2 \times 1930 = 3860 \text{ Btu/hr.}$$

Heat transfer through insulated
flanges,

$$2 \times \frac{1930}{3} = 1290 \text{ Btu/hr.}$$

$$\text{Total} = 5677 \text{ Btu/hr.}$$

The heat transfer by the resistance coefficient method was computed for each case and is presented in Table II-D.

TABLE II-D

Results of Heat Transfer Computations.

<u>Test Conditions</u>							
Test	Oil Flow Rate	Shell Temp.	Precool Inlet Temp.	Test Inlet Temp.	Test Outlet Temp.	Compressor Suction Pressure.	
	gal/min.	°F	°F	°F	°F	Psia.	Psig.
I	0	1.0	-	-	-	15.2	1.5
II	5.64	11.5	37.0	29.8	30.4	15.2	1.5
III	8.35	24.0	50.0	41.6	42.7	16.7	3.0
IV	12.71	56.0	71.5	68.0	69.0	16.6	3.0

<u>F-12 Flow Rate</u>		<u>Total Refrigeration Capacity</u>	
(1) By Heat Balance	(2) By Compressor Displacement	(3) Estimated	(4) Rated @ 590 R.P.M.
lb./sec.	lb./sec.	Btu/hr.	Btu/hr.
I	0.0450	8,640	33,400 @21.0 psig.
II	0.0739	16,250	27,700 @15.2 psig.
III	0.115	21,400	23,200 @10.7 psig.
IV	0.107	20,400	

<u>Heat Transfer from Oil, Btu/hr.</u>				(9) <u>Heat Transfer from Shell by Heat Balance Method, Btu/hr. (including losses)</u>
(5) Internal Energy Change	(6) Heat of Friction	(7) Kinetic Energy Change	(8) Total	
I 0	0	0	0	8,640
II 7,880	646	-19	8,510	7,740
III 13,000	2,360	-55	15,310	6,090
IV 6,640	6,540	-194	12,990	7,410

<u>Heat Transfer by Resistance</u> <u>Coefficient Method, Btu/hr.</u>				<u>Heat Expelled at Condenser,</u> <u>Btu/hr.</u>	
(10) Casing	(11) Flanges	(12) Total	(13) By Temp. of Cooling Water	(14) By Total Energy Balance	
I 527	5,150	5677	10,600	13,890	
II 457	3,470	3927	20,200	21,570	
III 302	2,330	2632	30,200	27,170	
IV 87	794	881	31,100	26,070	

Discussion of Results of Refrigeration Studies

Columns (8) and (12) of Table II-D give the estimated heat transfer through the shell by heat balance method and by resistance coefficient method, respectively. Comparison of values obtained, show that estimations by the latter method are lower. Heat transfer values shown in column (8) should be decreased by the amount of heat transfer due to external piping and the amount of heat transfer at the refrigerant expansion valves. No attempt was made to evaluate the heat transfer from these sources.

In general the heat transfer rates through the shell are high and show the need of further insulation. Transfer rates through the flanges (column 11), account for almost all the total heat transfer through the shell and indicate the necessity for adequate insulation of these flanges.

Estimated refrigeration capacities (column 3) indicate the need for a larger refrigeration unit. For example, if the minimum storage temperature is estimated at 30°F and the crude oil is to be tested at

20°F at a high flow rate, say 12.71 g.p.m. as in Test IV, the sensible heat transfer from the oil alone is:

$$q_o = \left(\frac{12.71 \text{ ft.}^3}{6.24 \text{ min.}} \right) (53.9 \frac{\text{lb.}}{\text{ft.}^3}) (0.41 \frac{\text{Btu}}{\text{lb.}^\circ\text{F}}) (\frac{60 \text{ min.}}{\text{hr.}}) (10^\circ\text{F.})$$

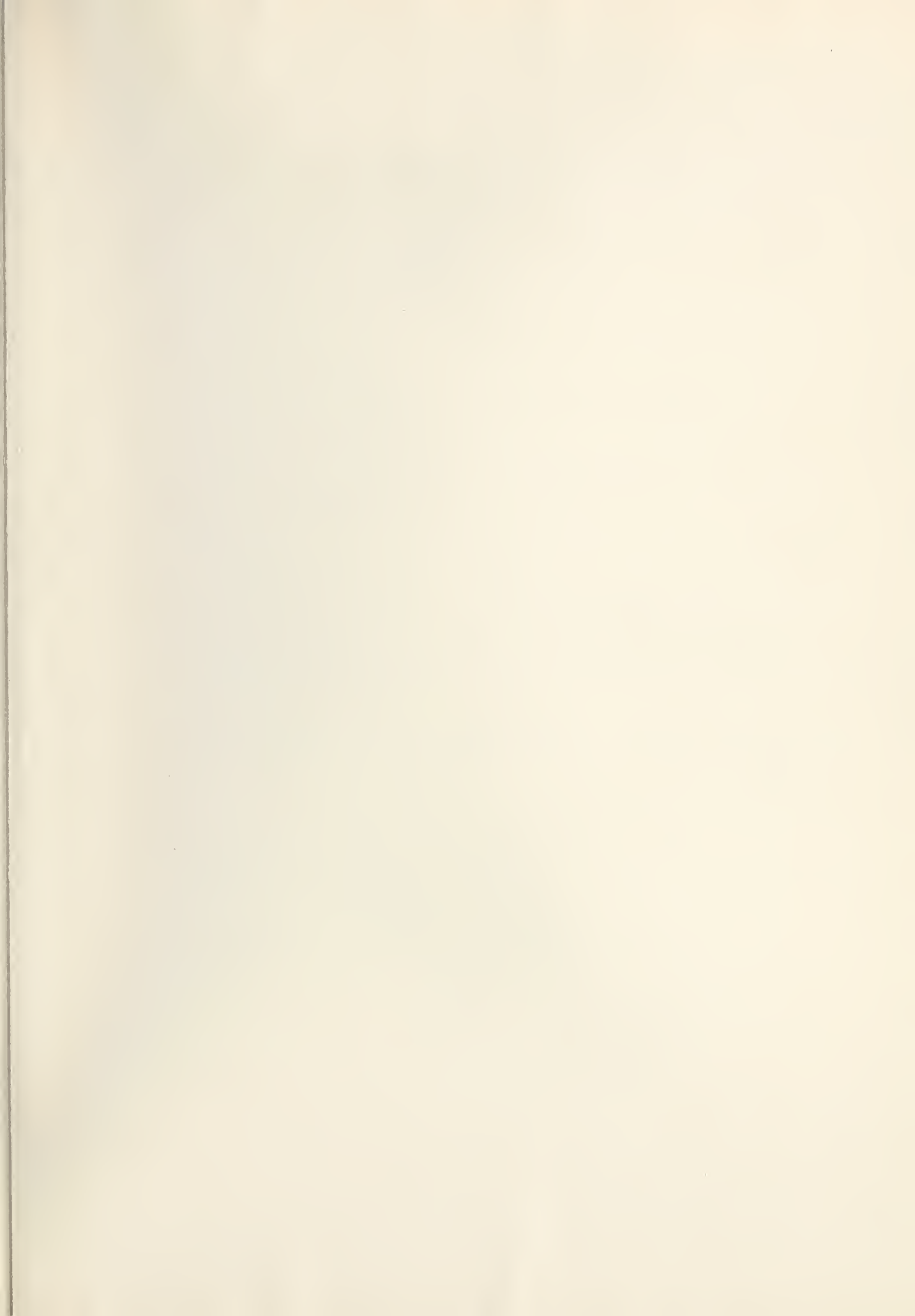
$$= 27,700 \text{ Btu/hr.}$$

The figures for test IV, column (6) show that approximately 6540 Btu/hr of heat will be generated due to friction at this flow rate.

The total amount of heat transfer without considering losses through the external piping system exceeds the refrigeration capacity of the unit. An alternative, to the replacement of the present unit may be through installation of an auxiliary precooling system. The cooling capacity of such a unit must be at least equal to the difference between the sum of heat transfer through the shell and heat transfer from the oil, less the capacity of the present unit.

Comparing the estimated refrigeration capacity (column 3) with the rated capacity (column 4), the refrigeration unit is operating near rated capacity for the suction pressure used. More efficient use could be made of the available refrigeration if a closer approach of test temperature to bath temperature could be realized. This would necessitate increased area of precool piping. Heat expelled by the condenser, columns 13 and 14, check within expectations and show that the results of computations by heat balance method are fairly accurate.

The flow rates computed by the sensible heat gained by the water for Case III and IV are considerably lower than those calculated by the compressor displacement method. The only explanation for this discrepancy is that inlet water temperatures measured by the 'pyrocon' gauge may have been in error.





B29770